DISCLAIMER:

This document does not meet the
current format guidelines of
the Graduate School at
The University of Texas at Austin.

It has been published for
informational use only.

The Dissertation Committee for Natasha Marie Sosanya certifies that this is the approved version of the following dissertation:

mTOR Dependent regulation of Kv1.1 in Normal and Disease States by the RNA binding factors, HuD and miR-129-5p

Committee:

Kimberly Raab-Graham, Supervisor

Nigel Atkinson

Nace Golding

Adron Harris

Vishwanath Iyer

mTOR Dependent regulation of Kv1.1 in Normal and Disease States by the RNA binding factors, HuD and miR-129-5p

By

Natasha Marie Sosanya, B.S.

Dissertation

Presented to the Faculty of the Graduate School of Natural Sciences

The University of Texas at Austin

in Partial Fulfillment

of the Requirements

for the Degree of

Doctor of Philosophy

The University of Texas at Austin

May 2014

This dissertation is dedicated to my Husband, Olakunle “Sosa” Sosanya.

Acknowledgments: This work was supported by the NSF grant IOS-1026527 and University of Texas Research Grant to K.R.G. I would also like to acknowledge my supervisor, Kimberly Raab-Graham, as well as the members of her lab, Farr Niere, Emily Workman, Sarah Wolfe, Luisa Cacheaux and former lab member, Peggy Huang. I would also like to acknowledge Darrin Brager from Dan Johnston's lab.

Abstract: mTOR Dependent regulation of Kv1.1 in Normal and Disease States by the RNA binding factors, HuD and miR-129-5p

Natasha Marie Sosanya, Ph.D.

The University of Texas at Austin, 2014

Supervisor: Kimberly Raab-Graham

Little is known about how a neuron undergoes site-specific changes in intrinsic excitability in normal and diseased conditions. We provide evidence for a novel mechanism for the mammalian Target of Rapamycin Complex 1 (mTORC1) kinase dependent translational regulation of the voltage-gated potassium channel Kv1.1 mRNA (Chapter 2). First, we identified a microRNA, miR-129-5p, that represses Kv1.1 mRNA translation when mTORC1 is active. When mTORC1 is inactive, we found that the RNA-binding protein, HuD, binds to Kv1.1 mRNA and promotes its translation. Surprisingly, mTORC1 activity does not alter levels of miR-129 and HuD to favor binding to Kv1.1 mRNA but affects the degradation of high-affinity HuD target mRNAs, freeing HuD to bind Kv1.1 mRNA. Thus, high affinity HuD target mRNAs can serve two purposes under normal physiological conditions: 1) to provide functional proteins, such as CaMKIIα, that change the

architecture of the synapse and 2) serve as a sponge sequestering HuD from translating mRNAs like Kv1.1.

To determine if this mechanism for repression of Kv1.1 expression is conserved in a disease model where mTORC1 activity is overactive, we assessed the expression levels of active mTORC1, Kv1.1, and miR-129-5p in a rat model of temporal lobe epilepsy (TLE; Chapter 3). We found that when mTOR activity is low in TLE, Kv1.1 expression is high and behavioral seizure number is low. In contrast, when behavioral seizure activity starts to rise there is a corresponding increase in mTOR activity and Kv1.1 protein levels dramatically drop. In addition, we found that miR-129-5p, the negative regulator of Kv1.1 mRNA translation increases by 21 days post status epilepticus (SE) to sustain Kv1.1 mRNA translational repression. Thus, long-term changes in Kv1.1 protein levels result in a hyperpolarized threshold for action potential firing. Our results suggest that increased mTOR activity following SE results in two phases of Kv1.1 repression (1) in an initial repression of Kv1.1 mRNA translation by mTOR activity that is followed by (2) an onset of elevated miR-129-5p expression that sustains Kv1.1 repression. These studies suggest that dynamic changes in miR-129-5p provide potential novel targets for epilepsy interventions.

mTOR is a protein kinase that promotes CaMKIIα mRNA translation (Sosanya et al., 2013; Chapter 2); however, the mechanism and site of dendritic expression are unknown. Herein (Chapter 4), we show that mTOR activity mediates the dendritic branch specific expression of CaMKIIα, favoring one

secondary, daughter branch over the other in a single neuron. Notably, reduction in mTOR activity decreases the overall dendritic expression of CaMKIIα protein and RNA through the shortening of its poly(A) tail. Overexpression of HuD both increases total CaMKIIα levels and rescues the selective expression of CaMKIIα in one daughter branch over the other. These results suggest that differential branch targeting of HuD may mediate the branch specific expression of CaMKIIα in neuronal dendrites during mTOR activity. Furthermore, when mTOR activity is reduced HuD releases CaMKIIα mRNA and thus exposes its poly(A) tail to be deadenylated, reducing its overall expression and eliminating its branch specific expression.

Table of Contents

Chapter 1: Dynamic Local Translation Promotes/Impairs Homeostatic Plasticity in Learning and Disease

Introduction

Local dendritic translation, in recent years, has emerged as a key regulator of neuronal development and plasticity (Di Liegro et al., 2014). Precise temporal and spatial regulation of local translation is required for normal brain function. When this precision is interrupted it can have a devastating impact leading to learning disorders or disease. Several pathways and regulators are important to maintain the precision associated with local translation. Here, we will discuss some pathways involved in regulating local translation and when dysregulated the potential consequences. We will also discuss how future treatment options that regulate local translation may exist.

Homeostatic Plasticity

Homeostatic plasticity is defined here as an adaptive, compensatory mechanism to maintain neuronal excitability within an optimal range. It is important to note that several forms of homeostatic plasticity mechanisms have been reported (Lee et al., 2013). Here, we focus on how local translation can either compensate for or contribute to learning difficulties or disease states.

ERK and mTOR Signaling Pathways:
Local Translational Regulation

Both the extracellular signal-regulated kinase (ERK) and mammalian target of rapamycin (mTOR) pathways are known to promote local translation (Wang et al., 2010). mTOR is a serine/threonine kinase that promotes cap-dependent translation by phosphorylating p70 S6 kinase (S6K) and elF4E binding protein (4E-BP). In neurons, mTOR kinase is activated by the Ca^{2+}-dependent activation of PI3Kinase and has been found to be active in dendrites (Hoeffer and Klann, 2009; Tang et al., 2002). ERK is known to promote local translation by phosphorylating p90 ribosomal S6 kinase (RSK) and Ca^{2+}-dependent ERK activation can underlie both LTP and LTD (Gallagher et al., 2004; Kelleher et al., 2004; Merlin et al., 1998; Pende et al., 2004; Thiels et al., 2002). Thus, mTOR- and ERK-dependent, local protein synthesis has the unique advantage over somatic translation and protein trafficking by making available a rapid and spatially specific source of new proteins that can function to maintain homeostatic plasticity or when dysregulated can facilitate an imbalanced network.

One example of mTOR-dependent local translation mediating homeostatic plasticity is the reversal of cocaine-evoked synaptic plasticity which, with acute cocaine exposure, is initially characterized by a reduction in excitation. This is due to GluA2-containing AMPARs being exchanged for GluA2-lacking receptors and decreased NMDAR function. Over time mTOR-mediated local translation of GluA2-containing AMPARs allows for the synapse to reset back to its original channel composition and function (Mameli et al., 2007). Thus, local translation may function as a neuroprotectant against drug abuse by regulating homeostatic plasticity. It will be interesting to

determine if local translation may act to reset channel composition with acute exposure to other drugs of abuse. For example, mTOR activity has been shown to be protective against craniofacial defects observed in fetal alcohol spectrum disorders (FASD) (McCarthy et al., 2013).

Epilepsy

One example of how local translation may push the neuron into a hyperexcitable state is in the development of chronic epilepsy. Temporal Lobe Epilepsy (TLE) is characterized by an increase in hyperexcitability within the neocortex and hippocampal neuronal network and this is associated with a variety of molecular changes. Traumatic brain insult such as stroke or infection can result in the development of TLE and the kainate animal model of acquired epilepsy recapitulates the neuropathological damage observed in the human brain (Buckmaster et al., 1997; Hellier et al., 1998; Dudek et al., 2006).

It is well documented that the mTOR and ERK pathways are deregulated in epilepsy and mTOR specific blockade can reverse seizure activity suggesting that mTOR inhibition could have anti-epileptogenic action (Wong and Crino, 2012; Zeng et al., 2009). Autism Spectrum Disorders, such as Tuberous Sclerosis complex (TSC) and Fragile X Syndrome (FXS), where both the mTOR and ERK pathways are dysregulated, have a greater susceptibility to developing epilepsy (Potter et al., 2013; Stafstrom et al., 2012). This may be, in part, due to the local translation of plasticity related genes, such as Arc. Local translation of Arc in FXS has been shown to result in the internalization of AMPA receptors contributing to epileptic firing (Bianchi et al., 2009; Bramham et al.,

2008; Nakamoto et al., 2007; Stafstom et al., 2012). It will be interesting to further determine how regulation of RNA binding factors contribute to the local translation of receptors and channels involved in seizure development.

Voltage Gated Potassium Channel: Kv1.1

The six transmembrane voltage gated potassium channel, Kv1.1, is transcribed from the KCNA1 gene. Kv1.1 is evolutionarily conserved from the Shaker potassium channel in *Drosophila* to its mammalian orthologue (Papazian et al., 1987; Tempel et al., 1987; Tempel et al., 1988). Kv1.1 can control the frequency and duration of the action potential (Smart et al., 1998; Foust et al., 2011; Bucher and Goaillard, 2011; Debanne et al., 2011). There are several Kv1.1 channelopathies, including a null mutation which can result in epilepsy (Smart et al., 1998). Mutations in Kv1.1 can also result in type 1 episodic ataxia which is characterized by ataxia (disrupted muscle coordination) with or without myokymia (Browne et al., 1994).

RNA editing of Kv1.1 has been recently investigated in patients with temporal lobe epilepsy (TLE). RNA editing of Kv1.1 leads to an amino acid exchange of isoleucine for valine in the S6 segment of Kv1.1 mRNA (Hoopengardner et al., 2003). It was found that there is a negative correlation between RNA editing of Kv1.1 and the length of time from seizure onset (Krestel et al., 2013). In vitro studies have shown that increased Kv1.1 RNA editing results in less affinity of Kv1.1 to bind an inactivation subunit resulting in more outward K+ current with membrane depolarization (Bhalla et al., 2004). Therefore, decreased I/V editing may conceivably result in disrupted repolarization and contribute to observed hyperexcitability in TLE (Krestel et al., 2013).

Further elucidation of the effect of RNA editing on Kv1.1 function and possible contribution to TLE is also needed.

Kv1 channels are present in both axons and neuronal dendrites (Storm, 1988; Metz et al., 2007). Kv1.1 mRNA also localizes to neuronal dendrites where it undergoes local translation under the control of the PI3K/mTOR pathway (Raab-Graham et al., 2006). We have recently found that the mTOR mediated negative regulation of Kv1.1 local translation is dependent on the microRNA, miR-129, and Kv1.1 expression in dendrites is promoted by the RNA binding protein, HuD (Sosanya et al., 2013, Chapter 2). Kv1.1 KO mice also either die early or develop spontaneous seizures (Rho et al., 1999) and it has been shown that Kv1.1 overexpression following seizure onset can reverse established seizure activity (Wykes et al., 2012). Collectively, these findings have led us to consider the relationship of miR-129 and HuD to Kv1.1 expression and function in TLE (Chapter 3).

RNA Binding Factors: microRNAs and miR-129

microRNAs (miRNAs) bind to and result in reversible translational suppression and/or degradation of their mRNA targets (Djuranovic et al., 2012). miRNAs are first transcribed, either from an intron or regulated by its own specific promoter, to its pri-miRNA form. This primary miRNA transcript is cleaved to its pre-miRNA (~70 nt) form by the Drosha complex. Following nuclear export, the Dicer complex cleaves this transcript to the active mature miRNA (21-23 nt). Regulation of miRNA expression can occur at any of these stages of miRNA biogenesis. The mature miRNA is then loaded

onto the Ago-RISC complex where it will be targeted to specific mRNA binding sequences.

mTOR activity itself can be regulated by RNA binding factors, including small noncoding microRNAs. Recently, several factors of the PI3K/AKT signaling pathway, including mTOR and S6K2, have been shown to be direct targets of the miRNA, miR-193a-3p/5p, where their mRNA levels are significantly depressed by miR-193a (Yu et al., 2014).

Contextual conditioning and NMDA neuronal stimulation results in changes in certain miRNA levels in the hippocampal CA1, including miR-129, (Jeong Kye et al., 2011) suggesting a possible key role for miR-129 in learning and memory. Several of these miRNAs are possible regulators of the mTOR pathway and in particular miR-19b suppression increased PTEN levels resulting in decreased mTOR activity (Jeong Kye et al., 2011).

Currently, miR-129 has been extensively studied in several types of cancer cells suggesting that aberrant expression of miR-129 may be important in several different disease types (Dyrskjøt et al., 2009). It has previously been shown that in both colorectal and gastric cancer, methylation of the miR-129-2 promoter results in the decreased expression of miR-129-5p (Bandres et al., 2009; Shen et al., 2010). Little is known about miR-129 role in the brain including its function in TLE.

RNA Binding Proteins: HuD

RNA binding proteins (RBPs) are *trans*-acting factors that are essential to the correct spatiotemporal expression of numerous proteins that function in multiple

processes, including learning and memory. *Cis*-acting elements or structures direct specific RBPs to bind certain mRNA targets (Bronicki and Jasmin, 2013; Lukong et al., 2008; Carninci, 2010). HuD is part of the ELAVl/Hu family of RBPs which have multiple functions, including stabilization and translation of its mRNA targets in neurons (Jain et al., 1997; Brennan and Steitz, 2001; Hinman and Lou, 2008; Pascale and Govoni, 2012). Other functions include alternative splicing, alternative polyadenylation, and cytoplasmic shuttling (Bronicki and Jamin 2013). Characterization of certain HuD targets revealed the following sequence, X-U/C-U-X-X-U/C?-U-U/C, as a specific binding motif (Wang and Tanaka Hall, 2001). Appropriate regulation and protein expression may depend on a balance between binding to either destabilizing or stabilizing RBPs (Bronicki and Jasmin, 2013). This may be determined by the levels of the RBPs themselves but it may also be a function of which mRNA targets are present considering that destabilizing or stabilizing RBPs can bind the same target concurrently. This critical expression of certain mRNAs may be regulated by multiple processes, including mRNA degradation. mRNA degradation may be promoted by multiple processes itself, including binding by destabilizing RBPs that can result in mRNA deadenylation and degradation (Bronicki and Jasmin, 2014). Small noncoding microRNAs have also been shown to promote suppression of translation followed by mRNA degradation (Bronicki and Jasmin, 2014). HuD has been shown to bind longer poly(A) tails via its third RRM to promote cap-dependent translation (Fukao et al., 2009). It is possible that deadenylation may result in the inability of HuD to bind to a target bound by a destabilizing RBP. Another possibility which has been observed is that a

lack of mTOR activity can result in mRNA decay by an unknown mechanism (Sosanya et al., 2013).

HuD Regulation

HuD expression levels may be regulated by several mechanisms (Bronicki and Jasmin, 2013). Post-translational modifications of HuD is one such mechanism. Protein Kinase C (PKC) phosphorylation of HuD results in key localization and stabilization of its target, GAP-43 (Lim and Alkon, 2012; Pascale et al., 2005). Co-activator associated arginine methyltransferase 1 (CARM1) methylation of HuD inhibits its stabilization function of specific mRNAs (Bedford and Clarke, 2009; Fujiwara et al., 2006; Hubers et al., 2011). Recently, HuD has also been shown to be regulated by the miRNA, miR-375, and diminished mTOR activity results in decreased HuD expression (Abdelmohsen et al., 2010; Sosanya et al., 2013). Other mechanisms regulating HuD levels include transcriptional and post-transcriptional control (Bronicki and Jasmin, 2013). One of the targets of HuD is the microtubule binding protein, Tau, which has recently been shown to attenuate hyperexcitability in Kv1.1 KO mice (Holth et al., 2013).

Epilepsy: HuD

Several recent studies have analyzed the expression of HuD and its targets in both the kainate and pilocarpine models of TLE. HuD levels and several of its target mRNAs increase expression in both models and dendritic localization of HuD increases following seizure development (Bolognani et al., 2007; Tiruchinapalli et al., 2008;

Winden et al., 2011). Our lab has also observed an increased expression of HuD and its target, Kv1.1, 5 days following SE (Sosanya et al., unpub.)

microRNAs as Disease Biomarkers

Circulating microRNAs can remain in blood plasma, unlike their mRNA targets, due to the high stability of the Ago2-miRNA complex (Turchinovich et al., 2001). This raises the possibility of miRNAs as biomarkers for disease and diagnosis. Studies have shown that detection of certain circulating miRNAs can discriminate between certain cancers and healthy controls (Siddeek et al., 2014). Several microRNAs have been shown to be up- or down- regulated in the blood following certain injuries, including 24 hr following kainate induced seizures (Liu et al., 2009; Jimenez-Mateos and Henshall, 2013). It will be interesting to determine if miR-129 could be a potential disease marker for TLE to aid in determining possible disease progression and treatment.

TLE Treatment: microRNAs

Forty percent of TLE patients are resistant to current treatment (Sharma et al., 2007). MicroRNAs are playing an increasing role in several diseases including TLE. Recently, it has been reported that inhibition of a single microRNA, miR-134, was neuroprotective against damage from recurrent seizures (Jimenez-Mateos et al., 2012). Not surprisingly, microRNAs may have a significant effect on driving the molecular changes that occur immediately following status epilepticus (SE) as well as after the development of chronic recurring seizures. It is possible that miR-129 may regulate multiple targets in TLE and therefore knockdown of miR-129 would decrease seizure

activity by removing its suppressive effects on multiple targets. Knockdown of the microRNA, miR-134, in the CA3 region of the hippocampus prevented seizure activity, substantiating the idea that removing a single microRNA may have considerable effects on disease prevention due to its effect on multiple targets (Jimenez-Mateos et al., 2012).

Conclusion

Local translation is a fundamental process that can either help or hinder the progression of a disease. This is due to local translation underlying the expression of channels, receptors, and their key regulators, leading to either a stable or erratic neuron. Many neurological disorders are characterized by dysregulation of factors, RNA binding proteins and microRNAs, involved in regulating local translation, development, and plasticity. Regulatory balance is a requirement of any neurological system and these factors offer another area of potential targets for therapeutic intervention. We have only begun to understand how regulating RNA binding factors may prevent disease progression.

Chapter 2: Degradation of High Affinity HuD Targets Releases Kv1.1 mRNA from miR-129 Repression by mTORC1

Introduction

During learning and memory, neurons undergo changes in excitability to enhance their efficacy. One way to modulate neuronal excitability is through regulating the number and composition of ion channels expressed on the cell membrane (Kim and Hoffman, 2008; Zhang and Linden, 2003). Such regulation can be achieved through controlling the local translation of dendritic mRNAs to provide a rapid response to neuronal activity and ensure proper temporal and spatial expression. Our previous work has shown that the local dendritic translation of an ion channel, Kv1.1, mRNA is repressed by mTORC1 kinase activity (Raab-Graham et al., 2006).

Kv1.1 is a dendrotoxin-sensitive voltage-gated potassium channel that is phylogenetically related to the Shaker channel in *Drosophila* (Hopkins et al., 1994; Tanouye and Ferrus, 1985). Kv1.1 is characterized as a delayed rectifier potassium channel that controls the frequency of the action potential (Brew et al., 2003). Unlike many ion channels that have redundant functions, Kv1.1 is essential. Mice lacking Kv1.1 either die early or have frequent spontaneous seizures (Smart et al., 1998). Furthermore, haploid insufficiency leads to episodic ataxia, a human neurological disease caused by mutations in Kv1.1 (Zerr et al., 1998). While a dendrotoxin-sensitive Kv current has been described in CA1 pyramidal dendrites, the molecular identity of this current remains inconclusive (Chen and Johnston, 2010; Golding et al., 1999; Metz et al., 2007; Storm, 1988). Moreover, prior to our report describing NMDA/mTORC1-

mediated suppression of Kv1.1 local translation in dendrites, Kv1.1 was considered to be only expressed in axons of hippocampal neurons (Chen and Johnston, 2010; Geiger and Jonas, 2000; Monaghan et al., 2001; Raab-Graham et al., 2006; Schechter, 1997; Southan and Owen, 1997). Here we report the molecular mechanism for the regulation of dendritic Kv1.1 mRNA translation.

Mammalian Target of Rapamycin (mTOR) is a ubiquitous serine/threonine kinase that forms two unique complexes, mTOR complex 1 (mTORC1) and mTOR complex 2 (mTORC2). mTORC1 kinase promotes cap-dependent translation via phosphorylation of S6K and 4E-BP, molecules critical for translational initiation. In neurons, mTORC1 kinase is activated by its upstream effectors, including neuronal receptors such as N-methyl-D-aspartate receptors (NMDAR) through the signaling molecules PI3K, Akt, and tuberous sclerosis complex proteins 1 and 2 (Tsc1/2) (Costa-Mattioli et al., 2009; Klann and Dever, 2004; Raab-Graham et al., 2006). Electrophysiological studies have shown that mTORC1 kinase activity is required for long-term depression (LTD) and late long-term potentiation (L-LTP) (Hoeffer and Klann, 2010; Ronesi and Huber, 2008; Volk et al., 2007). These persistent changes in excitatory neurotransmission have been widely accepted as a model for the cellular basis for learning and memory (Bliss and Lomo, 1973).

While mTORC1 kinase-dependent translational activation is well studied, how selective mRNAs undergo translational repression when mTORC1 kinase is active remains unclear. Translational repression can be achieved by mRNA binding molecules such as microRNAs (miRNAs) or RNA-binding proteins. miRNAs are ~18-25 nucleotide long, noncoding RNAs that bind to their target sequences in the 3' untranslated region

(UTR) of mRNAs, resulting in reduced protein expression via translational silencing or mRNA degradation (Bartel, 2009; Filipowicz et al., 2008a; Konecna et al., 2009; Kosik, 2006).

How mRNA repression is relieved to mediate bidirectional protein expression in an activity dependent manner is an important question. It was first hypothesized that miRNAs could directly or indirectly affect RNA-binding proteins ability to interact with their mRNA targets (George and Tenenbaum, 2006). Since then a growing body of evidence suggests that RNA-binding proteins can displace miRNAs from their target mRNAs even when the binding sites are located many nucleotides apart (Kundu et al., 2012; Meisner and Filipowicz, 2011; Srikantan et al., 2012; Xue et al., 2013).

Here we report the identification of a miRNA, miR-129, and a RNA-binding protein, HuD, both of which reversibly bind Kv1.1 mRNA when mTORC1 kinase is active and inactive, respectively. Using a local translation assay, we determined that removal of the miR-129 site releases the mTORC1 dependent repression of Kv1.1 mRNA translation. Furthermore, we provide evidence suggesting that HuD high affinity mRNA targets, such as CaMKIIα, GAP-43, and Homer1a, are degraded when mTORC1 is inhibited, allowing HuD to switch targets and overcome miR-129 repression of Kv1.1 mRNA.

Results

mTORC1 Kinase Activity Does not Affect Kv1.1 mRNA Levels

Previously, we have shown that mTORC1 kinase activity in cortical and hippocampal neurons suppresses the local protein synthesis of Kv1.1 mRNA in neuronal dendrites (Raab-Graham et al., 2006). When mTORC1 kinase activity is inhibited by its specific inhibitor, rapamycin, a significant increase in dendritic Kv1.1 protein is observed (Figure 2.1A; (Raab-Graham et al., 2006)). To determine the molecular mechanism for the change in Kv1.1 expression in dendrites we first assessed if there were corresponding changes in mRNA levels with mTORC1 activity. In cultured neurons (21 – 28 days in culture), mTORC1 kinase is phosphorylated and thus constitutively active (Figure 2.1A). Synaptoneurosomal (SN) preparation was checked for purity by western blot and immunostaining with nuclear marker (Figure S2.1A). Treatment with rapamycin inhibits mTORC1 kinase activity by reducing the active p-mTOR over total mTOR ratio to 59.20±4.67% and leads to a ~2 fold increase in Kv1.1 protein (Figure 2.1A; Kv1.1: DMSO 1.00±0.18; Rapa 2.00±0.26; (Raab-Graham et al., 2006). We next examined the mRNA levels in SN isolated from cortical neurons treated with rapamycin or carrier (DMSO) by quantitative real-time polymerase chain reaction (qPCR). The representative gel indicates the amplification of a specific Kv1.1 product for each condition (Figure 2.1B, above). Independent of mTORC1 kinase activity, the mRNA level remains constant (Figure 2.1B, bar graph), suggesting a mechanism of altered translation rather than changes in mRNA transport or degradation.

Kv1.1 3'UTR Is Required for mTORC1 Kinase-dependent Translational Repression

To investigate the molecular mechanism of such translational repression, we first searched for potential regulatory sequences in Kv1.1 mRNA that confer mTORC1 kinase-sensitive repression (Raab-Graham et al., 2006). Previously, we showed local translation of Kv1.1 when mTORC1 kinase is inhibited by blocking *N*-Methyl-D-aspartate receptors (NMDAR) or by the mTORC1 specific inhibitor rapamycin using the construct containing the coding region (CR) plus the 230 nucleotide (nt) 3'UTR of Kv1.1, cloned from synaptoneurosomal cDNA (Raab-Graham et al., 2006). Based on this finding, we hypothesized that a putative mTORC1 kinase repression sequence (mTRS) was present within this 3'UTR.

To verify the importance of the mTRS for Kv1.1 translation in neurons, we designed a competition assay in which excess 3'UTR was introduced to compete for the binding of factors that suppress endogenous Kv1.1, thus resulting in increased Kv1.1 expression (Figure S2.1). Exogenous 3'UTR containing the putative mTRS was introduced into neurons by a Sindbis virus coding for the fluorescent protein Kaede (Ando et al., 2002) fused to the 3'UTR. To control for nonspecific effects due to viral infection, neurons were infected with virus coding for Kaede fused to the dendritic targeting sequence (DTS) of MAP2 (Figure 2.2B; morphological similarity between neurons is demonstrated in Figure S2.1B; (Blichenberg et al., 1999)). The level of surface Kv1.1 protein was determined by immunocytochemistry on non-permeabilized neurons using an antibody that recognizes the extracellular domain of Kv1.1 (Raab-Graham et al., 2006; Tiffany et al., 2000). As expected, excess 3'UTR containing the

putative mTRS of Kv1.1 mRNA released endogenous Kv1.1 mRNA from repression, resulting in a ~5 fold (5.41±0.99) increase in Kv1.1 surface protein expression in the dendrites as determined by signal intensity of punctate structures with no significant change in the soma (Figure 2.2B; Figure S2.1C). Such an increase is comparable to the levels observed when mTORC1 kinase is inhibited by rapamycin, and excess mTRS does not further increase Kv1.1 expression in rapamycin treated neurons (Figure 2.2B). Collectively, these data suggest that the putative mTRS within the 3'UTR is required for repressing Kv1.1 translation in an mTORC1 kinase-sensitive manner.

miR-129 Binds Kv1.1 mRNA in an mTORC1 Kinase-dependent Manner

Notably, sequence alignment of the 3' UTR containing the mTRS with other mammalian Kv1.1 UTRs revealed a conserved binding site (or seed match sequence) for the microRNA, miR-129 (Figure 2.3A). Consistent with Kv1.1 mRNA levels remaining constant with changes in mTOR activity, the complementary of the miR-129 binding site to the 3' UTR sequence is considered to be weak, favoring a role in translational repression over degradation (Filipowicz et al., 2008). To determine if miR-129 binds to Kv1.1 mRNA and perhaps mediates the mTOR dependent-repression, we utilized an RNA affinity capture system (Kuwano et al., 2008). RNA was synthesized by *in vitro* transcription of cDNAs coding for Kv1.1: full-length (FL; coding region + 3'UTR), coding region (CR), or full-length with the predicted miR-129 binding site (seed match sequence) mutated to the complementary sequence (ΔmiR-129) (Figure 2.3B, above). The purified RNAs were then labeled with a biotin-linked oligonucleotide and served as bait to pull down binding factors from neuronal lysates harvested from cultured cortical

neurons treated with DMSO or rapamycin. Factors that bound to Kv1.1 RNA were then precipitated with streptavidin-coated magnetic beads and examined by qPCR for the presence of miR-129 (Figure S2.2A).

When mTORC1 kinase is active and Kv1.1 mRNA translation is suppressed, miR-129 was bound to the full-length RNA (Figure 2.3B, bar graph). As a negative control, the RNA affinity capture assay was carried out using *in vitro* synthesized RNA encoding the coding region alone (CR) or the full-length RNA with a mutated miR-129 binding site (ΔmiR-129). As expected, miR-129 binding was significantly reduced under both control conditions relative to the binding of the full-length RNA (CR: 11±9%, DMSO; ΔmiR-129: 6±5%, DMSO). However, when mTORC1 kinase was inhibited with rapamycin, miR-129 binding to the full-length RNA was reduced to 45±15% (Figure 2.3B). This level was not different from the background binding detected by the two constructs missing the miR-129 seed match sequence. Melt curve analysis was performed to verify that one product was amplified for miR-129 with a signature melting temperature determined by the input (Figure S2.2B). Similar to what we observed in cultured neurons, using solubilized synaptoneurosomes isolated from rat cortices, the full-length RNA bound significantly more miR-129 than the coding region RNA (52±1% relative to full-length; Figure S2.2C). These results suggest that miR-129 binds to the 3'UTR of Kv1.1 mRNA when mTORC1 kinase is active.

miR-129 Knockdown in Neurons Increases Kv1.1 Expression

We next examined the effect of miR-129 on Kv1.1 expression in neurons by transfecting a locked nucleic acid (LNA) probe complementary to miR-129 to knock

down (KD) its level in neurons. Total Kv1.1 protein was then determined by immunocytochemistry. The protein levels of another dendritic potassium channel, Kv4.2, were determined as a control. The effectiveness of miR-129 knockdown was established in cortical neurons showing a reduction in miR-129 levels by northern blot and an increase in the published miR-129 target, ERK2 (Figure S2.2D; (Wu et al., 2010)). If miR-129 suppresses the translation of Kv1.1 in dendrites, then knocking down miR-129 will increase the expression of Kv1.1. Indeed, we observed a significant 2-3 fold increase in signal intensity of Kv1.1 punctate structures in dendrites when miR-129 was knocked down compared to the negative EGFP or the scrambled LNA controls (Figure 2.3C, miR-129 KD vs. EGFP, 2.95±0.3; miR-129 KD vs. Scrambled LNA, 1.9±0.12, Figure S2.2E). Moreover, there was no change in Kv1.1 intensity in the cell body when miR-129 was knocked down (Figure S2.2E). Furthermore, no significant change was observed in dendritic staining for Kv4.2 (Figure 2.3D and S2.2E). These data suggest that miR-129 suppresses the translation of Kv1.1 mRNA in neuronal dendrites.

Overexpression of miR-129 Represses Kv1.1 mRNA Translation When mTORC1 Kinase is Inhibited

To test whether miR-129 mediates repression of Kv1.1 mRNA translation when mTORC1 kinase is active, we transduced neurons with a lentivirus coding for a precursor form of miR-129 (pre-miR-129-2). We predicted that increasing the level of miR-129 would mimic mTORC1 repression of Kv1.1 mRNA translation and thus prevent the increase in dendritic Kv1.1 expression when mTORC1 kinase is inhibited. Indeed,

overexpression of miR-129 prevents the observed increase in Kv1.1 dendritic protein with rapamycin, maintaining levels similar to the mTORC1 kinase active state (Figure 2.3E, Figure S.22F). These data suggest that miR-129 binding to Kv1.1 mRNA is necessary for repressing Kv1.1 translation when mTORC1 is active.

Repression of Local Protein Synthesis of Kv1.1 mRNA in Neurons is Relieved When the miR-129 Binding Site is Mutated

To further test the functional role of miR-129 in the regulation of Kv1.1 mRNA translation, we performed a local translation assay using Kaede fused to Kv1.1 as a translational reporter (Raab-Graham et al., 2006). Kaede is a fluorescent protein that changes color from green to red upon UV-induced photoconversion (Ando et al., 2002). To assess new protein synthesis, pre-existent Kaede-fused protein is first photoconverted to red, and newly synthesized green protein can thus be monitored and quantitated over time. Neurons expressing Kaede-Kv1.1 mRNA with either intact mTRS or with the predicted miR-129 binding site (seed match) sequence mutated (ΔmiR-129) were imaged for two hours after complete photoconversion. Detection of new “green” Kaede-Kv1.1 indicates Kv1.1 mRNA translation (Raab-Graham et al., 2006). Previously, we have shown that Kv1.1 protein appears in hot spots within the dendrite when mTORC1 kinase is inhibited. Furthermore, Kv1.1 was found to remain stationary within these hot spots. Transport rates were measured to be less than 15 µm per hour (Raab-Graham et al., 2006). Based on these data, we analyzed only new green Kaede-Kv1.1 puncta greater than 60 µm from the cell body to ensure all new protein was locally synthesized.

Z-stack images detecting the green signal were acquired over time and pseudocolored to reflect the signal intensity of newly synthesized green Kaede-Kv1.1 protein. As shown in Figure 2.4, mutating the miR-129 site in the 3'UTR of Kv1.1 mRNA results in an increase in Kv1.1 local mRNA translation by ~ 200% (215.1± 22.57%) when mTORC1 kinase was active, similar to the signal observed in neurons expressing Kaede-Kv1.1 with an intact miR-129 site when mTORC1 kinase is inhibited with rapamycin. Furthermore, in the absence of the miR-129 site, rapamycin treatment did not result in further increased translation, suggesting that the miR-129 binding site is the mTOR repressive sequence.

Binding of miR-129 Leads to Repression Rather than Degradation of Kv1.1 mRNA in Neuronal Dendrites

MicroRNAs have reported roles in both the repression and the degradation of their target mRNAs (Fabian et al., 2010). To verify that miR-129 represses translation without altering mRNA stability, we performed an *in situ* hybridization using an antisense oligo against EGFP (Raab-Graham et al., 2006; Wells et al., 2001) on neurons expressing EGFP fused to Kv1.1 with either an intact or mutated miR-129 binding site (Figure 2.5). If miR-129 binding leads to the degradation of Kv1.1 mRNA, we would predict that more RNA will be detected with the removal of the miR-129 binding site. However, if miR-129 binding represses Kv1.1 mRNA without degradation, then removal of the miR-129 site will lead to increased protein expression without altering mRNA levels. As expected, the overall RNA steady-state levels were the same between the two sets of neurons (FL, 1.0±0.06; ΔmiR-129, 1.1±0.06; Figure S2.3A),

whereas more protein was detected in the dendrites expressing Kv1.1 with the mutated sequence, as indicated by the ratio of EGFP/in situ hybridization signal (Figure 2.5 and Figure S2.3B: FL, 1.0±0.06; ΔmiR-129, 1.4±0.09). Considering that Kv1.1 mRNA level remains constant independent of mTORC1 kinase activity (Figure 2.1B) and that mutation of the miR-129 binding site does not change mRNA stability, these data thus support a mechanism of microRNA-mediated repression over degradation.

HuD Binds Kv1.1 mRNA when mTORC1 Kinase is Inactive and Overrides mTORC1 Kinase-dependent Repression

During neuronal transmission, signaling through the NMDA-R via the PI3K/mTORC1 pathway represses Kv1.1 mRNA translation. Although such translational repression of Kv1.1 may lead to increased excitability and provide an important positive feedback mechanism for learning and memory, homeostatic mechanisms that lower the membrane potential are required to maintain neuronal stability and allow new learning to occur (Davis and Goodman, 1998; Turrigiano and Nelson, 2000). Since we identified miR-129 as the translational repressor of Kv1.1 mRNA when mTORC1 kinase is active, how inactivating mTORC1 kinase with rapamycin releases such translational repression became the next question.

We first asked whether miR-129 levels would decrease upon rapamycin treatment, thus limiting the amount available to repress translation. To test this possibility, we performed qPCR to detect miR-129 in synaptoneurosomal RNA isolated from neurons where mTORC1 kinase was active (control, DMSO) or inhibited by rapamycin. Contrary to our prediction, we did not observe a significant change in miR-

129 levels between control and rapamycin treated neurons as determined by both RT-qPCR and northern blot (Figure 2.6A).

An alternative possibility is that additional factor(s) interact with Kv1.1 mRNA to relieve repression and promote translation when mTORC1 kinase is inhibited. We therefore searched for RNA-binding proteins that bind Kv1.1 mRNA in an mTORC1 kinase-sensitive manner. To find such candidates, we performed a bioinformatic scan for known binding sites for RNA-binding proteins within the full-length Kv1.1 mRNA. We identified 3 putative HuD-binding sites in the coding region of Kv1.1 mRNA (Figure S2.4A), consistent with a HuD binding motif previously reported by Wang and Tanaka-Hall (x-U/C-U-x-x-U/C-U-U/C; Figure S2.4A; (Wang and Tanaka Hall, 2001)). The Hu family of RNA-binding proteins has an established role in stabilizing mRNAs, promoting translation, and has been shown to be important for dendritic protein synthesis (Antic et al., 1999; Bolognani and Perrone-Bizzozero, 2008; Fukao et al., 2009; Tiruchinapalli et al., 2008). Moreover, similar to inhibiting mTORC1 kinase with rapamycin to prevent consolidation, mice that overexpress HuD have deficits in learning and memory (Bolognani et al., 2007).

To verify the predicted binding of HuD to Kv1.1mRNA, coimmunoprecipitation (co-IP) of transfected HEK cells was used to assess if HuD binds directly to Kv1.1 mRNA. HEK cells were co-transfected with myc-tagged HuD plus either Kaede-Kv1.1 full-length, Kaede-Kv1.1 coding region, or Kaede-Kv1.1 ΔmiR-129. mRNA protein complexes (mRNPs) containing HuD were immunoprecipitated from lysates using a myc specific antibody. Bound Kv1.1 mRNAs were then detected by RT-PCR using Kv1.1 specific primers. To control for antibody specificity, HEK cells were transfected

with Kaede-Kv1.1 and an empty vector without myc-HuD. We also included a negative control for nonspecific PCR amplification using myc-HuD and Kaede alone. As expected, Kaede-Kv1.1 full-length, coding region, and ΔmiR-129 mRNA all copurified with HuD protein (Figure 2.6B). This result is consistent with the predicted HuD binding elements found within the coding region of Kv1.1 mRNA (Figure S2.4A). Additionally, Kv1.1 specific PCR products were only detected from RNA immunoprecipitated from lysates expressing HuD and Kv1.1 (Figure 2.6B). Collectively, these results suggest that HuD binds to the coding region of Kv1.1 mRNA. A similar mechanism was recently shown for another member of the Hu protein family, HuR, which was found to displace miRISCs from target mRNAs even when its binding site and the miRNA site were not adjacent (Kundu et al., 2012).

A direct prediction of this hypothesis is that increasing HuD protein when mTORC1 kinase is active will overcome miR-129 mediated repression of Kv1.1 mRNA. To test this, we overexpressed HuD in cultured hippocampal neurons and measured dendritic Kv1.1 protein. Figure 2.6C shows that under conditions where mTORC1 kinase is active, neurons overexpressing HuD show a significant 3-4 fold (3.7±0.41) increase of Kv1.1 punctal intensity in dendrites with no significant change in Kv1.1 levels in the cell body (Figure S2.4B). Kv4.2 signal is not affected by HuD overexpression. This increase in Kv1.1 punctal signal is specifically inhibited by the presence of the well characterized protein synthesis inhibitor cycloheximide (0.3±0.04). Notably, cycloheximide further decreases the levels of both Kv1.1 and Kv4.2 relative to the control condition, indicating a decrease in basal translation (Kv1.1, 0.3±0.04; Kv4.2,

0.4±0.05). These results suggest that overexpression of HuD overrides mTORC1 kinase/miR-129 dependent repression of Kv1.1 mRNA translation.

We next tested whether HuD binding to Kv1.1 mRNA is altered with mTORC1 kinase activity. Purified GST-HuD fusion protein was incubated with total RNA isolated from carrier DMSO or rapamycin treated neurons and immunoprecipitated with a pan Hu antibody (Deschenes-Furry et al., 2007). Bound Kv1.1 mRNAs were then detected by RT-PCR with gene specific primers. GAP-43 and CaMKIIα mRNAs, known targets of HuD (Bolognani et al., 2010; Bolognani et al., 2006; Tiruchinapalli et al., 2008), were also assayed in parallel as controls. The differential binding of HuD with different mTORC1 activity to the three mRNAs assayed is reflected by the quantified ratio of mRNA pulled down in rapamycin over DMSO, as shown in Figure 2.6D (Note: a ratio of one indicates equal binding under both conditions, a ratio greater than one favors binding in the presence of rapamycin, a ratio less than one favors binding in DMSO). Interestingly, HuD only binds to GAP-43 mRNA in neurons treated with DMSO (Figure 2.6D, rapamycin/DMSO ratio significantly smaller than 1, one sample t-test, $p<0.05$) whereas HuD binds CaMKIIα mRNA under both conditions (Figure 2.6D, rapamycin/DMSO bound ratio = 1.4 ± 0.4 S.D. and was not considered significant from 1 by a one-sample t-test). In contrast, HuD only binds Kv1.1 mRNA in neurons treated with rapamycin (Figure 2.6D, with a ratio 8.6 ± 0.7 S.D., one sample t-test, $p<0.05$). The result that HuD only binds Kv1.1 mRNA in neurons treated with rapamycin supports a role for HuD in promoting Kv1.1 mRNA translation when mTORC1 is inhibited.

HuD Binding to Kv1.1 mRNA Coincides with the Reduced Level of Other HuD Target mRNAs

We next asked whether HuD protein levels increase with mTORC1 kinase inhibition which could lead to enhanced dendritic Kv1.1 levels. Western blot analysis using a HuD specific antibody was carried out on DMSO or rapamycin treated synaptoneurosomes. Contrary to what we expected, HuD levels significantly decrease when mTORC1 was inhibited (DMSO: 1.00±0.06; Rapa: 0.63±0.09; Figure 2.7A).

We then considered the possible relationship between mTORC1 activity and the abundance of other HuD targets. Notably in Figure 2.6D, the total input of the high affinity HuD target CaMKIIα with 32 predicted binding sites, some of which overlap (Bolognani et al., 2010), appears to be reduced when mTORC1 kinase is inhibited with rapamycin. To verify this observation in a quantitative manner, we performed RT-qPCR for CaMKIIα and Kv1.1 mRNAs by isolating total RNA from neurons treated with DMSO or rapamycin. As expected, CaMKIIα mRNA was reduced by ~70% when mTORC1 kinase was inhibited with rapamycin (rapamycin, 33.6±12.5% of control). Furthermore, when we assessed the relative abundance of two additional HuD targets, GAP-43 and Homer1a, we found they were both reduced by ~40% and were significantly different from control (GAP-43: rapamycin, 58.9±14% of control; Homer1a: rapamycin 59±12% of control; Figure 2.7B). In contrast, Kv1.1 mRNA levels remained the same between the two conditions (Kv1.1: rapamycin 89±27% of control; Figure 2.6D, input and Figure 2.7B). Moreover, the reduction of CaMKIIα mRNA is also reflected by the reduced protein level when mTORC1 kinase is inhibited (Figure 2.7C). Collectively, these data

led us to consider the possibility that HuD switches its targets in accordance with the mRNAs that are available to be translated.

To determine whether mTORC1 activity affects high affinity HuD target mRNAs levels at the transcriptional level or causes mRNA degradation, we treated neurons with the transcriptional inhibitor actinomycin for four hours prior to inhibiting mTORC1 activity with rapamycin and determined the mRNA levels of CaMKIIα. We predicted that if mTORC1 activity regulates the transcription of CaMKIIα, then pretreatment with actinomycin will reflect the same changes in mRNA levels as observed with rapamycin treatment alone. However, if inhibition of mTORC1 kinase activity by rapamycin promotes the degradation of CaMKIIα mRNA, rapamycin treatment in the presence of a transcriptional inhibitor will further decrease the amount of CaMKIIα mRNA. As shown in Figure 2.7D, quantitative PCR analysis of CaMKIIα mRNA levels showed a reduction by 61% (actinomycin, 100±0.9%; actinomycin+rapamycin, 39 ±18.3%) in neurons treated with both actinomycin and rapamycin relative to actinomycin alone, supporting CaMKIIα mRNA degradation over altered transcription upon mTORC1 inhibition (Figure 2.7D).

Overexpression of CaMKIIα UTRs Prevents the Increase in Dendritic Kv1.1 Protein when mTORC1 Kinase is Inhibited

If HuD binding to Kv1.1 mRNA requires the degradation of high affinity targets such as CaMKIIα mRNA, overexpression of CaMKIIα mRNA containing several HuD binding sites may affect the dendritic expression of Kv1.1 protein. We tested this prediction by overexpressing GFP-fused UTRs of CaMKIIα (5'UTR-GFP-3'UTR of CaMKIIα) (Aakalu et al., 2001) in neurons and measured the resulting dendritic Kv1.1 protein levels. The overexpressed CaMKIIα 3' UTR is predicted to carry 8 overlapping

HuD binding sites (Figure S2.4C). The ability of HuD to promote translation of this construct was first tested in HEK cells. Coexpression of HuD and GFP-CaMKIIα UTRs demonstrated a functional interaction by increasing the expression of GFP by ~3 fold over GFP-CaMKIIα UTRs alone (vector only control, 1.00±0.26; HuD, 3.24±0.59; Figure S2.4D). We then tested whether providing excess CaMKIIα UTRs for HuD binding in neurons will prevent the observed increase in Kv1.1 protein with mTORC1 kinase inhibition. Indeed, dendritic Kv1.1 protein levels no longer increased with rapamycin treatment in the presence of excess CaMKIIα UTRs (Figure 2.8A, GFP+DMSO, 1.00±0.12; GFP+rapamycin, 1.58±0.11; CaMKIIα UTRs+DMSO, 1.13±0.14; CaMKIIα UTRs+rapamycin, 0.88±0.11). To verify that repression of Kv1.1 mRNA translation with excess CaMKIIα UTR in the presence of rapamycin is due to HuD binding this construct, we removed the predicted HuD binding sites within the 3' UTR (CaMKIIα UTRΔHuD) by PCR based deletion. Indeed, with mTORC1 inhibition, dendritic Kv1.1 protein expression was restored and insensitive to overexpression of CaMKIIα UTRΔHuD relative to neurons expressing CaMKIIα UTR (Figure 2.8B, CaMKIIα UTRs +DMSO, 1.00±0.09; CaMKIIα UTRs +rapamycin, 1.36±0.11; CaMKIIα UTRsΔHuD +DMSO, 1.24±12; CaMKIIα UTRsΔHuD +rapamycin, 2.48±0.21). These results suggest that CaMKIIα and Kv1.1 mRNAs compete for HuD binding enabling translation. Collectively, our results support the hypothesis that mTORC1 kinase affects Kv1.1 mRNA translation by changing the availability of HuD via degradation of other high affinity HuD target mRNAs.

Discussion

Reversible binding of RNA-binding Factors to Kv1.1 mRNA with mTORC1 Activity Regulates Dendritic Expression of Kv1.1

mTORC1 regulation of Kv1.1 mRNA translation provides an example for how RNA-binding factors may determine the bidirectional expression of dendritic ion channels. As depicted in Figure S2.5, our findings support a model where the levels of Kv1.1 expression can be titrated by the interplay between mTORC1 kinase-dependent reversible binding of miR-129 and HuD to Kv1.1 mRNA. We have provided several lines of evidence demonstrating the repressive role of miR-129. We found that miR-129 binds to Kv1.1 mTRS only when mTORC1 kinase is active and knocking down miR-129 in neurons increases Kv1.1 expression in dendrites; whereas overexpressing miR-129 prevents the rapamycin dependent increase in dendritic Kv1.1. Consistent with these results, mutating the miR-129 binding site released the local translation of Kv1.1 mRNA from mTORC1 kinase mediated repression. All these data suggest that NMDAR activation (Raab-Graham et al., 2006) and mTORC1 kinase signaling may lead to a positive feedback mechanism that reduces the expression of Kv1.1 channels via miR-129, perhaps rendering the dendrite more excitable (Figure S2.5, left dendrite).

A major concern of a positive feedback loop is that if left unchecked it will lead to neuronal instability and prevent further acquisition of new information (Turrigiano and Nelson, 2000). Our findings support a homeostatic mechanism to possibly reduce dendritic excitability by increasing Kv1.1 mRNA translation via the RNA-binding protein,

HuD. We found that expression of dendritic Kv1.1 is determined by mTORC1 kinase-dependent availability of HuD for Kv1.1 mRNA in the dendrite. We show that HuD binds to high affinity mRNA targets, such as CaMKIIα mRNA, when mTORC1 kinase is active. Those mRNAs degrade when mTORC1 kinase is inhibited, thus releasing HuD to bind to the coding region of Kv1.1 mRNA and possibly releasing miR-129-containing miRISC from the 3' UTR of this mRNA. Furthermore, neurons overexpressing HuD show protein synthesis-dependent increase of Kv1.1 expression. We thus propose that HuD binds to Kv1.1 mRNA when mTORC1 kinase is inhibited and promotes its translation (Figure S2.5, right dendrite). Collectively, our results suggest that mTORC1 kinase serves as a molecular switch for bidirectional changes in dendritic expression of Kv1.1.

One surprising and novel finding from our data is that mTORC1 kinase activity affects the degradation of high affinity HuD mRNA targets, such as CaMKIIα, GAP-43 and Homer1a, instead of affecting miR-129 or HuD levels to favor Kv1.1 mRNA binding. In yeast, rapid degradation of some mRNAs, but not all, has been reported with nutrient limitation or TORC1 kinase inhibition by accelerating the deadenylation-decapping pathway (Albig and Decker, 2001). To our knowledge, our study is the first example of mRNA degradation serving as a way to recycle RNA-binding factors and thus promote the translation of other targets. Consistent with a recycling mechanism, overexpression of CaMKIIα UTRs occludes the increase in dendritic Kv1.1 protein in rapamycin treated neurons. Furthermore, with mTORC1 inhibition, CaMKIIα UTRs with the HuD binding sites removed rescued this reduction of endogenous dendritic Kv1.1. Our results thus suggest that changing the local availability of the regulatory factors may provide a rapid

and spatially restricted response, therefore bypassing the need for new transcription or translation of those factors.

miR-129 and HuD may be Important Regulators of Memory and Disease mediated by mTORC1 activity

The importance of miRNAs in neuronal development and plasticity is emerging (Kosik, 2006; Schratt, 2009). miR-129 has been identified to be specifically enriched in the brain (Kim et al., 2004; Landgraf et al., 2007; Miska et al., 2004); however, its role in neuronal function has not been identified. Our data reveal that miR-129 represses the expression of Kv1.1 when mTORC1 is active, which may partially contribute to the increased risk for seizures in disease states with hyperactive mTORC1 kinase (Sahin, 2012; Sharma et al., 2010; Zeng et al., 2009).

The discovery of mTORC1 mediated switching of HuD binding targets provides clues for the importance of mTORC1 in memory. As memory requires both the induction of positive regulators, (such as CaMKIIα that can enhance synaptic strength), and the removal of negative constraints (Abel et al., 1998), (such as potassium channels that can dampen action potentials), translational control of those regulators by HuD via mTORC1 mediated mRNA degradation is thus conceivably important for memory. Our findings may thus explain why HuD has been found to be important for memory (Bolognani et al., 2004; Pascale et al., 2004), but overproduction of HuD in transgenic mouse led to memory deficits (Bolognani et al., 2007). In other words, the physiological role of HuD may be determined by the ratio of available high to low affinity targets such as CaMKIIα and Kv1.1, respectively.

Since hundreds of dendritic mRNAs have been identified (Martin and Zukin, 2006) and Kv1.1 was the first example of a voltage-gated ion channel being locally translated (Raab-Graham et al., 2006), other mRNAs that are critical to site-specific changes in dendritic excitability may utilize the same mechanism to regulate their local translation. Our study may thus lead to the future discovery of other functionally related mRNAs suppressed by mTORC1 kinase activity. Moreover, Kv1.1, miR-129, and HuD may serve as important targets and/or biomarkers for mTORC1 kinase-related diseases such as epilepsy, Fragile X Syndrome, Tuberous sclerosis complex and Alzheimer's disease (Richter and Klann, 2009; Sharma et al., 2010).

Materials and Methods

Antibodies Used

Primary antibodies: mouse anti-NeuN (1:500, Millipore), mouse anti-Kv1.1 extracellular, 1:1000 (Neuromab 75-105), mouse anti-Kv1.1, 1:1000 (Neuromab 75-007), mouse anti-Kv4.2 (Neuromab 75-016), rabbit anti-Kaede, 1:500 (MBL PM012), rabbit anti-Phospho mTOR, 1:500 (Cell Signaling 2971S), mouse anti-tubulin, 1:1000 (Sigma-Aldrich T6074); rabbit anti-HuD, 1:1000 (Millipore AB5971; epitope: 26-42 nt), rabbit anti-ERK2, 1:1000 (Cell Signaling Technology, 9108S) rabbit anti-myc 1:150 (Sigma-Aldrich c3956), rabbit anti-GFP 1:1000 (Abcam ab6556), rabbit anti-HuD (Santa Cruz, sc-25360, for GST pulldown). Western blot signals were detected by secondary antibodies conjugated to HRP (1:1000, Jackson labs) for chemilluminescence or IR conjugated

secondary antibodies (1:5000, IR680; 1:5000, IR800) for Licor Infrared Imaging system. For immunostaining, secondary antibodies conjugated to either Alexa-488 (1:400, Invitrogen), Cy3 (1:500, Jackson labs), Alexa 647 (1:200, Invitrogen) or Cy5 (1:200, Jackson labs) were used.

Preparation of Primary Cultured Neurons

Primary neurons were prepared as previously described (Ma et al., 2002). Briefly, cortices from E18-19 rats were collected, dissociated, and plated. Neurons were plated at densities of 15 million neurons/100 mm dish for affinity RNA capture experiments, 2 million/35 mm well for western blot and qPCR, 400,000 neurons/12 mm coverslip for imaging in figure 2.2 and 200,000 neurons/12 mm coverslip for imaging in figure 2.3.

Isolation of Synaptoneurosomes (SN) and neuronal lysates

SN were isolated by a modified method as previously described (Quinlan et al., 1999). Briefly, neurons were harvested in buffer B (20 mM HEPES, pH 7.4, 5 mM EDTA, pH 8.0, protease inhibitor cocktail (Complete, Roche), phosphatase inhibitor, RNase inhibitor Superase-In (Ambion) or RNaseOut (Invitrogen) at 40 units/ml) and homogenized. After pelleting nuclei and unbroken cells at 80x g for 10 min, the supernatant was filtered first through a sterile 100 μm nylon filter followed by a 5 μm filter. SN was pelleted at 14,000xg for 20 min. For mRNA quantification, total RNA was isolated using RNeasy columns as outlined by the manufacturer (Qiagen). For miRNA experiments, total RNA was isolated using TRI Reagent (Applied Biosystems). For RNA

affinity capture, SN pellet was solubilized with RIPA buffer (150 mM NaCl, 10 mM Tris, pH 7.4, 0.1% SDS, 1% Triton X-100, 1% deoxycholate, 5 mM EDTA supplemented with protease inhibitor cocktail tablet and RNase inhibitor) at 4°C overnight and centrifuged at 55,000xg for 1 hour to remove any insoluble aggregates. For neuronal lysates, DIV21 cultured cortical neurons were harvested, homogenized and centrifuged similarly as SN without further filtrations or centrifugation. The supernatant after removing P1 pellet was collected and used for RNA affinity capture experiments.

Measure SN purity

Prior to SN preparation, an aliquot was removed and served as total lysate. Total and concentrated SN was smeared directly onto glass slides, fixed, permeabilized and then stained using DAPI (1:1000) wash in PBS. Imaged using 20x objective. This staining method was adapted from Williams et al., 2009.

Sindbis virus generation

All the constructs listed below were subcloned into SinRep5 virus vector (Invitrogen) and pseudovirions produced according to the manufacturer's directions.

Kaede-Kv1.1-mTRS: Kaede-Kv1.1 in the SinRep5 vector was digested with Bcl I. The region of DNA between nucleotide 153 and 1477 (accession number M26161) was dropped out. The backbone DNA was religated.

Kaede-Map2-dendritic targeting sequence (DTS): The 3'UTR of MAP2 between nucleotide 2418 and 3096 (accession number U30938) was cloned by PCR using

specific primers including a Not I restriction site in the forward primer and an Xba I site in the reverse primer (listed in the primers section) (Blichenberg et al., 1999). The PCR product was digested with Not I and Xba I and ligated into the corresponding restriction sites within the multiple cloning site after the stop codon of Kaede in the Living Color vector (Clontech). Kaede-MAP2-DTS was subcloned into the SinRep5 vector by a blunt end ligation.

Kaede-Kv1.1 and EGFP-Kv1.1 FL and ΔmiR-129: Kaede or EGFP fused to full length Kv1.1 coding region and mTRS were previously cloned into pCDNA3 as described in Raab-Graham et. al., 2006. Mutation of miR-129 binding site (seed match sequence) was then achieved by performing Quick Change Site Directed Mutagenesis (Stratagene) using primers 5'caaaaccaaccaaacaacgtttttgaaaaaaaaaacccaac3' and 5'gttgggttttttttttcaaaaacgttgtttggttggttttg3' (mutations indicated as underlined sequence). The resulting constructs were then subcloned into SinRep5 vector for virus production.

Competition Assays

For figure 2.2, DIV21 cortical neurons were infected with Sindbis virus coding for Kaede-MAP2-DTS (control) or Kaede-Kv1.1-mTRS. 18 hours post infection, neurons were treated with DMSO or rapamycin (200 nM) in HEPES based aCSF for 75 min at 37°C. Following treatment, neurons were fixed with 4% paraformaldehyde for 10 min on ice. Neurons were immunostained and imaged as outlined in immunofluorescence section. Surface expression was quantitated by blindly choosing Kaede positive neurons.

For Figure 2.8, CaMKIIα 5'- 3'UTR fused to destabilized GFP (dGFP- 5', 3'UTR) cDNA was obtained from Addgene, generously deposited there by Dr. Michael Sutton and reported by Aakalu et al (Aakalu et al., 2001). DIV 17 neurons were transfected with EGFP (control) or dGFP- CaMKIIα-5', 3'UTR cDNA alone. At DIV 21 transfected neurons were treated with DMSO or rapamycin (200 nM) for 100 min at 37°C. After treatment they were fixed with 4% paraformaldehyde for 20 min at room temperature. Neurons were immunostained and imaged as outlined under immunofluorescence. Putative HuD binding sites were removed by quick change mutagenesis using two complimentary oligos (sense strand: 5-CACTCACACCACTTCCTTCCACCA CTCTCTCCCTCTTCCTGGGTTTGGCTC-3; antisense strand: 5-CACTCACACCACTTCCTTCCACCACTCTCTCCCTCTTCCTGG GTTTGGCTC -3). The PCR protocol used to generate loopout was 95°C for 1 minute followed by 20 cycles of 95°C for 30s, 50°C for 1 minute, and 68°C for 22 minutes. Nucleotides removed are highlighted in yellow in Figure S2.4C.

Immunofluorescence and Image Analysis Immunofluorescence was performed as outlined in Raab-Graham et al., 2006. For staining of total protein, neurons were fixed with 4% paraformaldehyde, permeabilized with 0.25% Triton-X 100, and incubated with primary antibodies overnight at 4°C. Secondary antibodies conjugated to either Alexa-488 (1:400, Invitrogen), Cy3 (1:500, Jackson labs), Alexa 647 (1:200, Invitrogen) or Cy5 (1:200, Jackson labs) were used in appropriate combinations. For staining of surface expressed Kv1.1, fixed but non-permeabilized neurons were incubated overnight at 4°C

with Kv1.1 antibody (1:1000, Neuromab) that recognizes the extracellular epitope. Neurons were washed extensively with PBS for at least one hour to remove all excess antibodies before permeabilization. Z-stack images were acquired using a Leica SP5 (Leica DM6000 CFS) confocal microscope (63X oil objective lens, N.A. 1.2) by sequential scanning. The Leica application suite advanced fluorescence (LAS AF) software was used for imaging acquisition. Dendrites were chosen blindly based on Kaede or EGFP signal that were at least 60 μm in length. Signal intensity of puncta was determined by first tracing dendrites up to 150 μm on maximum projected images using the line scan tool in the LAS AF software package. Background was subtracted by determining the signal in a region close to the dendrite but void of all processes. Signal intensity for Kv1.1 puncta was defined as peaks that exceeded the mean signal intensity in control dendrites plus one standard deviation.

Cell Body Analysis

For analysis of cell bodies, a region of interest encompassing the cell body was drawn using ImageJ. The average intensity was measured for Kv1.1 and normalized to Kaede (Figure S2.1C), DsRed (Figure S2F), or EGFP (Figure S2.2E and Figure S2.4B). All integrated signal intensities were between the range of 0 and 255, to ensure that measurements were taken within the linear range.

RNA Affinity Capture of miRNAs Associating with Kv1.1 mRNA

Kv1.1 FL, CR, or ΔmiR129 were PCR amplified using primers containing a T7 promoter and an extra connecting sequence of 20 nt. The PCR products were then purified and *in vitro* transcribed with T7 polymerase (Ambion) to generate RNA. The RNA fragments were then purified and hybridized with the synthesized Biotin-oligonucleotide (IDT) against the 20 nt tag, resulting in 5' specific Biotin labeling of the RNA. 40 µg of cell extract from synaptoneurosomes (SN) or total neurons was then used to incubate with 4 µg of Biotinylated RNA for 1 hour at room temperature (RT) in reaction buffer (10 mM HEPES, pH7.4, 150 mM NaCl, 3 mM $MgCl_2$, 2.5% glycerol, 0.5% NP40, 0.2 mg/ml yeast t-RNA, protease inhibitor cocktail, 5 mM EDTA, RNase inhibitor 40 U/ml, 0.2 mM TCEP). The associated protein/RNA complex was pulled down with 10 µl of streptavidin-coated magnetic beads (Promega) by additional incubation of 1 hour at RT. The magnetic beads were then washed 3 times with reaction buffer and eluted with high salt buffer followed by heating at 95ºC for 5 min. The eluent was subjected to miRNA detection using miRNA PCR system (Exiqon) with primers specific for miR-129 (Exiqon).

Quantitative PCR for mRNA or miRNA

Quantitative PCR was performed by using a SYBR Green PCR Master Mix as outlined by the manufacturer (Applied Biosystems) using a BioRad icycler. Fold changes were calculated as outlined by Raab-Graham et al. (2006). For steady state mRNA quantification (Figure 2.1B) primers against GAPDH were used as an internal housekeeping gene to control for variation between samples. For miRNA pull down (Figure 2.3), 10% total input RNA was used for internal control. All experiments were

performed in triplicate. Relative ratios were calculated by the equation: ratio= ($2^{\Delta CPtarget(control\text{-}sample)} \div 2^{\Delta CPreference(control\text{-}sample)}$), adapted from Pfaffle et al., 2001, where CP is the threshold cycle, the target is the transcript of interest, and the reference is GAPDH, 5S rRNA or 10% total RNA.

Primers Used

For cloning of MAP2-DTS: forward primer (5'ggcgcggccgcgatctagcactaaaatatcatttttc3') and reverse primer (5'gcggtctagattactggaccttcttctttagttacc3').

For *in vitro* transcription of RNA for RNA affinity capture assay: Kv1.1 FL, forward primer (5' ccaagcttctaatacgactcactatagggagaggccggacaacgtcaaggctatgacgg3') and reverse primer (5'gttgggttttttttttctttttgcttgtttgg3'); mTRS, same forward primer as FL and reverse primer (5'ttaaacatcggtcaggagc3').

For 5' specific biotinylation of mRNAs, Biotin labeled-5'agccttgacgttgtccggcc-3' was used to hybridize with *in vitro* transcribed mRNAs.

For detection of Kv1.1 mRNA pulled downed by HuD: Kv1.1 FL and ΔmiR-129, forward primer (5' gccgccgcagctcctctactatcag3') and reverse primer (5'gcttttgattgcttgcctggtgctt3'); Kv1.1 CR, forward primer (5'ggccatcctcagggtcatccgcttg3') and reverse primer (5'acaccaccgcccaccagaaagcatc3'); CaMKIIα, forward primer (5' cccttggatgttgctggaattctc3') and reverse primer (5' gggtgggtcaacactggagacaaac3'); GAP-43 forward primer (5'ggaataaggatccgaggaggaaagg3') and reverse primer

(5’cttaaagttcaggcatgttcttggt3’); GAPDH forward primer (5’gcaagagagaggccctcag3’) and reverse primer (5’tgtgagggagatgctcagtg3’);

Homer1a forward primer (5’ tgggtgtctggagttcttcccttt 3’) and reverse primer (5’ atgaagacccatctgccacgatca 3’; adapted from Keene et al., 2008).

LNA Transfection of Cultured Neurons

DIV12 neurons were transfected using Lipofectamine2000. For each well, 0.4 □g of EGFP DNA and 100 nM of LNA (either the scrambled or miR-129 specific probes from Exiqon) were used for transfection in a 1:5 dilution with Neurobasal medium. Neurons were incubated with the transfection mix for 2 hours at 37^{o}C and returned to conditioned media afterwards. 24 hours post-transfection, neurons were fixed, permeabilized, and immunostained with Kv1.1 antibody as described in the immunofluorescence section. Signal quantitated by blindly choosing EGFP positive neurons. Fluorescent images of eGFP-transfected neurons and Kv1.1 signals were then taken as outlined in immunofluorescence section.

miR-129 Overexpression Assay

Cultured hippocampal neurons were transduced with control or miR-129-2 precursor lentivirus (3 X 10^5 IU; Biosettia) at DIV14. Neurons were treated at DIV21 for 75 min with DMSO or rapamycin. miR-129 overexpressing neurons were detected by

immunostaining for Dsred. Kv1.1 surface protein was detected by using an antibody that detects an extracellular domain of Kv1.1 (Neuromab) using nonpermeabilized neurons.

Northern blot analysis

4 micrograms of total RNA from DMSO or rapamycin treated cells or 2.5 micrograms of total RNA from scrambled or LNA transfected cells was separated on a Tris-borate-EDTA-Urea-15% polyacrylamide gel. The gel was transferred onto a piece of Amersham Hybond N^+ membrane (GE Healthcare, Illinois). The blot was UV-crosslinked using the HL-200 HybriLinker (UVP, California). The blot was probed for hsa-miR-129 5p miRNA as previously described (citation below). The blot was stripped with boiling hot stripping buffer (0.1% sodium dodecyl sulfate [Sigma-Aldrich, Missouri] in double-distilled water), and then probed for hsa-let-7a. The sequences for the probes used were as follows: hsa-miR-129-5p, GCAAGCCCAGACCGCAAAAAG; hsa-let-7a-5p, AACTATACAACCTACTACCTCA. Quantitative values for the northern blot analysis were obtained using the Quantity One Analysis Software (Bio-Rad, California). (Grundhoff et al., 2006)

Local Translation Assay

Local Translation assay was carried out essentially as reported by Raab-Graham et al.(Raab-Graham et al., 2006) with the following modifications: primary culture of neurons (DIV 14 – 28) infected with Sindbis virus coding for Kaede-Kv1.1 FL or Kaede-Kv1.1ΔmiR-129 for 18 to 24 hours were placed in 35mm dish containing HEPES based

aCSF with either DMSO or rapamycin (200 nM) and immediately imaged (before photoconversion). Confocal excitation imaging was accomplished using an upright microscope (Leica SP5) with a water immersion lens (HCX APO L20x/0.05W U-V-I) at room temperature. A 488 nm laser was used to excite Kaede-Kv1.1 and green emission was detected at 498 – 534 nm. Serial 1.0 µm z-sections of a neuron expressing Kaede-Kv1.1 were acquired and then photo-converted using a DAPI filter for 30 seconds. After the initial photoconversion, the final image was acquired at 120 min post-photoconversion. Maximum projected images from z-compressed stacks were used for data analysis using Leica SP5 software. For each neuron, the mean intensity of 8 -10 puncta more than 60 µm from the soma was measured. All images were analyzed blindly using photoconverted protein as an unbiased selection of puncta. The magnitude of new protein synthesis was calculated by determining the fold increase of the mean green pixel intensity of puncta 120 min after photo-conversion (F) as compared to that immediately after photo-conversion (F_0; time point 0) and calculated using the equation $\Delta F/F=(F- F_0)/ F_0$. Average basal translation under control conditions (Kaede-Kv1.1 FL, DMSO) was set equal to 100% and relative new translation measured with rapamycin or Kaede-Kv1.1ΔmiR-129 +/- rapamycin are reported as a percent increase over the average basal translation.

In situ Hybridization of Kv1.1 mRNA in Cultured Neurons

For in situ hybridization of infected neurons, cultures (DIV 21-28) were infected with Sindbis virus encoding either EGFP-Kv1.1 or EGFP as outlined previously (Raab-

Graham et al., 2006). Briefly, 18 hours post infection, DIV21-28 neurons were fixed in 4% paraformaldehyde, 4% sucrose for 18 minutes on ice. Neurons were washed 3X in PBS and 1X in SSC for 5 minutes. Neurons were permeabilized with 1% Triton-X 100, 1X SSC for 30 minutes at room temperature followed by EGFP antisense (nt 5'-ATATAGACGTTGTGGCTGTTGTAGTTGTACTCCAGCTTCT-3') DIG labeled oligo hybridization with an overnight incubation at 37^{o}C. DIG labeled oligo was detected using a mouse anti-dig antibody (Roche) followed by an anti-mouse cy5 antibody (Jackson; www.singerlab.org).

Transfection and Isolation of HEK293T cells

HEK293T cells were transfected with Lipofectamine2000 as outlined by the manufacturer (Invitrogen). 48 hours post-transfection, cells were harvested by scraping the cells into buffer A (in mM; 150 NaCl, 10 HEPES [pH 7.4], 3 KCl, 2 $CaCl_2$, 1 $MgCl_2$, 10 glucose, 250 sucrose, 5 TCEP) containing protease inhibitors (Complete, Roche) and phosphatase inhibitors (Sigma). Cells were lysed by homogenization. Lysates were centrifuged at 106 xg for 10 min at 4^{o} C. Supernatant was transferred to a new tube and centrifuged for 17,000 xg for 20 min at 4^{o} C. P2 pellet was resuspended in 100 µl of buffer A. SDS-sample buffer was added to a final concentration of 1X and samples were resolved on a 10% SDS-PAGE gel and transferred to nitrocellulose for western blot analysis.

HuD Pulldown of Kv1.1 mRNA from HEK Cells

HEK293T cells were co-transfected with pCDNA3-myc-HuD and pCDNA3-Kaede-Kv1.1-FL, CR, or ΔmiR-129. pCDNA3 alone and Kaede alone were used as controls. Cell lysates were harvested in polysome lysis buffer (100 mM KCl, 5 mM $MgCl_2$, 10 mM HEPES, 0.5% NP-40, TCEP 0.4 μl/ml, RNaseOut 100 U/ml, 0.2% vanadyl ribonucleoside complexes, and EDTA free protease inhibitor tablet) followed by homogenization. After centrifugation at 14,000 xg, 4ºC, for 10 min, the supernatant was pre-cleared with 20 μl/ml protein A/G beads (Santa Cruz) for 1 hr at 4ºC. Protein A/G beads (20 μl/reaction) were coated with myc antibody (Sigma) (2 μg/reaction) by incubating at RT for 2 hs in NT2 buffer (50 mM Tris, pH 7.4, 150 mM NaCl, 1 mM $MgCl_2$, 0.05% NP-40, 15 mM EDTA, 8 U/ml RNaseOut, and 0.4 μl/ml TCEP) supplemented with 5% BSA. The myc-antibody coated beads were then washed 6 times in NT2 buffer. Pre-cleared lysates were incubated with myc-antibody coated beads or beads alone in NT2 buffer supplemented with 3 μl/ml RNaseOut at 4ºC overnight. After washing 6 times with NT2 buffer, beads were treated with protease K (30 μg/ml in NT2 buffer containing 0.1% SDS) at 55 ºC for 30 min and subjected to RNA extraction using TRI-LS reagent (Molecular Research Center, Inc) following the manufacturer's protocol. Purified RNAs were further treated with DNase (Ambion Turbo DNase kit) following the manufacturer's protocol and used for reverse transcription (Superscript III kit from Invitrogen) with oligo dT primer. The reverse-transcribed cDNAs were then treated with RNase H (Invitrogen) for 30 min at 37 ºC and used for PCR with Kv1.1 specific primers (see primers used section).

HuD Overexpression in Cultured Neurons

Cultured hippocampal neurons were transfected at DIV12 with cDNAs coding for myc-tagged HuD or pCDNA3 with eGFP. 48 hours post-transfection neurons were treated with DMSO or cycloheximide (50 μM) for 4 hours, fixed and immunostained with Kv1.1 or Kv4.2 specific antibodies (Neuromab).

GST Pulldown

Neurons were treated at DIV21 with 200 nM Rapa or DMSO for 75 min at 37 ºC in aCSF. Neuronal lysates were isolated in HB buffer and homogenized. Nuclei and unbroken cells were removed by low speed centrifugation (900 rpm, 10 min) and supernatant was transferred to a new tube containing TRI-LS reagent. RNA was isolated following manufacturer instructions (Molecular Research Center, Inc). 500 ng of GST or GST-HuD was incubated with 2.25 μg RNA for 45 min at room temperature in binding buffer (20 mM HEPES, pH 7.9; 3 mM Magnesium acetate; 50 mM Potassium acetate; yeast tRNA (0.2 μg/μl), TCEP, RNaseOut and 5% glycerol). Protein agarose A/G beads (Santa cruz) were precoated with rabbit pan Hu antibody in binding buffer or rabbit-IgG (Santa cruz) in binding buffer without the yeast tRNA, TCEP, RNaseOut and glycerol for 2 hrs at room temperature. 50 μl of the precoated IgG beads were used to preclear GST/RNA in solution for 1 hr at room temperature. IgG beads were removed by centrifugation and supernatant was added to precoated rabbit anti-HuD beads and

incubated for 2 hrs at room temperature. Beads were washed with diluted binding buffer (0.5X) without glycerol 6 times and then eluted with TRI reagent following manufacturer's protocol (Zymogen, the Direct-zol RNA minikit). Isolated RNA was treated with Dnase I (Ambion Turbo DNase kit) and reverse transcribed using the iScript cDNA Synthesis kit (Bio-Rad) following manufacturer's protocol. cDNA was treated with RNase H and subjected to PCR using Kv1.1, GAP43 and CaMKIIα specific primers (see primers used section). PCR was done using the iQ SYBR green kit (Biorad). PCR was terminated between cycle 25-30 to prevent saturation.

mRNA Degradation Assay

mRNA degradation assay was carried out essentially as previously described (Origanti et al., 2012). In brief, DIV 21 cultured cortical neurons were treated with actinomycin (12μM) for 4 hrs prior to the addition of rapamycin (200 nM). Neurons were treated with rapamycin or DMSO plus actinomycin for 75 min in HEPES-based ACSF at 37 ºC. Neurons were harvested in HB buffer containing TCEP and RNaseOut and homogenized. Following a low speed centrifugation (900 rpm, 10 min), the supernatant was removed to a new tube containing TRI-LS. RNA was isolated following manufacturer instructions (ABI). Total RNA was treated with DNAse, quantitated, and subjected to quantitative RT-PCR using CaMKIIα specific primers as outlined under quantitative PCR section. Degradation was measured as a percent remaining after treatment with rapamycin as compared to DMSO treated neurons.

Chapter 3: Dynamic changes in the RNA-binding factor miR-129-5p result in resetting the action potential threshold in CA1 pyramidal neurons by Kv1.1 in Temporal Lobe Epilepsy

Introduction

Neuronal insult or injury is often followed by changes in intracellular signaling that, in some cases, can lead to a persistent state of neuronal hyperexcitablity such as temporal lobe epilepsy (TLE). The serine/threonine kinase mTOR is overactive following status epilepicus (SE) in models of TLE (Brewster et al., 2013; Zeng et al., 2009). mTOR is best characterized for its role in promoting translation of mRNAs. Therefore, it is often hypothesized that overactive mTOR in neurological disorders results in excessive protein synthesis (Hoeffer and Klann, 2010). However, a number of studies suggest that there is a reduction or loss of protein expression with respect to voltage-gated ion channels (Poolos and Johnston, 2012). Our previous work established a link between mTOR activity and the dendritic expression of the delayed rectifier potassium channel Kv1.1. Findings from that study showed that activation of mTOR represses the local protein synthesis of Kv1.1 in neuronal dendrites (Raab-Graham et al., 2006). Remarkably, increased seizure susceptibility directly correlates with a decrease in Kv1.1 gene expression (Rho et al., 1999; Robbins and Tempel, 2012; Smart et al., 1998). Likewise, overexpression of Kv1.1 has been shown to eliminate seizures in a rat model of epilepsy (Wykes et al., 2012).

Identifying mechanisms through which mTOR activity represses the translation of ion channel mRNA may be important for understanding the causative nature of epilepsy. RNA-binding proteins and microRNAs can bind to the same target mRNAs and antagonize each other's function (Meisner and Filipowicz, 2011). Recent work from our laboratory determined the microRNA, miR-129-5p and the RNA binding protein HuD display this exact relationship with respect to KV1.1 translation (Sosanya et al., 2013). mTOR-dependent repression of Kv1.1 mRNA translation is mediated by binding of miR-129-5p while under conditions where mTOR activity is reduced, miR-129-5p binding is relieved and HuD restores translation (Sosanya et al., 2013). These findings have led us to ask the questions (1) is Kv1.1 protein reduced in epilepsy when mTOR is overactive, (2) what is the physiological consequence of changes in Kv1.1 protein expression, and (3) are the RNA-binding factors that regulate Kv1.1 mRNA translation aberrantly expressed in epilepsy?

Herein we report that Kv1.1 protein dynamically changes over the course of several days following status epilepticus, a critical period during which neuronal remodeling occurs that contributes to chronic epilepsy. Interestingly, Kv1.1 expression sharply increases 5 days post status epilepticus (post-SE) peaking at 14 days post-SE followed by a dramatic decrease at 15 days post-SE which is significantly different from control by 21-30 days post-SE, a time point associated with the onset of behavioral seizures (Mascott et al., 1994) and where we observe significant increase in the number of behavioral seizures. Consistent with the changes in Kv1.1 protein, the threshold for action potential firing is lower by 21-30 days compared to control. This overall decrease

in Kv1.1 expression 21-30 d post-SE corresponds to an increase in mTOR activity and a significant increase in miR-129-5p. Collectively, these data suggest that mTOR/miR-129-5p-mediated repression of Kv1.1 translation contributes to the neuronal hyperexcitability observed in epilepsy.

Methods

Animals. Status epilepticus (SE) was induced in 8-week old male Sprague-Dawley rats by intraperitoneal injection of kainic acid (10 mg/kg). The behavior of the animals was observed, and seizures were scored according to the Racine scale (Racine, 1972). One hour after the onset of SE (Class V on the Racine scale), seizures were terminated by subcutaneous injection of sodium pentobarbital (PB; 30 mg/kg). All animal experiments were performed in accordance with guidelines approved by the Institutional Animal Care and Use Committee (IACUC) at The University of Texas-Austin.

Continuous Video Monitoring. KA rats (n=3) were video monitored from d2 to d30 post-SE. Videos were watched and scored by a 3rd party over an 8 hour period. Only behavioral seizures ranging from Class III to Class V on the Racine scale were counted.

Slice Preparation. Animals were anesthetized using a lethal dose of ketamine and xylazine. Once deeply anesthetized, animals were perfused intracardially with ice-cold modified ACSF containing (in mM) 210 sucrose, 2.5 KCl, 1.2 NaH_2PO_4, 25 $NaHCO_3$, 0.5 $CaCl_2$, 7.0 $MgCl_2$, and 7.0 dextrose bubbled with 95%O_2 / 5%CO_2. The brain was removed and bisected along the midline. One hemisphere was used for slice preparation for electrophysiological recording and the other hemisphere was used for

biochemical analyses (see below). The hemisphere was mounted and 350 µm thick slices were made using a microtome (Vibratome, St. Louis MO). Slices were placed in a holding chamber filled with ACSF containing (mM): 125 NaCl, 2.5 KCl, 1.25 NaH_2PO_4, 25 $NaHCO_3$, 2 $CaCl_2$, 2 $MgCl_2$, and 12.5 dextrose warmed to 35°C for 20 min and then placed at room temperature for < 6 hrs until needed for recording.

Electrophysiology. Slices were placed individually as needed into a submerged recording chamber continuously perfused with control extracellular saline (see below). Slices were viewed with a Zeiss Axioskop using infrared video microscopy and differential interference contrast (DIC) optics. For all recordings, the ACSF solution contained (mM): 125 NaCl, 3 KCl, 1.25 NaH_2PO_4, 25 $NaHCO_3$, 2 $CaCl_2$, 1 $MgCl_2$, and 12.5 dextrose and was bubbled continuously with 95%O_2 / 5% CO_2 at 31-33°C. Fast glutamatergic and GABAergic synaptic transmission was blocked by a combination of 20 µM DNQX, 50 µM AP5, 2 µM gabazine, and 5 µM CGP55845.

Patch pipettes were pulled from borosilicate glass and had a resistance of 4-8 MΩ when filled with the internal recording solution containing (in mM): 120 potassium gluconate, 20 KCl, 10 HEPES, 4 NaCl, 4 MgATP, 0.3 Na-GTP and 7 phosphocreatine (pH 7.3 with KOH). Whole cell recordings were made from the soma of CA1 pyramidal neurons using a Multiclamp 700A or Dagan BVC in current clamp mode. Series resistance was monitored throughout the recording, and experiments in which the series resistance exceeded 30 MΩ were discarded.

Data Acquisition and Analysis. Data were sampled at 40 kHz, filtered at 5 kHz and digitized by an ITC-18 interface connected to computer running Axograph X. Data analyses were performed with Axograph X.

Western blot analysis. Synaptoneurosomal (SN) protein and RNA was harvested from the hippocampus as outlined by Sosanya et al. (2013). Proteins were separated by SDS-PAGE, transferred to nitrocellulose, and blocked with 5% milk+Tween 20. Blots were then probed with antibodies against Kv1.1 (1:500; neuromab), p-mTOR (1:500, Cell Signaling), mTOR (1:500, Invitrogen), HuD (1:500; Millipore), and Tubulin (1:2000). Alexa680 or Alexa800 (1:2000; invitrogen) were used as secondary antibodies and imaged on the Leica Odyssey.

Immunohistochemistry. Control and KA injected rats were perfused with ice cold PBS and post fixed with 4% formaldehyde overnight at 4^{o}C. 80 µm thick coronal sections of the hippocampus were taken on a vibratome and placed in PBS. Hippocampal slices with similar morphology were double stained for Kv1.1 and tubulin. Slices were blocked overnight at 4oC in blocking solution (10% goat serum with 0.3% Triton X-100 in PBS). and then incubated in primary antibody (m anti- Kv1.1 (1:200, neuromab) and rb anti tubulin (1:200)) overnight at RT in blocking solution. The following day, slices were washed in PBS for 1x10min, 1x30min, and 1x40 min and then incubated in blocking solution for 2 hr at RT. Slices were then incubated overnight in secondary antibody followed by same washing protocol as above. Once mounted on glass slides slices were imaged on a Leica microscope using a 20x objective.

Reverse Transcription-quantitative PCR (RT-PCR). SN RNA was isolated using Zymogen Direct-zol RNA miniprep kit according to the manufacturer's directions. RT-PCR for miR-129-5p or 5S rRNA was done using the miRCURY LNA Universal RT microRNA PCR kits (Exiqon; universal cDNA #203300 and Sybr green master mix #203450) using miR-129 specific primers (Exiqon) according to the manufacturer's directions. Fold changes were calculated as outlined by Raab-Graham et al. (2006) and Sosanya et al. (2013). Relative ratios were calculated by the model as previously described (Pfaffl, 2001) and calculated by the equation: ratio= (2∆CPtarget(control-sample) ÷ 2∆CPreference(control-sample)), where CP is the threshold cycle, the target is the transcript of interest, and the reference is 5S rRNA.

Statistical Analyses. All data are expressed as mean ± S.E.M. Statistical comparisons were made using one-way or two-way ANOVA followed by Tukey-Kramer or Dunnett's multiple comparisons post-hoc test or Student's t-test (paired or unpaired as appropriate) with Prism software (GraphPad). Linear fits and correlations were made using Prism. Data were considered statistically significant if $p < 0.05$.

Results

Number of Behavioral Seizures peak at 21 days post-SE when compared to earlier time points.

The kanic acid (KA) model of TLE has been useful for identifying molecular changes that occur during epileptogenesis leading to the progression of spontaneous

recurrent behavioral seizures. To determine the time course for the development of seizure activity KA injected rats were continuously video monitored and behavioral seizures ranging from Class III-V (Racine, 1972) were scored from 2 to 21 days post-SE. Interestingly, seizure number was depressed at day 14 post-SE and then gradually increased from day 15 to day 21 where seizure number became significantly higher when compared to all other time points (Figure 3.1).

Increased mTOR activity corresponds to peak number of behavioral seizures.

Previously, it was reported that mTOR was overactive in the kainic acid model of TLE (Zeng et al., 2009). In light of the behavioral progression data (Figure 3.1) we set out to determine the time course of mTOR activity post-SE. To address this question, we examined mTOR activity in the hippocampus of control rats (0d, no KA) and rats 2, 5, 14, 15, and 21-30 days post-SE. Synaptoneurosomes isolated from hippocampi were subjected to Western blot analysis for phospho-mTOR (pmTOR) and total mTOR. The ratio of pmTOR/mTOR served as a readout for mTOR activity. Notably, mTOR activity was significantly depressed 14d post-SE followed by a sharp increase at 15d post-SE which was significantly different from control by 21-30d post-SE (control: 1.00±0.02, 2d post-SE: 1.03±0.05, 5d post-SE: 1.03±0.04; 14d post-SE: 0.56±0.25, 15d post-SE: 1.22±0.19, 21-30d post-SE: 1.25±0.11; Figure 3.2A). This significant increase in mTOR activity corresponds to the significantly higher number of seizures 21 days post-SE. As a further control, we measured mTOR activity in KA injected rats that did not progress

past Class III on the Racine scale and observed no change in mTOR activity when compared to control (Figure 3.2B)

Bidirectional changes in Kv1.1 expression in TLE.

Shortly after periods of intense activity neurons may undergo changes in ion channel function and/or expression that can reduce the overall activity of the neuron (Fan et al., 2005; Narayanan and Johnston, 2010; Shin et al., 2008). However following status epilepticus, these changes are often transient, resulting in persistent states of neuronal hyperexcitability and ultimately leading to the onset of recurrent seizure activity (Sun et al., 2013). The overexpression of Kv1.1 can provide protection against seizures in drug resistant focal neocortical epilepsy (Wykes et al., 2012). We therefore asked if Kv1.1 expression undergoes changes following kainic acid induced status epilepticus (SE): higher expression in the short-term, to dampen neuronal excitability, followed by a reduction of expression that contributes to a state of hyperexcitability. To test our prediction, we measured Kv1.1 expression at distinct time periods (0, 2, 5, 14 and 15 days after KA injection) and then again at late post-SE (21 – 30 days after KA injection) when behavioral seizures are significantly different from all other time points. As predicted, in Western blot analysis of isolated hippocampal synaptoneurosomes there was an increase in Kv1.1 expression of ~27% by 5 days post-SE and of ~71% by 14 days post-SE (0d no-SE: 1.00±0.04, 2d post-SE: 1.07±0.08, 5d post-SE: 1.27±0.09; 14d post-SE: 1.71±0.25; 15d post-SE: 0.98±0.05; Figure 3.3A). In contrast, 21-30d post SE, resulted in reduced Kv1.1 levels by ~50% relative to control (21-30d post-SE:

0.54±0.15; Figure 3.3A). As a further control, we observed no change in Kv1.1 expression between control and KA injected rats that did not reach SE (Figure 3.3B). These results suggest that the potential neuroprotective increase in Kv1.1 expression early after SE fails to be sustained at later stages of TLE and may contribute to the gradual increase in behavioral seizures from day 15 to day 21 post-SE as mTOR activity increases.

Bidirectional changes in Kv1.1 expression post-SE in the hippocampus.

To determine the regional distribution of changes in Kv1.1 expression post-SE we perfused and sectioned the hippocampus from control, 14d, and 21-30d post-SE animals. Slices within the same region of the hippocampus were immunostained for Kv1.1 and Tubulin. Consistent with our western blot results, we observed an increase in Kv1.1 protein expression both in the CA1 and CA3 regions 14 d post-SE when compared to control (Figure 3.4A), with a significant decrease by 30days post-SE relative to control animals (Figure 3.4B).

Dynamic changes in Kv1.1 expression post-SE alter the threshold for action potential firing.

In cortical neurons, dynamic changes in Kv1 channels reset the threshold for action potential firing (Vth) (Higgs and Spain, 2011). Thus, one possible functional consequence of the changes in KV1.1 expression post-SE would be to alter Vth in hippocampal pyramidal neurons. To test if Vth is altered, we recorded single action

potentials elicited in CA1 pyramidal neurons from KA and saline injected rats. The amplitude of a 100-msec current pulse was adjusted so that a single action potential occurred in the middle (~ 50 msec latency) of the current injection.

Since behavioral seizures in KA-treated rats are significantly higher starting at 21 days post-SE compared to control animals (Figure 3.1), we measured the contribution of Kv1.1 to the threshold of action potential firing at this time point. Consistent with our Western blot analysis, we found that Vth with 100ms current injections in 21-30d post-SE CA1 pyramidal neurons was hyperpolarized by ~3 mV compared to control neurons (Figure 3.5A and B). Moreover, blocking Kv1-containing channels with 4-AP (50 µM) significantly hyperpolarized Vth in control neurons (Figure 3.5A, B, and D). Consistent with a reduction in Kv1.1 protein expression, there was however, no significant effect of 4-AP on the Vth with the 100ms current injections in KA neurons (Figure 3.5A, B and D). The Vth of action potentials elicited with 2-msec current injections was not significantly different between control and 21-30d post SE animals and was insensitive to 4-AP (Figure 3.5C and D). These data support the hypothesis that Kv1.1 expression is reduced 21-30 days post-SE and that this loss of Kv1.1 contributes to CA1 pyramidal hyperexcitability by reducing the threshold for action potential firing.

miR-129-5p, a negative Kv1.1 regulator, levels are heightened when Kv1.1 is reduced.

What is the molecular mechanism accounting for reduced Kv1.1 expression in TLE? Recently, our laboratory determined that the microRNA, miR-129-5p negatively regulates the expression of Kv1.1 in neurons when mTOR is active and that the RNA-binding protein HuD positively regulates the translation of Kv1.1 mRNA when mTOR is inhibited (Sosanya et al., 2013). To determine if changes in the dynamic relationship between miR-129-5p, HuD, and Kv1.1 is altered post-SE, we determined the expression levels of HuD and miR-129-5p 21-30d post-SE. Based on our model, for Kv1.1 expression to decrease 21-30d post-SE either miR-129-5p levels will increase or HuD levels will be reduced. Figure 3.6A shows that miR-129-5p levels increase by ~70% 21-30d post-SE corresponding to reduced Kv1.1 levels (Figure 3.6A; control: 1.00±0.06, 21-30d post-SE: 1.76±0.33) and HuD levels remain constant (Figure 3.6B, control: 1.00±0.21, 21-30d post-SE: 0.95±0.30). Together this data suggests that increased levels of miR-129-5p in TLE favor translational repression of Kv1.1 mRNA resulting in reduced protein levels and a lower Vth for firing an action potential.

Discussion

Many ion channels are dynamically regulated during epileptogenesis (Poolos and Johnston, 2012) and a growing number are being linked to changes in mTOR activity (Brewster et al., 2013; Lee et al., 2011). We recently described a mechanism by which

mTOR can influence the expression of the delayed rectifier potassium channel Kv1.1 by regulating two RNA-binding factors, HuD and miR-129-5p, that promote and repress KV1.1 mRNA translation, respectively (Sosanya et al., 2013). In this study, we found that hippocampal expression of Kv1.1 is higher 5 to 14 days post-SE. This increase in Kv1.1 expression is likely due to the low levels of mTOR activity, a condition that favors the release of miR-129 repression (Figure 3.7, left panel). In contrast, when miR-129-5p levels are heightened 21-30 days post-SE possibly shifting the balance toward Kv1.1 mRNA repression thus leading to lower expression of Kv1.1 and a significant hyperpolarization of CA1 pyramidal neuron action potential threshold (Figure 3.7, right panel, Late TLE, red arrow). This may contribute to hippocampal pyramidal neuron hyperexcitability during a time when recurrent spontaneous seizures occur (Figure 3.1). Our findings propose a mechanistic model explaining the posttranscriptional regulation of an ion channel by mTOR activity in a model of TLE (Figure 3.7).

Interestingly, in a different model of epilepsy, Brewster et al., demonstrated that while there is a trend toward a decrease in Kv1.1 protein two weeks post status epilepticus, the chronic use of the mTORC1 inhibitor rapamycin did not reverse interictal epileptiform activity or increase the levels of Kv1.1 in the hippocampus of epileptic rats (Brewster et al., 2013). Collectively, our results suggest that to effectively increase Kv1.1protein in TLE, miR-129-5p levels need to be reduced and HuD levels need to increase. Consistent with this idea, HuD protein has been shown to decrease with acute treatment of rapamycin (Sosanya et al., 2013). Perhaps chronic use of rapamycin

reduces HuD protein to dangerously low levels, further decreasing the probability for it to bind to Kv1.1 mRNA.

The initial rise in ion channel expression in TLE, reported in this study for Kv1.1 and previously seen with HCN channels (Shin et al., 2008), may help explain the reduced numbers of behavioral seizures during the early stages or latent period. Moreover, the failure to sustain elevated levels of these channels may lead to chronic epilepsy. The concurrent increase in mTOR activity coincides with the decline in channel expression. Why mTOR activity fails to renormalize in TLE is an open question. Interestingly, a recent report suggests that mTOR activity also inhibits the expression of the homeostasis protein polo-like kinase 2 (PLK2) in a neonatal seizure model (Sun et al., 2013). Although the mechanism of repression has not been established, it has been shown that PLK2 down regulates mTOR signaling through its interaction with the upstream inhibitor tuberous sclerosis complex 1 (Matthew et al., 2009). Collectively, these studies suggest that mRNAs that are repressed by mTOR activity may be good antiepileptic targets.

In summary, activity dependent mRNA translation through the competition of RNA binding factors for their target mRNAs suggests that altered levels of these factors can shift the balance toward repression or translation and lead to disease. The present study shows that elevated expression of miR-129-5p that is not properly counter balanced by HuD may lead to the reduced Kv1.1 expression and a depolarized action potential threshold resulting in neuronal hyperexcitability. Although Kv1.1 mRNA is not the only mRNA translationally regulated by miR-129-5p and HuD, its function is not

compensated by other potassium channel since deletion or loss of function mutations of the kv1.1 gene causes epilepsy in mice (D'Adamo et al., 2013). These studies provide a unique model of regulating ion channel expression which may be relevant to other mTOR related diseases associated with epilepsy, such as Tuber Sclerosis Complex, Fragile X syndrome, and Alzheimer's disease (Ma et al., 2010; Narayanan et al., 2007; Pei and Hugon, 2008; Sharma et al., 2010; Spilman et al., 2010; Zeng et al., 2011).

Chapter 4: The RNA-binding protein HuD mediates CaMKIIα Branch - specific expression

Introduction

mTOR is a protein kinase whose activity is required for late-LTP (L-LTP) and memory consolidation. mTOR consists of two subunits TORC1 and TORC2. mTORC1 is a serine/threonine kinase that promotes cap-dependent translation by phosphorylating p70 S6 kinase (S6K) and eIF4E binding protein (4E-BP). In neurons, mTOR kinase is activated by the Ca^{2+}- dependent activation of PI3Kinase and has been found to be active in dendrites (Hoeffer and Klann, 2009; Tang et al., 2002).

One notable plasticity related protein whose mRNA translation is regulated by mTORC1 is Ca^{2+}/calmodulin-dependent protein kinase II alpha (CaMKIIα) (Gong et al., 2006; Sosanya et al., 2013). Several studies have verified the importance of CaMKIIα both in the induction phase and maintenance (late) phase of LTP and memory (Mayford et al, 1996; Miller et al., 2002). The importance of locally translated CaMKIIα mRNA to memory consolidation was demonstrated in a mouse where the dendritic targeting sequence of CaMKIIα in the genome was disrupted (Miller et al., 2002). Moreover, recent data demonstrates that synapses undergoing protein synthesis- LTP tend to occur within the same dendritic branch (Govindarajan et al., 2010). Thus, further insight into the subcellular loci of CaMKIIα mRNA translation in dendrites may yield information regarding the importance of dendritic branches in memory formation.

HuD is an RNA-binding protein whose expression has been correlated with both spatial learning and contextual fear conditioning (Bolognani et al., 2006). Overexpression of several targets of HuD are associated with improved cognition. Moreover, HuD has gained recent attention for its ability to relieve microRNA repression (Kundu et al., 2012; Sosanya et al., 2013). Collectively, these data strongly support a role for HuD to relieve mRNA repression and promote the translation of mRNAs that support learning and memory.

Recently, we determined that mTORC1 kinase serves as a switch for translation of specific mRNAs through the RBP HuD. When mTORC1 is active HuD binds to its high affinity target mRNAs, one of them being CaMKIIα mRNA, stabilizing the mRNA and promoting its translation. When mTORC1 is inhibited CaMKIIα mRNA degrades, thus releasing HuD allowing it to bind to low affinity target mRNAs, such as the voltage-gated potassium channel Kv1.1. Whether HuD unbinds CaMKIIα mRNA prior to degradation and how the mRNA is degraded is unclear.

A great deal is known about global mTORC1 regulation of translation; however, little is known about how mTORC1 may regulate translation in a site-specific manner. Based on our previous work the RNA binding protein HuD appears limited and determines which mRNAs are translated based on affinity in an mTORC1-dependent manner (Sosanya et al., 2013). Herein, we demonstrate the unexpected role for HuD in mTORC1 regulated mRNA translation of CaMKIIα in a branch specific manner. We have previously demonstrated that both CaMKIIα mRNA and protein expression decrease when mTOR is inhibited (Sosanya et al., 2013). Using immunocytochemistry

to map CaMKIIα protein, we determined that HuD increases the expression of CaMKIIα by protecting it from degradation via HuD differential branch targeting. Thus, HuD differential branch expression may affect the propensity of a dendritic branch to undergo site-specific and long-lasting forms of plasticity.

Experimental Procedures

Transfection and Immunocytochemistry

Neurons were cultured as previously described in Sosanya et al., 2013. Cultured hippocampal neurons were transfected with pCDNA+eGFP or HuD+eGFP at DIV 17-20 using Lipofectamine2000 (Invitrogen). At DIV 21-24, neurons were treated with 200 nM Rapamycin or DMSO (vehicle) for 75 min. Following treatment, neurons were fixed for 20 min at RT in 4% paraformaldehyde followed by 3 washes in 1X PBS. Neurons were then permeabilized for 5 min with 0.25% triton and blocked for 1 hour in Blocking Solution (8% Goat serum, 0.25% Triton, 1X PBS). Primary antibody was incubated ON at 4^{o}C and Secondary antibody was incubated for 1 hour at RT in Blocking Solution. 3-10 min washes in 1X PBS were performed after each antibody incubation. Coverslips were mounted with Flourmount and imaged the following day using the Leica Confocal Microscope 63x objective.

Antibodies

Primary antibodies used for immunostaining include mouse anti-CaMKIIα (1:200, Lifespan), chicken anti-GFP (1:200, Aves), mouse anti-Kv1.1 extracellular (Neuromab,

1:200), rabbit anti-myc (1:200). Secondary antibodies used for immunostaining are Alexa488 anti-GFP (1:400), Alexa555 anti-mouse (1:400), and Alexa647 anti-rabbit (1:400).

PAT Assay

PAT assay was carried out according to Wu et al. and similar to Udagawa et al. (8,9). Cultured cortical neurons between DIV21-28 were treated in aCSF for 10 min for time point 0 or Rapamycin for 60, 90, or 180 min. Neurons were harvested in HB buffer B (20 mM HEPES, pH 7.4, 5 mM EDTA, pH 8.0, with RNaseOut and TCEP) and homogenized. Following a low-speed spin (900rpm, 10min) total RNA was isolated using Tri-LS following the manufacturer protocol (ABI). Reverse transcription was performed with the anchor-oligo dT primer (5' GCGAGCTCCGCGGCCGCGT$_{(12)}$) using superscript III first strand cDNA synthesis kit (Invitrogen). Subsequent PCR with 100ng of cDNA using Amplitaq Gold (ABI) with specific CaMKIIα forward (5'CCGAAGCTTCTCTCTCTTTCTTTTTTATTATGTGGCTGTG; oligo#1) and reverse (5' GCTCTAGACACATAAATTTGTAGCTATTTATTCC) primers were used (Wu et al., 1998). To detect the poly(A) tail oligo#1 was used in combination with the anchor-oligo dT primer. PCR was done with an initial denaturation step (95^{o}C, 5min) followed by 10 cycles of (15 sec at 95^{o}C, 15 sec at 45^{o}C, 1min at 72^{o}C) and then 50 cycles of (15 sec at 95^{o}C, 15 sec at 58^{o}C, 1min at 72^{o}C) and finally 7 min at 72^{o}C. The PCR products were resolved in a 2% agarose gel. As a control for the PAT assay, 600 ng of total RNA was treated with RNase H and oligo dT for 20 min at 37 ^{o}C prior to RT-PCR.

Results

mTORC1 regulates the expression of CaMKIIα in a branch specific manner

N-methyl-D-aspartate receptor (NMDAR) activity is necessary for many forms of plasticity. We have previously demonstrated that in cultured hippocampal and cortical neurons (21 – 28 days in culture), mTORC1 kinase is phosphorylated and thus active through NMDAR stimulation (Raab-Graham et al., 2006; Sosanya et al., 2013). Acute treatment with rapamycin reduces mTORC1 kinase activity (Raab-Graham et al., 2013).

Neuronal activity stimulates the mTOR-dependent local protein synthesis of CaMKIIα mRNA (Gong et al., 2006; Miller et al., 2002; Tang et al., 200); however, whether mTOR regulated translation of CaMKIIα mRNA occurs in one daughter branch over the other is unknown. To determine if mTORC1 activity regulates CaMKIIα expression in a branch specific manner we treated eGFP expressing neurons with the carrier or the mTORC1 inhibitor rapamycin for 75 minutes and stained for CaMKIIα protein with a specific antibody. eGFP allowed us to clearly visualize individual neurons and quantitate branch-specific expression changes using the eGFP signal as a way to normalize for individual dendritic volume between branches. We first confirmed that mTOR activity increases the expression level of CaMKIIα in dendrites by measuring the CaMKIIα signal in the primary apical dendrite prior to the first branch point. As previously, observed inhibition of mTOR with rapamycin reduced the dendritic expression of CamKIIα to ~ 49% ± 0.05 (Figure 4.1A and B). Next, we measured the average signal intensity of CaMKIIα in each daughter branch within 5μm of the branch point normalized by eGFP. Again, mTOR activity increases the overall expression of

CaMKIIα in the secondary branches (Figure 4.1B). As a control we measured Kv1.1 dendritic protein expression following mTORC1 inhibition. As previously observed inhibition of mTOR with rapamycin increased the dendritic expression of Kv1.1 (Figure 4.1C; Primary branch: Control: 1.00±0.17; Rapa: 2.00±0.45; Daughter branch: Control: 1.00±0.13; Rapa: 1.72±0.27). To determine the branch specific expression of CaMKIIα we developed a branch variability index where we took the absolute value of the normalized CaMKIIα signal in daughter branch A – daughter branch B. A value above zero suggests that more protein is expressed in one branch over the other. Indeed, CaMKIIα protein favors one branch over the other by ~55 ± 15% in neurons where mTOR is active relative neurons treated with the mTOR inhibitor rapamycin (Figure 4.1D; Control: 1.00±0.15; Rapa: 0.45±0.07). However, Kv1.1 branch variability remains constant with mTORC1 inhibition (Figure 4.1D).

mTOR inhibition causes the rapid degradation of CaMKIIα mRNA by the removal of its poly(A) tail.

How does mTOR inhibition reduce the branch specific expression of CaMKIIα? We recently demonstrated that the mTOR-dependent expression of CaMKIIα relies on its mRNA binding to the RNA-stabilizing protein HuD. Notably, when mTOR activity is inhibited with rapamycin high affinity HuD target mRNAs such as CaMKIIα protein is significantly reduced and its mRNA rapidly degrades. HuD is known to stabilize its target mRNAs by delaying the onset of mRNA degradation, a process that depends on the length of the poly(A) tail (Beckel et al., 2002). Furthermore, in yeast, it has been

reported that inhibition of TORC1 kinase accelerates the deadenylation-decapping pathway (Albig and Decker, 2001). mRNAs that decay rapidly in the presence of rapamycin have shorter poly(A) tails possibly through rapid deadenylation (Albig and Decker, 2001). In light of these data, we predict that overexpression of HuD may restore CaMKIIα branch variability index back to levels when mTOR is active by preventing its mRNA degradation with rapamycin in one branch over the other. To address this question we first assessed if mTOR activity promotes the degradation of CaMKIIα mRNA degradation by shortening its poly(A) tail. We analyzed the length of the poly(A) tail of CaMKIIα mRNA when mTORC1 kinase was active and/or inhibited by rapamycin. As shown in Figure 4.1E, the poly(A) tail of CaMKIIα mRNA is indeed shorter in neurons treated with rapamycin and is sensitive to RNase H treatment (Figure 4.1F), supporting the idea that CaMKIIα mRNA degrades when mTORC1 kinase is inhibited. As a further control, we measured the poly(A) tail length of Kv1.1. Consistent with the idea that mTOR inhibition reduces the branch specific expression of CaMKIIα through mRNA degradation, Kv1.1 mRNA levels and the length of its poly(A) tail remain the same regardless of mTOR activity (Figure 4.1G; Sosanya et al., 2013).

The RNA-binding protein HuD rescues CaMKIIα protein expression and branch variability when mTOR is inhibited.

Next we asked if overexpression of HuD can restore the CaMKIIα BVI when mTOR is inhibited by rapamycin by stabilizing CaMKIIα mRNA as indicated by an

increase in protein levels (Sosanya et al., 2013). Indeed, CaMKIIα protein expression increased significantly in the HuD overexpressing primary dendrite both when mTOR is active and inhibited with rapamycin (Figure 4.2A and B; HuD DMSO: 1.12±0.13; HuD Rapa: 1.52±0.23). Furthermore, the levels of CaMKIIα in the HuD overexpressing secondary branches were relative to control levels with rapamycin (Figure 4.2C). Interestingly, overexpression of HuD did not further increase the branch variability index for CaMKIIα when mTOR is active; however, it did restore it back to control levels when mTOR is inhibited with rapamycin (Figure 4.2D; HuD DMSO: 0.97±0.12; HuD Rapa: 0.82±0.13). These results suggest that HuD stabilizes the expression of CaMKIIα mRNAs in one daughter-branch over the other.

myc-HuD targets one branch over the other resulting in its differential branch expression

How does HuD rescue CaMKIIα differential branch expression when mTORC1 is inhibitied? To address this question, we measured overexpressed myc tagged HuD (myc-HuD) levels following mTORC1 inhibition in both primary and daughter branches. myc-HuD levels do not change with mTORC1 inhibition in either primary or daughter branches (Figure 4.2E, F and G; Primary: HuD DMSO: 1.00±0.11, HuD Rapa: 1.01±0.11; Daughter branch: HuD DMSO: 0.99±0.09, HuD Rapa: 0.92±0.06). Surprisingly, myc-HuD favors expression in one daughter branch over the other with rapamycin treatment as indicated by its increased BVI (Figure 4.2 E and H; HuD DMSO: 1.00±0.16, HuD Rapa: 2.27±0.59). This suggests that myc-HuD is more available to

protect CaMKIIα from degradation in one branch over the other resulting in CaMKIIα selective branch expression.

Discussion

Temporal and spatial regulation of protein expression is critical for a neuron to modify its synaptic input in an experience-dependent manner (Kandel, 2001; Govindariajan et al., 2006). It's widely accepted that proteins synthesized in response to strong stimuli at one set of synapses are available to other nearby synapses to facilitate plasticity at both sets of synapses known as "synaptic tag and capture" (Frey and Morris, 1997). Synapses that are "bound" together and distributed on a single dendritic branch increase the probability that excitatory postsynaptic potential (EPSP) amplification will occur (Govindarianjan, et al., 2006). Molecular mechanisms that mediate branch-specific expression of proteins that facilitate plasticity are unknown. One such mechanism may be the local translation of mRNAs coding for proteins that are required for lasting changes in synaptic efficacy, such as CaMKIIα. We determined that overexpression of HuD, the RNA-binding protein that promotes the expression of CaMKIIα, can prevent it from being degraded when mTOR activity is reduced and mediates its branch specific expression.

Chapter 5: Conclusion

Here, we discovered the molecular mechanism of mTOR mediated repression of Kv1.1. Previously, a novel mechanism of mTOR repression of local Kv1.1 translation was reported (Raab-Graham et al., 2006). With mTOR activity, the microRNA, miR-129-5p, binds to and suppresses the local translation of Kv1.1. We found that in order to relieve repression the RNA binding protein, HuD, binds Kv1.1 mRNA and promotes its local translation. Surprisingly, HuD levels do not change to relieve miR-129-5p binding to Kv1.1. Instead, when mTOR levels are repressed, other HuD high affinity targets, including CaMKIIα, Homer1a, and GAP-43, mRNAs degrade releasing HuD to bind its low affinity targets, such as Kv1.1.

This in vitro model allowed us to determine if these factors, miR-129-5p and HuD, regulate Kv1.1 expression in a disease model such as Temporal Lobe Epilepsy (TLE), where acute mTOR activity occurs. Previously, it has been shown that rapamycin treatment can prevent seizures in TLE suggesting that mTOR signaling is critical in TLE development (Zeng et al., 2009). We first determined the time course of mTOR dependent regulation of Kv1.1 following status epilepticus (SE). mTOR levels significantly drop 14 days post-SE corresponding to the peak of Kv1.1 levels in TLE. When mTOR levels were elevated at 21-30 days post-SE resulting in a significant increase in the number of behavioral seizures, Kv1.1 expression was significantly impeded by miR-129-5p. This drop in Kv1.1 led to a hyperpolarized action potential

threshold which could potentially contribute to the increased hyperexcitability observed in TLE.

This work has raised several new interesting questions. One of those questions is elucidating how a drop in mTOR activity may result in specific mRNAs to degrade. We have begun to address this question of elucidating how certain mRNAs may be targeted to degrade once mTOR activity drops (Chapter 4) and how this mRNA degradation may mediate differential branch expression. Secondly, are these regulatory factors of Kv1.1, important for the development of other diseases where mTOR activity is affected, including Alzheimer, Parkinson's, and Cancer (Costa-Mattioli and Monteggia, 2013; Hoeffer and Klann, 2010; Wong 2013). Thirdly, how are miR-129-5p levels elevated in TLE and finally, there are several predicated targets of miR-129-5p that have significant functions in the nervous system that may be regulated similarly to Kv1.1.

There is a growing body of evidence illustrating the importance of proper control of local translation and maintaining the balance of regulatory factors that oversee local translation. mTOR activity also has an important role as disruption of this key signaling pathway underlies many neurodegenerative diseases. The importance of the proper regulation and expression of Kv1.1 cannot be overstated. Lack of Kv1.1 results in development of seizures and therapeutic intervention with Kv1.1 overexpression blocks seizure activity (Wykes et al., 2012). Inhibition of mTOR with rapamycin blocks seizure progression (Zeng et al., 2009). However, long term treatment with rapamycin may have

severe side effects due to mTOR being a major signaling pathway involved in several important neural system functions (Costa-Mattioli and Monteggia, 2013; Hoeffer and Klann, 2010; Wong 2013). Finding key targets downstream of mTOR, such as Kv1.1 and possibly miR-129-5p, to effect may have less adverse side effects while still preventing disease.

Chapter 2 Figures

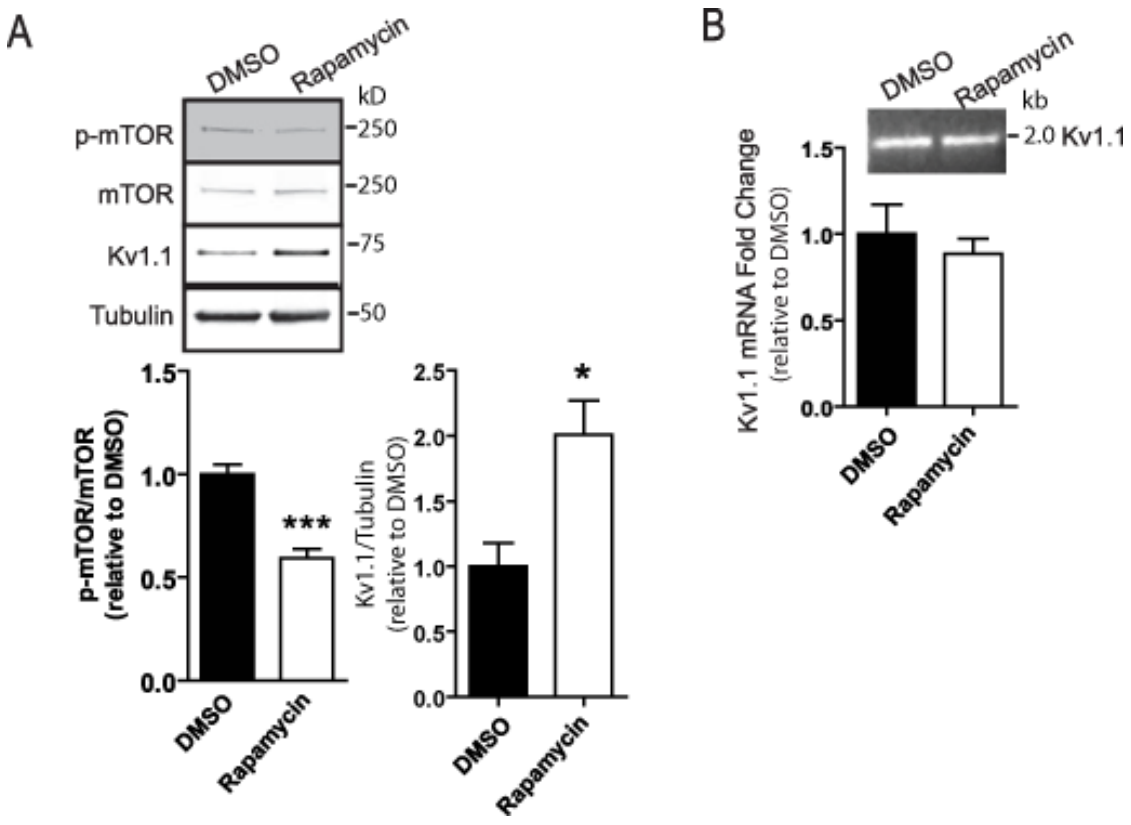

Figure 2.1. mTORC1 Kinase-dependent Repression of Kv1.1 is not Due to mRNA Stability

(A) SN were isolated from DMSO or rapamycin treated DIV21 cortical neurons. Representative western blots and quantification indicate the relative level of p-mTOR/mTOR and Kv1.1/tubulin (loading control). *** p< 0.001. *< 0.05, unpaired student's t-test. Error bars = SEM. p-mTOR: n=7; Kv1.1: n=5 over 2 independent cultures.

(B) SN RNA was isolated from DMSO or rapamycin treated cortical neurons and Kv1.1 mRNA was detected via RT-qPCR. Representative DNA gel of RT-qPCR samples showing amplification of a specific Kv1.1 band. Error bars =SEM. DMSO: n=5; rapamycin: n=6 over 3 independent cultures

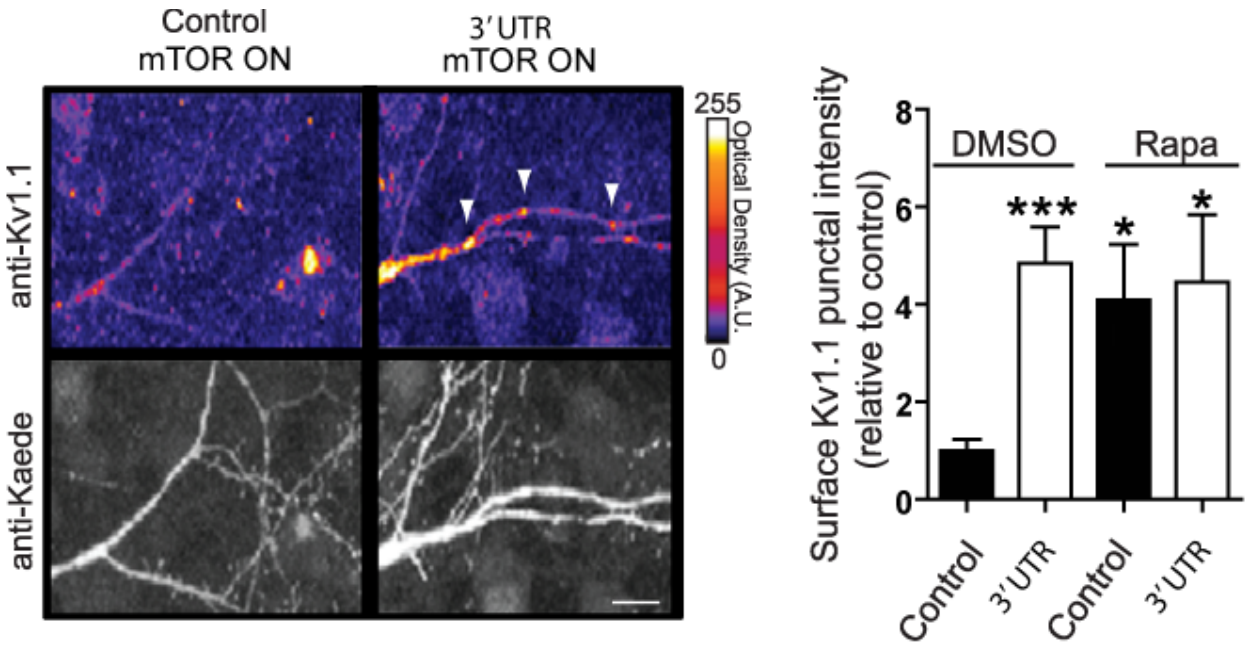

Figure 2.2. Overexpression of Kv1.1 3' UTR removes endogenous repression factors leading to increased Kv1.1 protein.

Left, representative neurons infected with Sindbis virus coding for control RNA (Kaede-MAP2 DTS) or Kv1.1 3' UTR (DIV21). Neurons were treated with DMSO or rapamycin. Scale bar = 20 µm. Right, quantification of surface expression of Kv1.1. ***p< 0.001, unpaired student's t-test. Control+DMSO: n=16 neurons, 21 dendrites; 3' UTR+ DMSO: n=17 neurons; 20 dendrites, control+Rapa: n=7 neurons, 8 dendrites, 3' UTR+Rapa: n=10 neurons, 11 dendrites. Error bars =SEM.

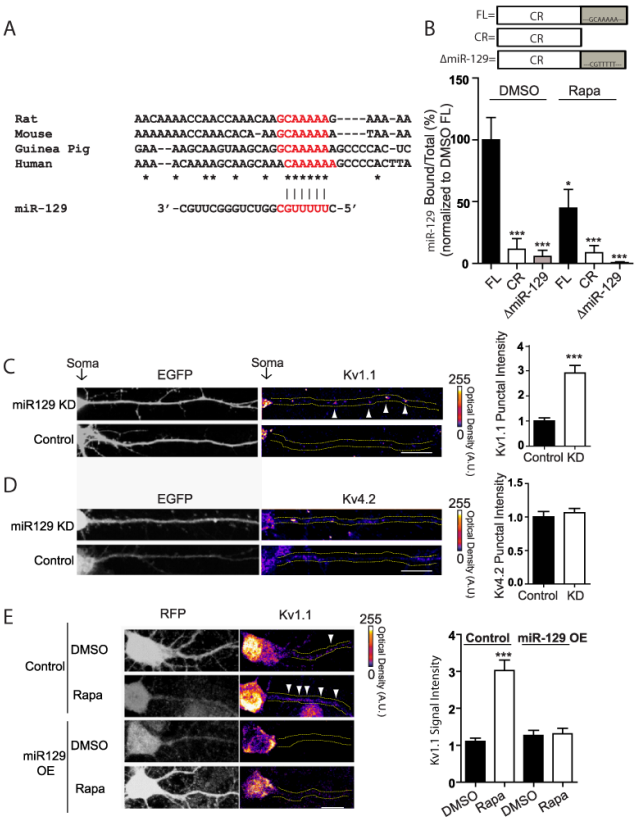

Figure 2.3: miR-129 Binds Kv1.1 RNA when mTORC1 Kinase is Active.

(A) Sequence alignment of Kv1.1 3'UTR indicates that the miR-129 seed match sequence (binding to nucleotide (nt) 2-8 of miR-129) is conserved among rat, mouse, guinea pig, and human, with nt 1 and 8 being less conserved. The miR-129 binding site is highlighted in red. Nucleotide number after the stop codon of each sequence shown: Rat, 181-212 nt; mouse, 177-207 nt; guinea pig, 1-34 nt; human 1-35 nt. The NCBI accession numbers are: rat M26161.1, mouse NM_010595, and human BC101733.1. For guinea pig, the UCSC genome browser database was used. The sequence is located in scaffold_107:2955798-2955831. (B) Above, schematic of RNA fragments used as bait to determine miR-129 binding to Kv1.1. mTRS indicated by gray box illustrating the miR-129 seed match sequence (FL) or the mutated sequence (ΔmiR-129). Below, qPCR of miR-129 pulled down from DMSO or rapa treated neurons. *p<0.05, ***p<0.001, one-way ANOVA, Dunnett's post-test compared to the FL DMSO. DMSO: FL n=11, CR n=8, ΔmiR-129 n=5; rapa: FL n=6, CR n=8, ΔmiR-129 n=4 over at least 4 independent cultures. CR: coding region; FL: Full-length. (C) Left, representative neurons transfected with EGFP alone (control) or with LNA to specifically knockdown miR-129 (KD). Arrows indicate Kv1.1 puncta in dendrites. Scale bar = 20 µm. Right, quantification of dendritic Kv1.1 punctal signal intensity. # dendrites: control: n=12; miR-129 KD: n=14. 9 neurons for each condition. ***p<0.001, unpaired student's t-test. (D) Left, representative neurons transfected with EGFP alone (control) or with LNA against miR-129 (KD). Right, quantification of dendritic Kv4.2 puncta. # dendrites: control: n=12; miR-129 KD: n=17. n= 8 and 10 neurons for control and miR-129 knockdown, respectively. (E) Left, hippocampal neurons transduced with either DsRed-control or DsRed-pre-miR129-2 lentivirus at DIV14. DMSO or rapa treated DIV21 neurons were stained and imaged for RFP and Kv1.1. Right, quantification of signal intensity. *** < 0.001, one-way ANOVA Tukey post-test. n=9 neurons per treatment. # dendrites: DMSO, Rapa: control n=17; n=14 and 15 for miR-129 OE.

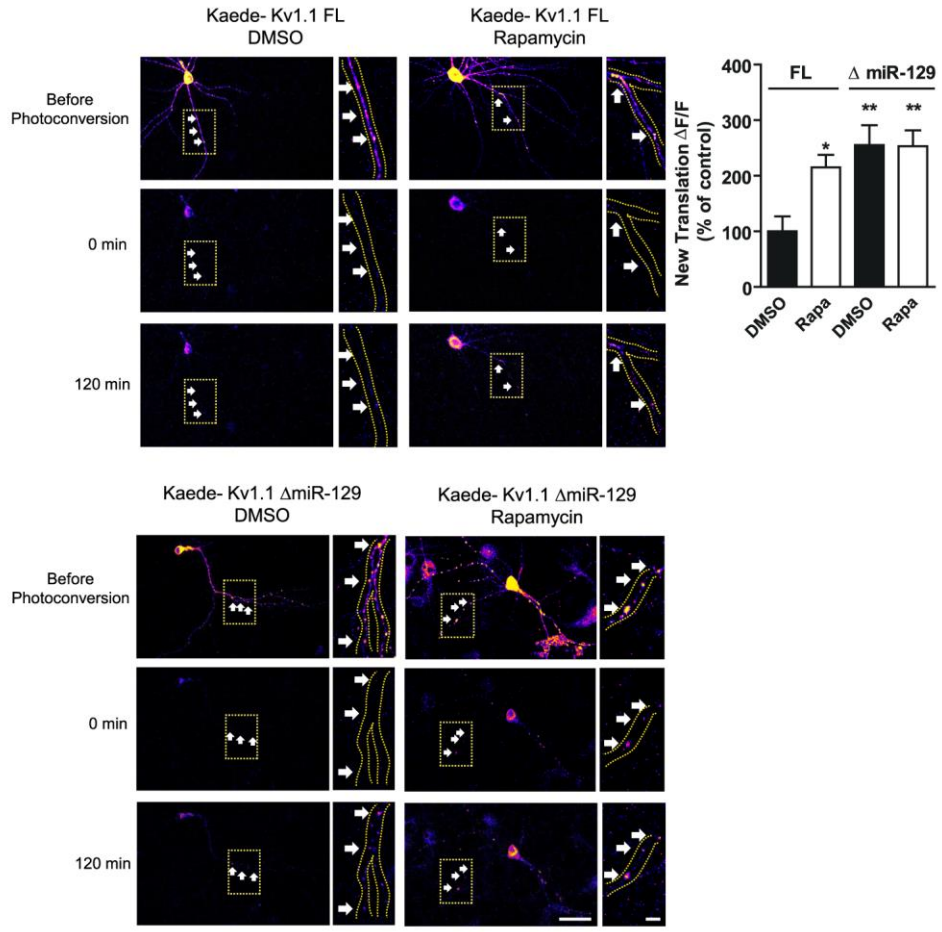

Figure 2.4: Mutating the miR-129 Seed Match Sequence in Kaede-Kv1.1 mRNA Results in mTORC1-independent New Translation in Neuronal Dendrites.

Live imaging of cultured hippocampal neurons expressing Kaede-Kv1.1 with (top panel, FL) or without (bottom panel, ΔmiR-129) seed match sequence of miR-129 in aCSF containing DMSO (left, control) or rapamycin (right, 200 nM) before, immediately after (0 time point), and 120 min after UV exposure to photoconvert Kaede-Kv1.1. Left: entire representative neuron. Right: blown up representative dendrite, indicated by arrows, greater than 60 µm from the soma. Large image: scale bar=50 µm, Insert: scale bar=10 µm. DMSO: FL n= 58 puncta, ΔmiR129 n=67 puncta; Rapamycin: FL n=51 puncta, ΔmiR-129 n=64. *p< 0.05 and **p< 0.01 one-way ANOVA, Tukey post-test, relative to Kaede-Kv1.1-FL DMSO. Error bars = SEM.

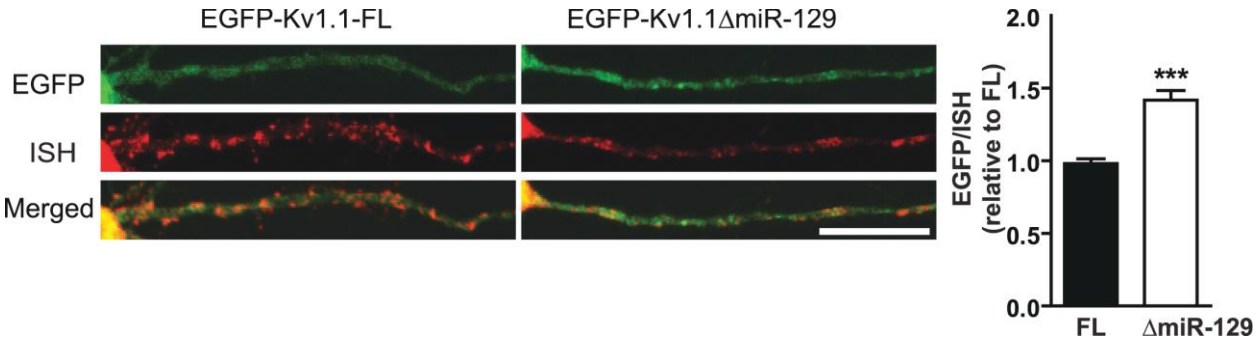

Figure 2.5. Mutating the miR-129 Seed Match Sequence in EGFP-Kv1.1 RNAIncreases Protein Levels without Changing RNA Levels.

Representative images of dendritic localization of EGFP-Kv1.1 RNA (red) and protein (green) with the intact (left, FL) or mutated (right, ΔmiR-129) miR-129 binding site revealed by *in situ* hybridization using a digoxigenin-labeled antisense oligo against EGFP. Scale bar = 20 μM, n=12 and 13 neurons for FL and ΔmiR-129, 40 dendrites each. Error bars = SEM.

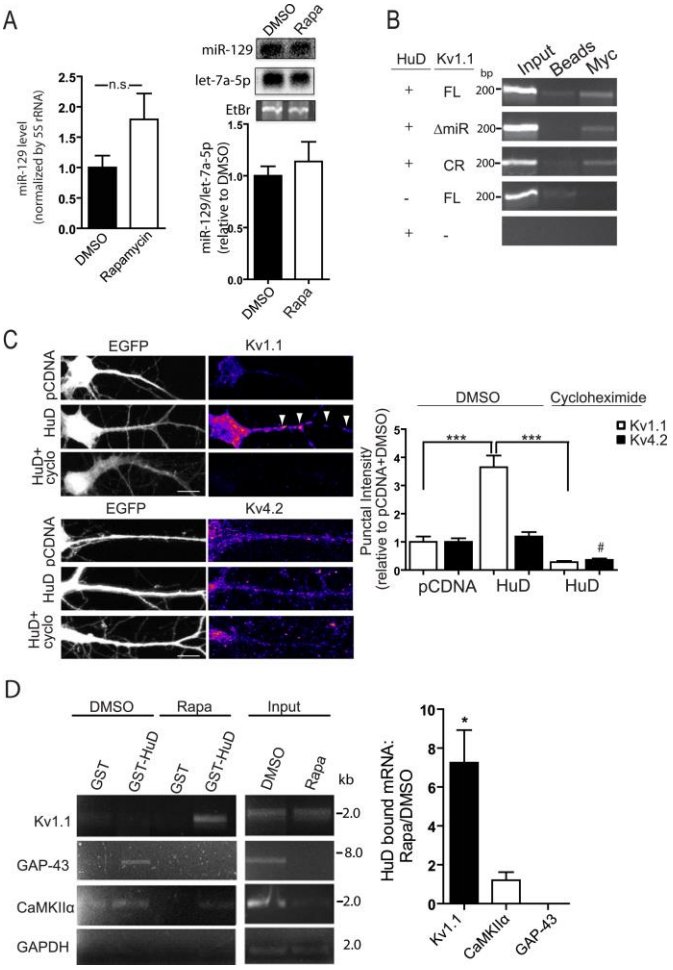

Figure 2.6. HuD Binds Kv1.1 mRNA when mTORC1 Kinase is Inhibited and Increases Kv1.1 Expression that is Reversed with Cycloheximide.

(A) Left, RT-qPCR amplification of miR-129 from neurons treated with DMSO or rapamycin. n=3 independent cultures and each sample was done in triplicate. The signal intensity for miR-129 was normalized to the signal intensity for let-7a which remained constant between DMSO or rapamycin treated neurons. As a loading control, ethidium bromide-stained low-molecular-weight RNA is shown in the bottom panel (labeled as EtBr). (B) RT-PCR amplification of Kv1.1 mRNA pulled down by HuD in HEK cells. HEK cells were co-transfected with myc-HuD and Kaede-Kv1.1 FL, CR, or ΔmiR-129. Anti-myc coated beads were used to pull down HuD bound to Kv1.1 mRNA outlined above. n=2 independent cultures. (C) Left, representative neurons (DIV14) co-transfected with EGFP and either pcDNA or HuD cDNA. Neurons were treated with DMSO or cycloheximide (50 µM) and Kv1.1 and Kv4.2 were detected with specific antibodies. Right, quantification of Kv1.1 and Kv4.2 punctal intensity in dendrites. # dendrites: DMSO: Kv1.1 pCDNA n=15, HuD n=18; Kv4.2 pCDNA n=17, HuD n=16. Cycloheximide: Kv1.1 HuD n=14, Kv4.2 HuD n=17. ***p<0.001, one-way ANOVA, Tukey's post-test. # Kv4.2 punctal intensity significant from DMSO+HuD. (D) RT-PCR amplification of Kv1.1 (top panel), GAP-43 or CaMKIIα (middle panel) mRNA copurified with GST-HuD or GST from DMSO or rapamycin treated cortical neurons (DIV21). GAPDH mRNA was detected in input but not pulldown (bottom panel). The ratio (Rapa/DMSO; right of the images) is determined by subtracting signal intensity of background GST band from the specific GST-HuD band and normalizing each band by their respective GAPDH input mRNA levels. HuD-RNA pulldown was replicated with 3 independent cultures for Kv1.1 mRNA and two independent cultures for CaMKIIα and GAP-43 mRNA. Significance for each mRNA was determined by a single t-test. *p<0.05 indicating the binding is significantly different from 1. A value of 1 suggests equal binding in both treatments.

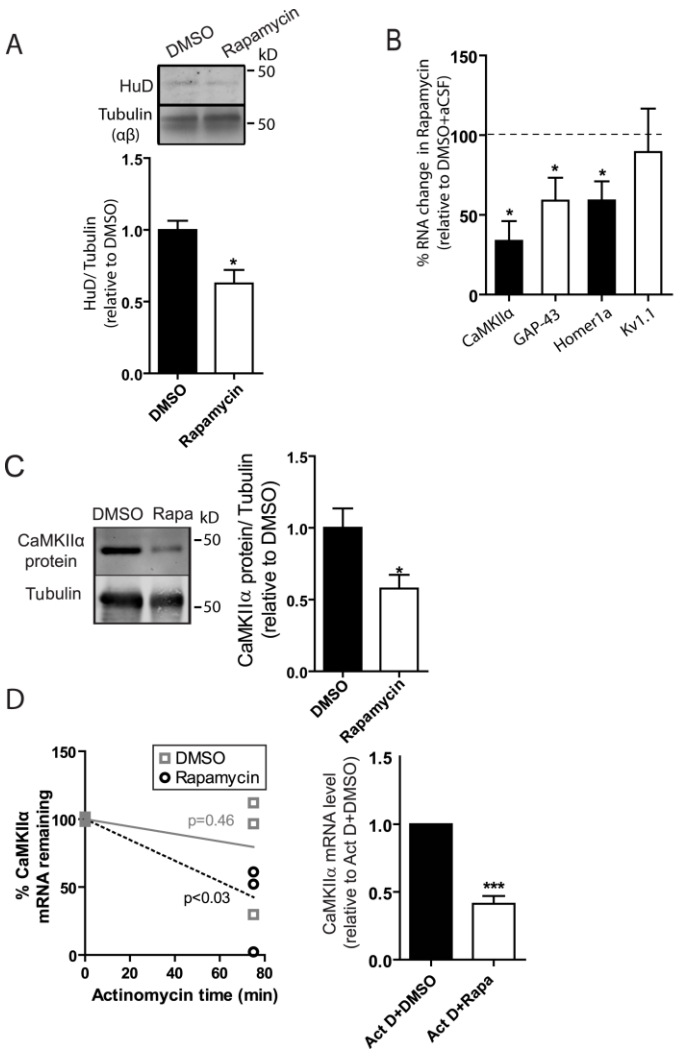

Figure 2.7. HuD Binding to Kv1.1 mRNA Coincides with Reduced Levels of other HuD Target mRNAs.

(A) Western blot analysis of HuD from synaptoneurosomes isolated from neurons treated with DMSO or rapamycin. DMSO: n=3; Rapa: n=4 over 2 independent cultures. (B) RT-qPCR analysis of CaMKIIα, GAP-43, Homer1a, and Kv1.1 mRNA isolated from control or rapamycin (200 nM) treated neurons normalized to the internal housekeeping gene, GAPDH which remains constant between the two conditions. CaMKIIα and Kv1.1: n=3, GAP-43: n=5, Homer1a: n=4; three-five independent cultures. Control was normalized to 100% and is indicated by dotted line on the graph. The mRNA target of HuD is shown as % remaining following rapamycin treatment. One-sample t-test was done to determine statistical significance from control. Error bars = SEM. *p<0.05. (C) Representative blot and quantification of SNCaMKIIα protein isolated from DMSO or rapa treated cortical neurons. Error bars = SEM. *p<0.05. DMSO: n=5; Rapa: n=6. (D) Neurons were treated with Actinomycin D (12 µM) for 4-5 hrs prior to treating with DMSO or rapamycin for 75 min. Degradation was measured by RT-qPCR for CaMKIIα mRNA and reported as the percent decrease with the addition of rapamycin relative to actinomycin alone. Error bars = SEM. n=5 per treatment. ***p<0.001.

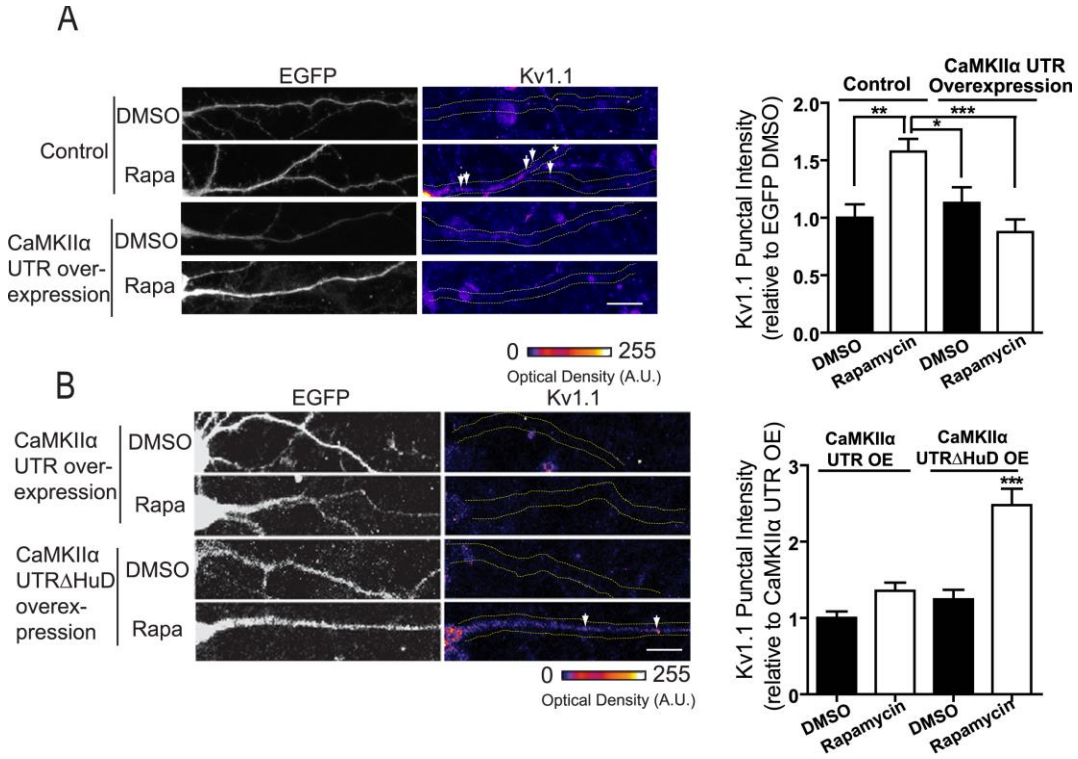

Figure 2.8. Overexpression of the CaMKIIα UTR with Multiple HuD Sites Occludes the Increase in Dendritic Kv1.1 Expression.

(A) Representative neurons (DIV 21) transfected with cDNA coding for EGFP or dGFP CaMKIIα UTRs were treated with DMSO or rapamycin (200 nM), fixed and immunostained for EGFP and Kv1.1. Quantification of dendritic Kv1.1 signal intensity for control (EGFP) or CaMKIIα UTR overexpression normalized by baseline signal for dendritic Kv1.1 under control conditions (EGFP/DMSO). # dendrites: DMSO: control n=22, CaMKIIα UTR OE n=29; rapamycin: control n=33, CaMKIIα UTR OE n=31. *p<0.05, **p<0.01, ***p<0.001, one-way ANOVA, Tukey's post-test.
(B) Representative neurons expressing dGFP CaMKIIα UTR without the putative HuD binding sites treated with DMSO or rapamycin (200 nM) were quantitated as outlined in (A) of this figure. # dendrites: CaMKIIα UTR OE, DMSO: control n= 20; CaMKIIα UTR OE, rapamycin n= 23; ΔHuD OE, DMSO n= 20; ΔHuD OE, rapamycin n= 24. ***p<0.001 relative to all other conditions, one-way ANOVA, Tukey's post-test.

Chapter 2 Supplemental Figures

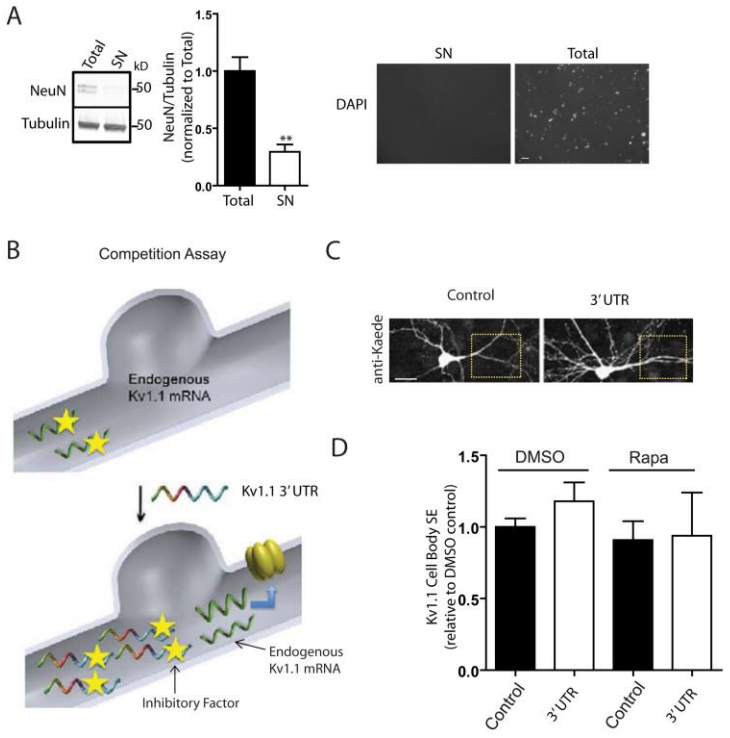

Figure S2.1. Post-transcriptional Regulation of Kv1.1 mRNA Mediated by mTORC1 Kinase Repressive Sequence in the 3'UTR of Kv1.1.

(A) Left, representative western blot of total lysate or synaptoneurosomal (SN) preparation probed for the nuclear marker, NeuN. Quantification is shown of NeuN/Tubulin protein. Total: n=4; SN: n=3 over 2 independent culture. Right, total lysate or SN preparation stained for the nuclear marker, DAPI. Scale bar = 10µm.

(B) Schematic of competition assay where DIV21 cortical neurons were infected with a Sindbis virus coding for the 3' UTR of Kv1.1. Overexpression of Kv1.1 3' UTR is predicted to remove the inhibitory factor(s) from endogenous Kv1.1 and therefore result in an increase in the endogenous surface expression of Kv1.1. (C) Representative neurons infected with Sindbis virus coding for control RNA (Kaede-MAP2 DTS) or Kv1.1 3' UTR (DIV21) show similar morphology. Scale bar = 20 µm. (D) Surface expression of Kv1.1 in the cell body of neurons infected with either control RNA (Kaede-MAP2 DTS) or Kv1.1 3' UTR. 18 hours post-infection neurons were treated with either carrier (DMSO) or rapamycin. Kv1.1 intensity is normalized to Kaede expression. Related to Figure 2.2. Error bars represent SEM.

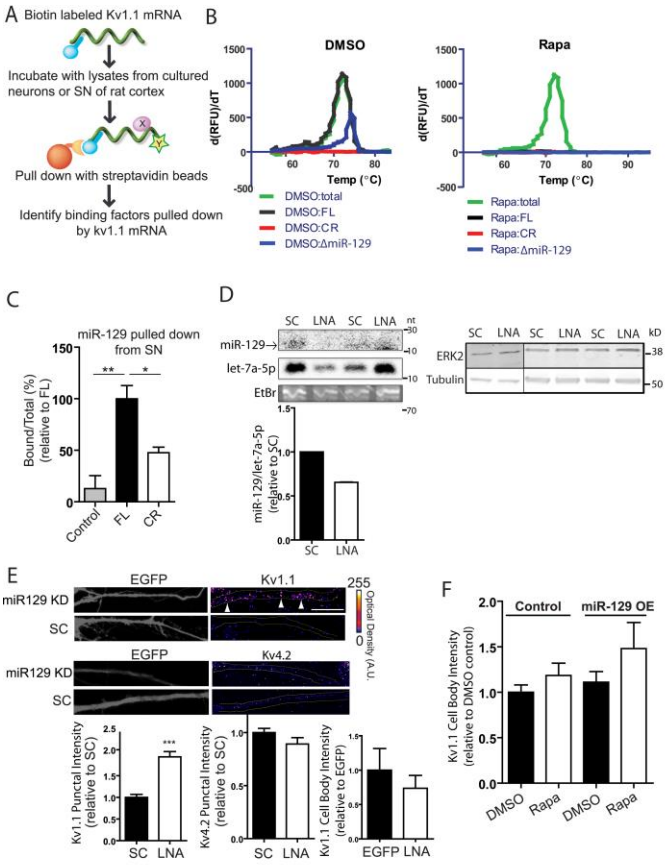

Figure S2.2. miR-129 Binds to Kv1.1 mRNA when mTOR is On and Reduces Kv1.1 Expression.

(A) Schematic of RNA affinity capture assay used to identify factors binding to Kv1.1 mRNA. Kv1.1 FL, Kv1.1 CR, or Kv1.1 (B) Representative melt curves of real-time PCR for miR-129 pulled down by Kv1.1 RNA (related to Figure 2.3B; n=3 independent cultures). FL, full length Kv1.1 RNA with mTRS; CR, coding region of Kv1.1 RNA; ΔmiR-129 , full length Kv1.1 RNA with miR-129 seed match sequence mutated; RFU, relative fluorescent unit. (C) miR-129 pull-down from SN as determined by qPCR and normalized to 10% total RNA input. (n=3 rats done in duplicate) Control, no RNA. * indicates $p<0.05$, ** indicates $p<0.01$. Error bars indicate SEM. (D) miR-129 levels were reduced in cortical neurons transfected with LNA against miR-129 compared to scrambled LNA, as shown by northern blot analysis. miR-129 levels were normalized to the miRNA, let7; The data shown are from a single representative experiment out of two repeats; For the experiment shown n=2. Error bar = SEM. As a positive control for LNA inhibition of miR-129, SNs isolated from transfected cortical neurons were immunoblotted using an ERK2 specific antibody. SC and LNA: n=3 over 2 independent cultures. (E) Top: Representative neurons EGFP+Scrambled (SC) or EGFP+miR-129 Knockdown (KD) LNA for Kv1.1 and Kv4.2. Bottom left, quantification of Kv1.1 showed ~2 fold increase in punctal signal intensity with no change in Kv4.2 (middle). *** indicates $p<0.001$. Kv1.1, SC: n=9 and 12, LNA: n=7 and 12, neurons and dendrites, respectively. Kv4.2, SC: n=9 and 14, LNA: n=5 and 8 neurons and dendrites, respectively. Bottom, right: cell body analysis of neurons co-transfected with EGFP+SC or EGFP+miR-129 KD LNA. Kv1.1 intensity is normalized to EGFP signal. Error bars indicate SEM. (F) Kv1.1 intensity measured in the cell body of hippocampal neurons transduced with either DsRed-control or DsRed-pre-miR-129-2 lentivirus at DIV14. At DIV21 neurons were treated with either DMSO or rapamycin. Kv1.1 intensity is normalized to Red fluorescent protein signal. Related to Figure 2.3E. Error bars represent SEM.

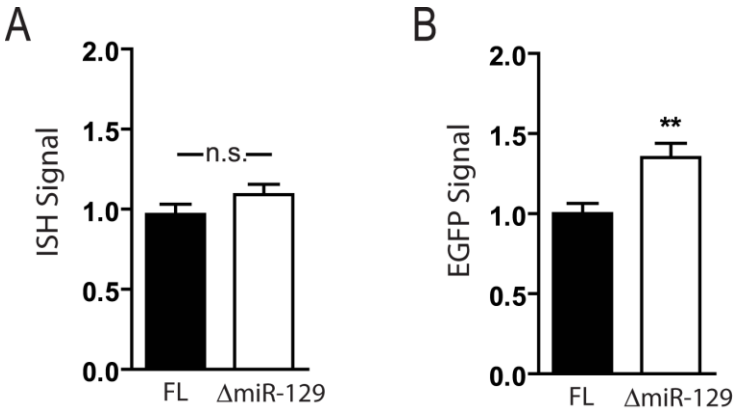

Figure S2.3. Mutation of miR-129 Binding Site in mTRS Increases Kv1.1 Protein Level without Changing the RNA Level.

As described in figure 2.4, neurons were infected with sindbis virus coding for EGFP-Kv1.1 RNA with the intact (FL) or mutated (ΔmiR-129) miR-129 binding site. Kv1.1 protein level was then determined by immunofluorescence and the RNA level determined by in situ hybridization (ISH) using a digoxigenin-labeled antisense oligo against EGFP. (A) Quantification of ISH signal (representing the RNA level). (B) Quantification of EGFP signal to control for volume (representing the Kv1.1 protein level). The result reveals that the exogenous RNA levels are relatively equal between constructs with a significant increase in protein level with ΔmiR-129. FL: n=12 neurons; ΔmiR-129: 13 neurons; n=40 dendrites each. Error Bars represent SEM.

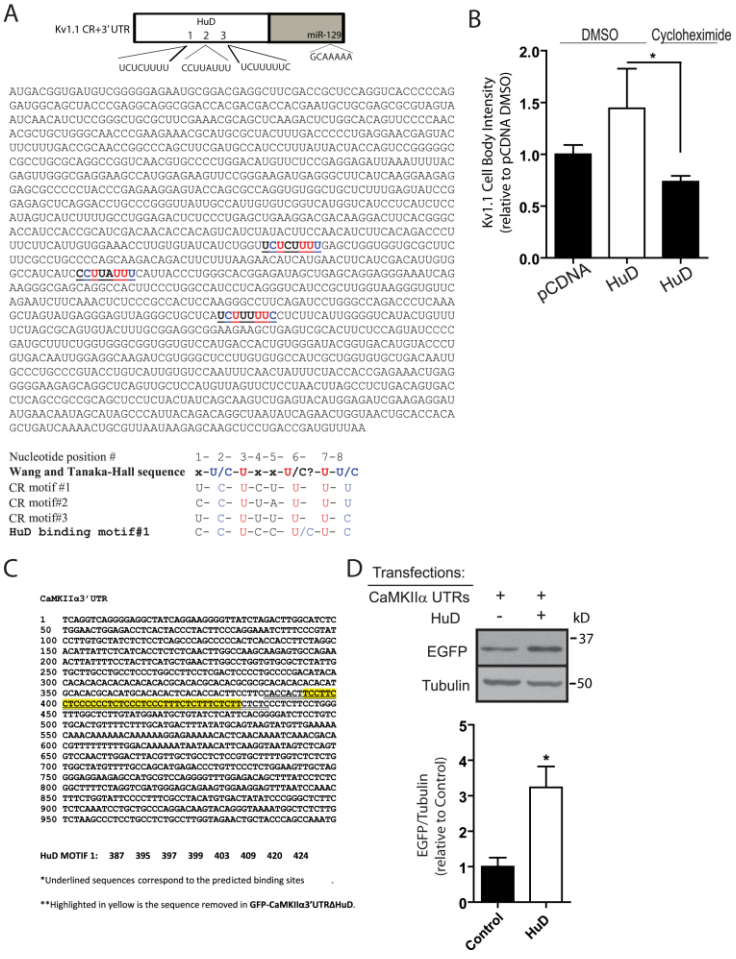

Figure S2.4. Predicted Low-Affinity HuD Binding Sites in the CR of Kv1.1 mRNA and HuD Binding to EGFP-CaMKIIα UTR, with Predicted HuD Binding sites, results in Increased EGFP levels.

(A) Top, cartoon of Kv1.1 coding region (CR) and mTRS indicating the approximate sites of the predicted HuD and verified miR-129 binding sites. Below, the CR of Kv1.1 has 3 motifs that are consistent with the 8-nucleotide consensus sequence identified by Wang and Tanaka-Hall, and are equivalent to recently identified HuD binding motif #1(1,2). The alignment of these potential HuD binding sites with the consensus sequences are shown below with red residues representing U, blue residues representing C or U, and black residues representing arbitrary nucleotides. (B) Kv1.1 intensity measured in the cell body of neurons co-transfected with EGFP and either pcDNA or HuD cDNA. Neurons were treated with DMSO or cycloheximide (50 µM). Kv1.1 intensity is normalized to EGFP. Related to Figure 2.6C. Error bars represent SEM. * < 0.05. (C) Sequence of CaMKIIα cDNA coding for the 3' UTR included in the construct used for the competition assay in Figure 2.7A and B. Underlined sequence indicates region of 8 putative HuD binding sites as denoted below by nucleotide number (HuD motif 1). Highlighted in yellow is the region removed to eliminate the HuD binding sites as a control for Figure 2.7B.
(D) HEK293T cells were transfected with EGFP-CaMKIIα UTRs plus either pCDNA or HuD and total protein was isolated. Representative blot of EGFP and Tubulin are shown with quantification below. HuD overexpression resulted in a significant increase in EGFP protein as a possible result of binding CaMKIIα UTRs. There are 8 predicted overlapping HuD binding sites within this 3'UTR of CaMKIIα. Error bars represent SEM. * indicates $p<0.05$. n=4 for control and HuD.

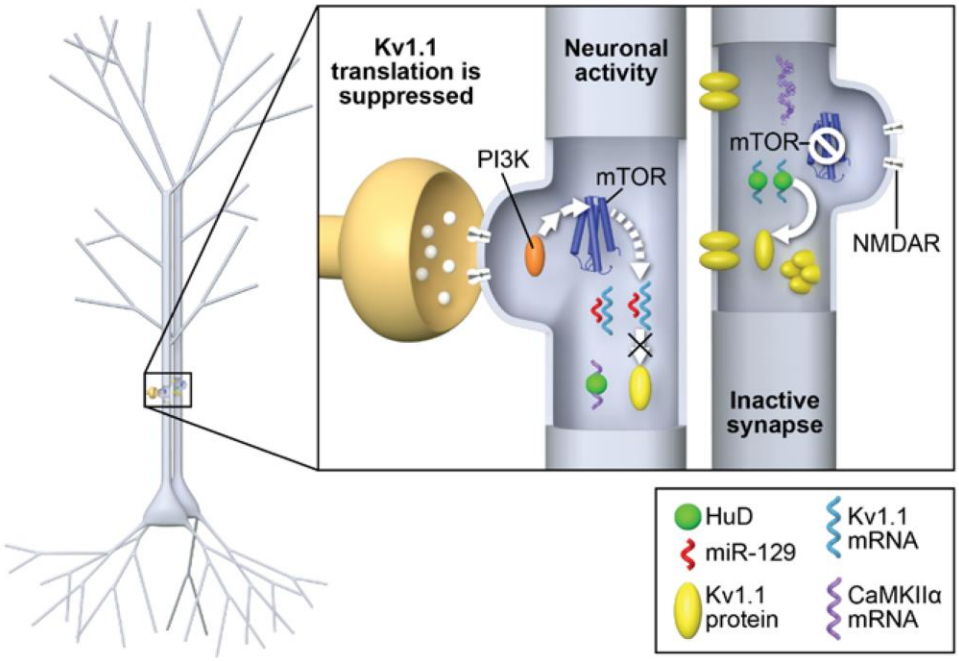

Figure S2.5. Model for Bidirectional Regulation of Kv1.1 mRNA Translation.

With NMDAR/mTORC1 activation, miR-129 binds Kv1.1 mRNA while HuD binds to its high-affinity targets, such as CaMKIIα mRNA, repressing Kv1.1 mRNA translation (left dendrite). With mTORC1 inhibition, HuD's high affinity targets are degraded, increasing the available HuD to bind to its low affinity targets. As a result, HuD binds to Kv1.1 mRNA and miR-129 binding is relieved, promoting Kv1.1 mRNA translation resulting in more Kv1.1 channels on the dendritic membrane (right dendrite). mTORC1 regulated CaMKIIα mRNA degradation serves as a switch to release HuD and allow its binding to Kv1.1 mRNA mediating the local translation of Kv1.1 mRNA.

Chapter 3 Figures

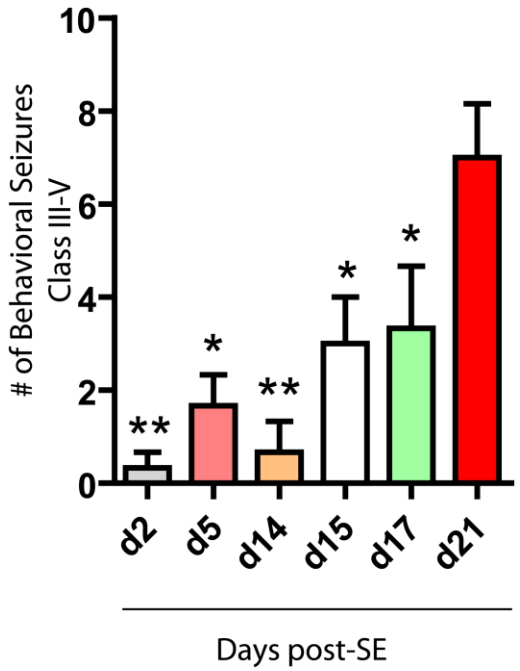

Figure 3.1: Number of Behavioral Seizures increase at 21 days post-SE.

Day 2 after KA injected rats reached SE, they were placed in an isolated room where they were continuously video monitored for the progression of behavioral seizures until day 21 post-SE. KA rats were scored by number of behavioral seizures ranging from Class III-V. *<0.05; **<0.01. P value represents significance to 21 days post-SE by One-way ANOVA Newman-Keuls post test.

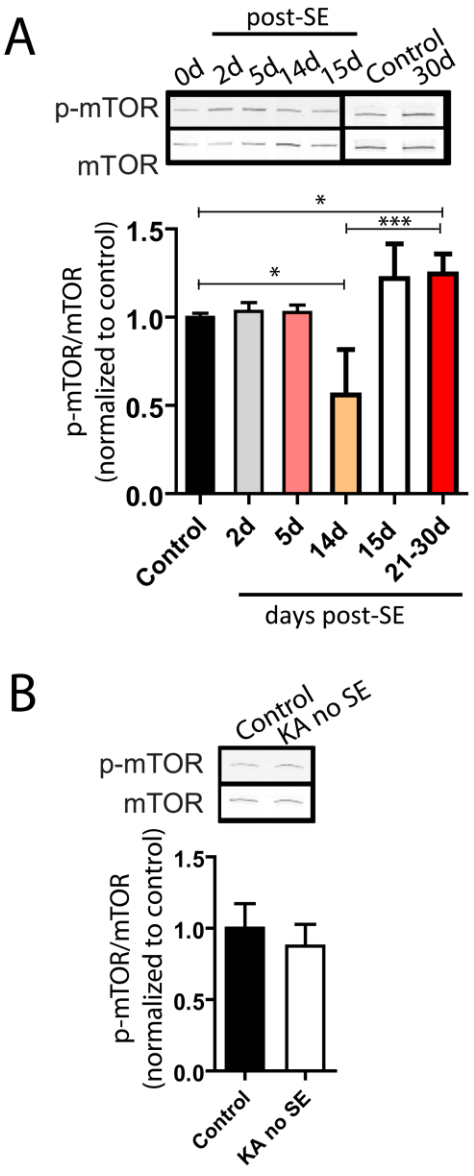

Figure 3.2: Differential mTOR activity occurs post-SE.

(A) Hippocampal SN protein was isolated from 0d (control, saline+PB) and kainic acid (KA+PB) treated animals 2, 5, 14, 15 and 21-30 days post-SE. Top, representative Western blot of a SDS-PAGE gradient gel probed with antibodies against p-mTOR and mTOR. Quantification of p-mTOR signal normalized by mTOR levels and relative to 0d is shown below. control: n=20, 2d post-SE: n=6, 5d post-SE: n=5, 14d post-SE: 2, 15d post-SE: 3, 21-30d post-SE: n=9. *<0.05, ***<0.005. One-way ANOVA Dunnett post test.

(B) Hippocampal SN protein was isolated from control (saline+PB) and kainic acid (no SE) treated animals that did not progress past class III. ~90% of animals injected with KA reach Class V. Representative Western blot of a SDS-PAGE gradient gel probed with antibodies against p-mTOR and mTOR with the quantification of p-mTOR signal normalized by mTOR levels is shown. Control: n=4, no SE: n= 5. Error bars are SEM.

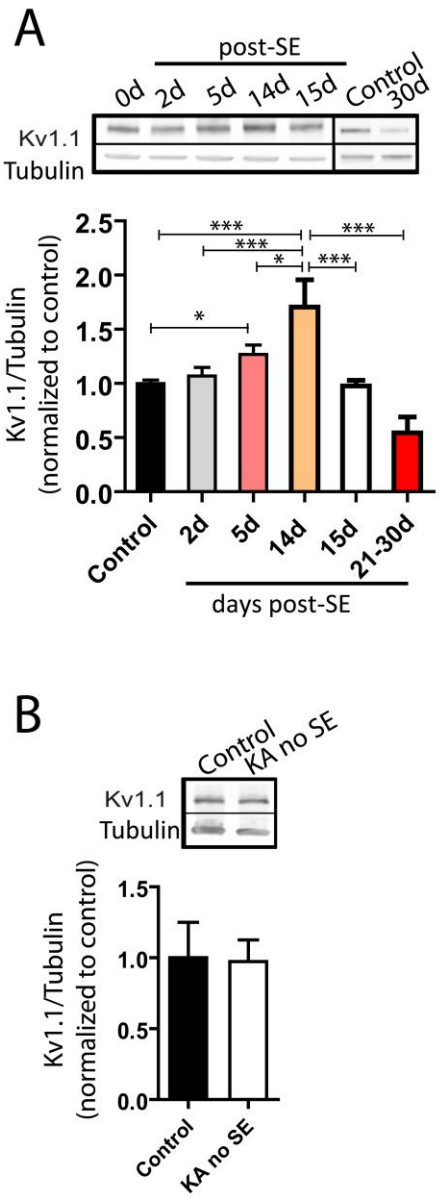

Figure 3.3: Reduced mTOR activity results in peak Kv1.1 protein levels at 14d post-SE whereas when mTOR activity is increased 21-30 days post-SE Kv1.1 levels drop.

(A) Hippocampal SN protein was isolated from 0d (control, saline+PB) and kainic acid (KA+PB) treated animals 2, 5, 14, 15 and 21-30 days post SE. Top, representative Western blot of a SDS-PAGE gradient gel probed with antibodies against Kv1.1 and tubulin. Quantification of Kv1.1 signal normalized by tubulin levels and relative to 0d is shown below. *p<0.05. ***p<0.005. One-way ANOVA Tukey post test. Control: n=18, 2d post-SE: n=6, 5d post-SE: n=5, 14d post-SE: n=2, 15d post-SE: n=3, 21-30d post-SE: n=5. Error bars represent SEM.

(B) Representative Western blot of a SDS-PAGE gradient gel probed with antibodies against Kv1.1 and tubulin and quantification of Kv1.1 signal normalized by tubulin levels is shown. Control: n=4, no SE: n= 5. Error bars represent SEM.

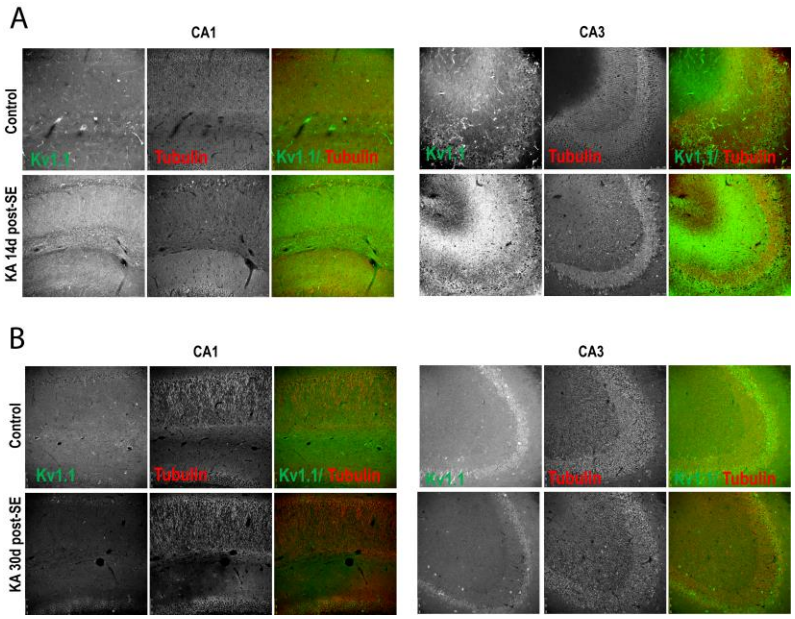

Figure 3.4: Kv1.1 protein increases 14 days post-SE and decreases 30 days post-SE in the CA1 and CA3 region.

(A) Coronal slices from control and 14 days post-SE rats were immunostained for Kv1.1 and tubulin (volume control) followed by imaging with the Leica microscope 20x objective. Representative slices are shown of the CA1 and CA3 region from 14 days post-SE rats. Kv1.1 is pseudocolored green and tubulin is pseudocolored red.

(B) Coronal slices from control and 21-30 days post-SE rats were immunostained for Kv1.1 and tubulin (volume control) followed by imaging with the Leica microscope 20x objective. Representative slices are shown of the CA1 and CA3 region from 30 days post-SE rat. Kv1.1 is pseudocolored green and tubulin is pseudocolored red.

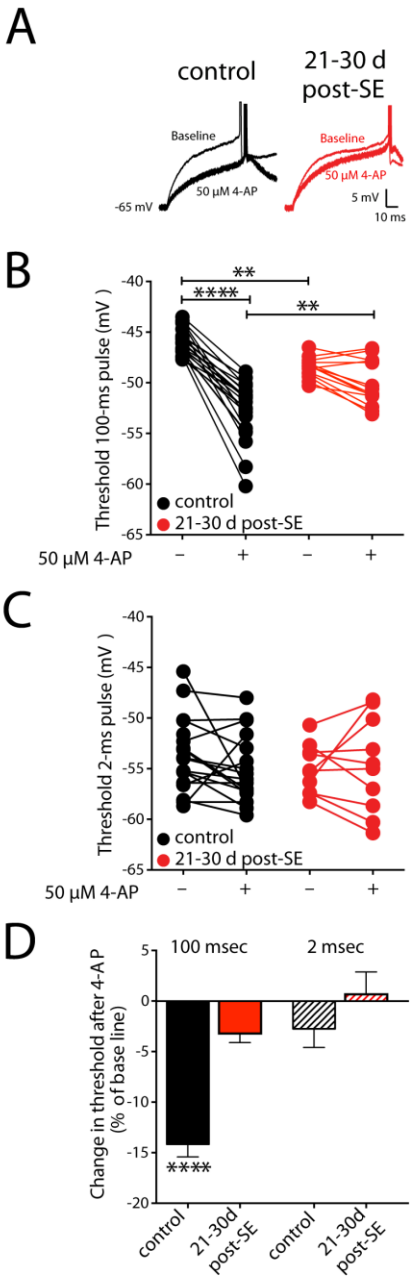

Figure 3.5: CA1 pyramidal neurons have a more hyperpolarized action potential threshold and reduced 4-AP sensitivity post SE.

(A) Voltage recordings showing a single action potential elicited by a 100-msec current injection before (thin line) and after (thick line) application of 50 µM 4-AP from control (black) and 21-30d post-SE (red) CA1 neurons. (B) The threshold of action potentials elicited by 100-msec current injection is significantly hyperpolarized at 21-30d post-SE relative to control. 4-AP application significantly hyperpolarized the threshold of action potentials in control but not 21-30d post-SE neurons. **p<0.01, ****p<0.001. (C) There is no significant difference in action potential threshold elicited during the 2-msec steps between control and 21-30d post-SE CA1 neurons. 4-AP has no significant effect on action potential threshold in either control or 21-30d post-SE neurons. (D) Summary data showing that 4-AP significantly hyperpolarized action potential threshold in control but not 21-30d post-SE neurons for the 100-msec current injection. ****p<0.001 compared to 21-30d post-SE.

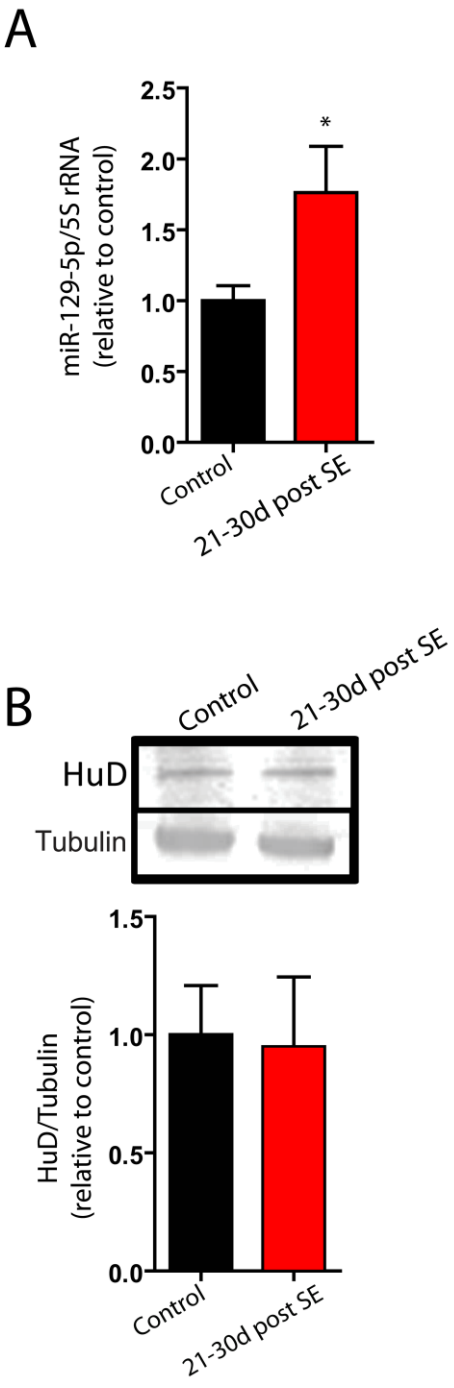

Figure 3.6: The negative regulator of Kv1.1 expression (miR-129-5p) is elevated 21-30d post-SE correlating with decreased Kv1.1 and a hyperpolarized action potential

(A) Hippocampal SN RNA isolated from 0d (saline+PB) and kainic acid (KA+PB) treated animals 21-30 days post SE. RT-qPCR analysis of miR-129-5p levels normalized to 5S rRNA is shown. Note, increased miR-129-5p levels are shown 21-30 days post-SE. 0d: n=9, 21-30d: 10. *<0.05 Error bars = SEM.

(B) Hippocampal SN protein isolated from 0d (saline+PB) and kainic acid (KA+PB) treated animals 21-30 days post SE. Representative blot of HuD and tubulin is shown. Quantification of HuD normalized to tubulin is shown below. 0d no-SE: n=7, 21-30d post-SE: n=7 Error bars represent SEM.

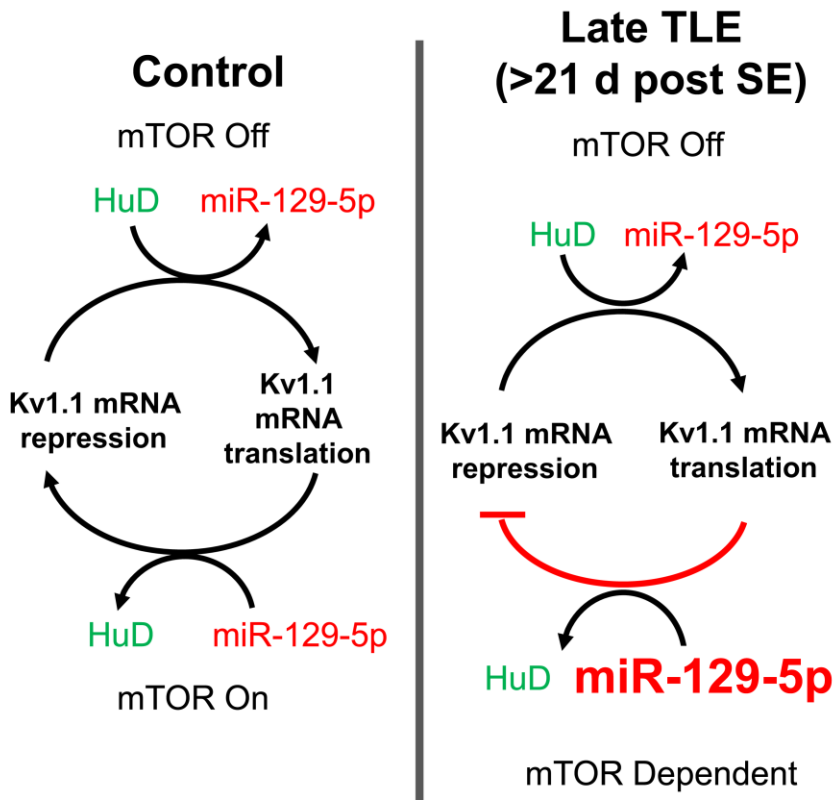

Figure 3.7: Model for post-transcriptional regulation of bidirectional changes in Kv1.1 expression in TLE.

Left panel, under conditions where mTOR activity is off Kv1.1 mRNA repression via miR-129-5p is relieved by HuD resulting in Kv1.1 expression. In contrast, when mTOR activity is on miR-129-5p binds to Kv1.1 mRNA and HuD is released. Under normal conditions the relative levels of miR-129-5p and HuD do not change to favor Kv1.1 binding (Sosanya et al., 2013). At later stages of TLE (21-30 days post-SE), when mTOR activity is elevated, miR-129-5p levels increase favoring translational repression of Kv1.1 mRNA (red arrow) leading to neuronal hyperexcitability.

Chapter 4 Figures

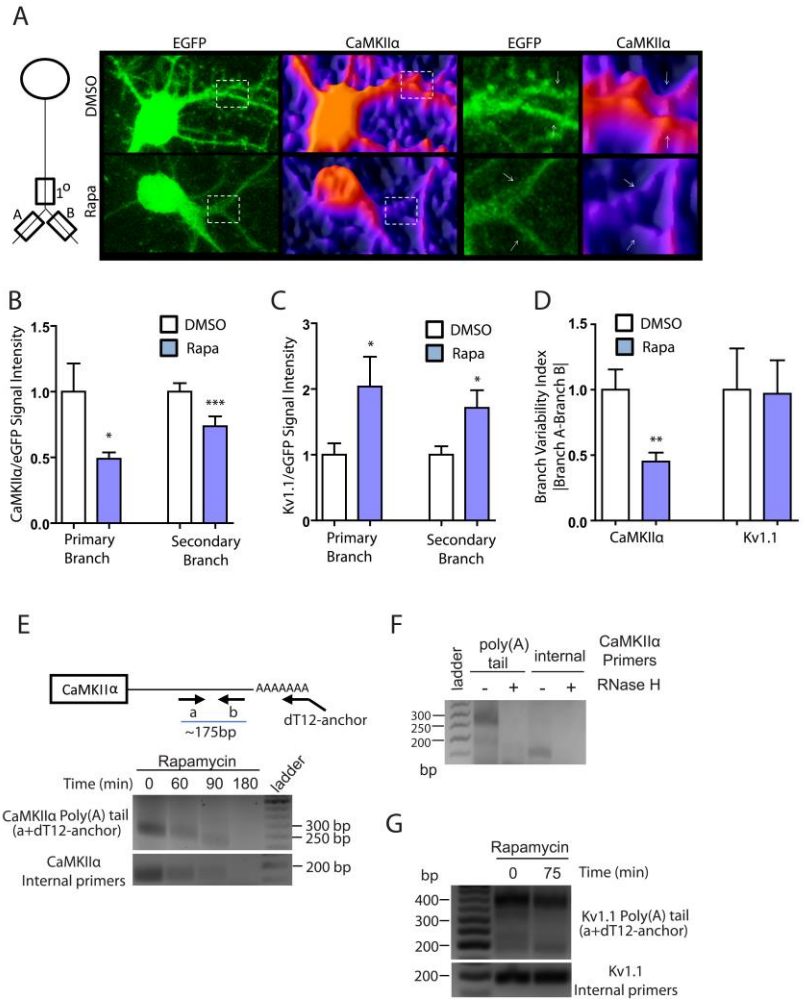

Figure 4.1. mTOR blockade removes CaMKIIα branch variability by promoting the rapid degradation of CaMKIIα. (A) Cultured hippocampal neurons transfected with pCDNA+eGFP were treated with DMSO or Rapamycin and immunostained for CaMKIIα. Representative neurons are shown. White boxes indicate the primary and secondary branches where signal intensity measurements were taken in B, C, and D. (B) The signal intensity of CaMKIIα in neurons treated with DMSO or Rapamycin was measured as a ratio over eGFP, 10 µm before the branch point. As a control, Kv1.1 signal intensity was also measured. *<0.05, ***<0.005. (C) The signal intensity of CaMKIIα in neurons treated with DMSO or Rapamycin was measured as a ratio over eGFP, 10 µm after the branch point. Note, CaMKIIα protein decreases with rapamycin treatment. As a control, Kv1.1 signal intensity was also measured. *<0.05. (D) The difference between CaMKIIα protein was measured between daughter branches and graphed as branch variability index or BVI. **<0.01. (E) Neurons treated with rapamycin for 0, 60, 90, and 180 min were harvested from cultured neurons and PCR was performed with specific primers. Above, schematic of CaMKIIα internal primers (a and b) and primers that recognize the poly(A) tail of CaMKIIα. (F) As a control, PCR was performed following RNase H treatment. (G) As a control, PCR was performed using Kv1.1 specific primers and primers that recognize the poly(A) tail of Kv1.1. Note, neither the poly(A) tail or the mRNA levels of Kv1.1 change in rapamycin treated neurons.

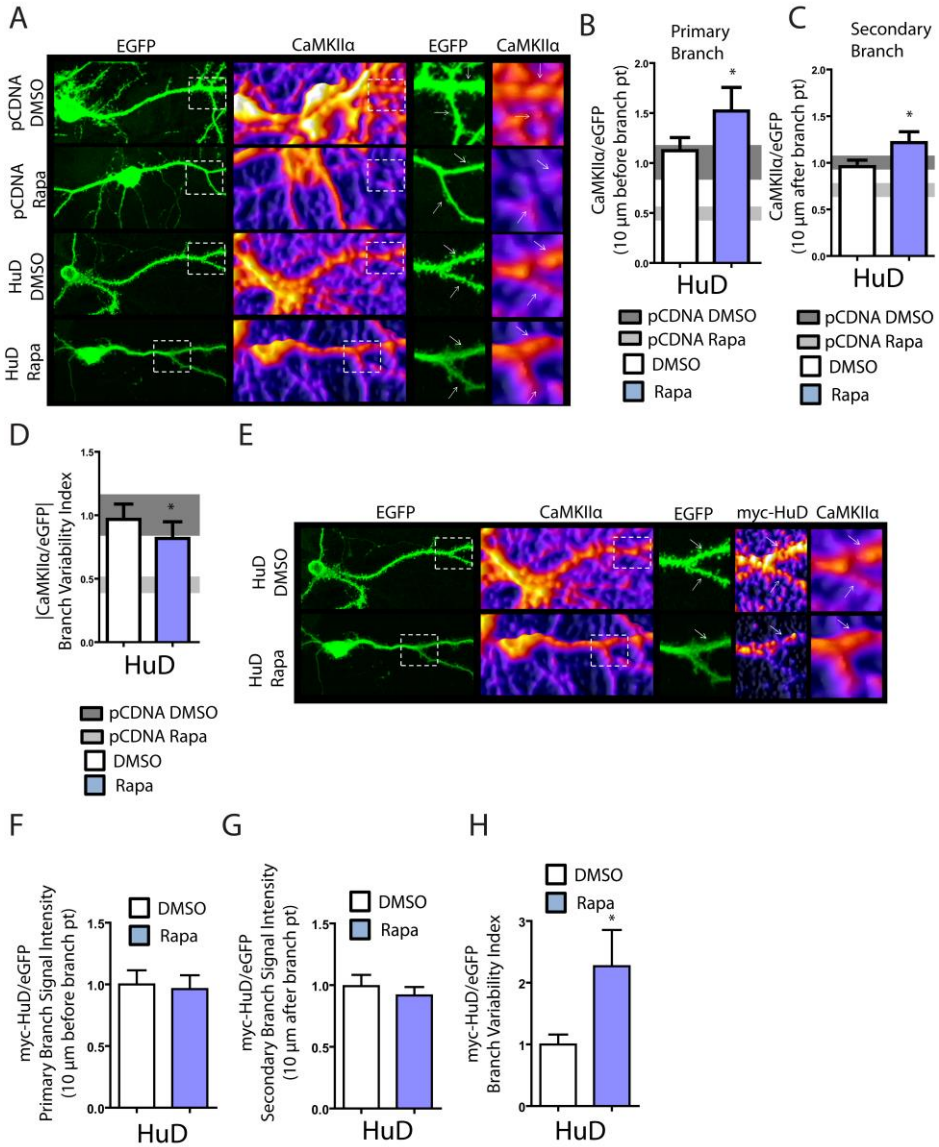

Figure 4.2. myc-HuD differential branch expression rescues reduced CaMKIIα Branch Variability.

(A) Cultured hippocampal neurons were transfected with pCDNA+eGFP or HuD+eGFP, and treated with either carrier (DMSO) or rapamycin. Representative neurons stained for CaMKIIα are shown. CaMKIIα protein is indicated as a heat map. (B) Primary (10 µm before branch point) dendritic CaMKIIα protein was measured as a ratio over eGFP. *<0.05 significantly different from pCDNA DMSO neurons. (C) CaMKIIα protein in daughter branches (10 µm after the branch point) was measured as a ratio over eGFP. *<0.05 significantly different from pCDNA Rapa neurons. (D) The difference between CaMKIIα/eGFP protein was measured between daughter branches and graphed as BVI. *<0.05 significantly different from pCDNA Rapa neurons. (E) Cultured hippocampal neurons were transfected with pCDNA+eGFP or HuD+eGFP, and treated with either carrier (DMSO) or rapamycin. Representative neurons stained for myc-HuD are shown. myc-HuD protein is indicated as a heat map. (F) Primary (10 µm before branch point) dendritic myc-HuD protein was measured as a ratio over eGFP. (G) myc-HuD protein in daughter branches (10 µm after the branch point) was measured as a ratio over eGFP. (H) The difference between myc-HuD/eGFP protein was measured between daughter branches and graphed as BVI. *<0.05.

Works Cited

Aakalu, G., W.B. Smith, N. Nguyen, C. Jiang, and E.M. Schuman. 2001. Dynamic visualization of local protein synthesis in hippocampal neurons. *Neuron*. 30:489-502.

Abdelmohsen, K., Hutchison, E.R., Lee, E.K., Kuwano, Y., Kim, M.M., Masuda, K., Srikantan, S., Subaran, S.S., Marasa, B.S., Mattson, M.P., et al. 2010. miR-375 inhibits differentiation of neurites by lowering HuD levels. *Mol. Cell. Biol*. 30, 4197–4210.

Abel, T., K.C. Martin, D. Bartsch, and E.R. Kandel. 1998. Memory suppressor genes: inhibitory constraints on the storage of long-term memory. *Science*. 279:338-341.

Albig, A.R., and C.J. Decker. 2001. The target of rapamycin signaling pathway regulates mRNA turnover in the yeast Saccharomyces cerevisiae. *Mol Biol Cell*. 12:3428-3438.

Allen, M. L., Koh, D. S., and Tempel, B. L. 1998. Cyclic AMP regulates potassium channel expression in C6 glioma by destabilizing Kv1.1 mRNA. *Proceedings of the National Academy of Sciences of the United States of America* 95, 7693-7698.

Ando, R., H. Hama, M. Yamamoto-Hino, H. Mizuno, and A. Miyawaki. 2002. An optical marker based on the UV-induced green-to-red photoconversion of a fluorescent protein. *Proceedings of the National Academy of Sciences of the United States of America*. 99:12651-12656.

Antic, D., N. Lu, and J.D. Keene. 1999. ELAV tumor antigen, Hel-N1, increases translation of neurofilament M mRNA and induces formation of neurites in human teratocarcinoma cells. *Genes Dev*. 13:449-461.

Bandres, E., Agirre, X., Bitarte, N., Ramirez, N., Zarate, R., Roman-Gomez, J., Prosper, F., and Garcia-Foncillas, J. 2009. Epigenetic regulation of microRNA expression in colorectal cancer. *Int. J. Cancer* 125, 2737–2743.

Bartel, D.P. 2009. MicroRNAs: target recognition and regulatory functions. *Cell*. 136:215-233.

Beckel-Mitchener, A. C., Miera, A., Keller, R., and Perrone-Bizzozero, N. I. 2002. *The Journal of biological chemistry* 277: 27996-28002

Bedford, M.T., and Clarke, S.G. 2009. Protein arginine methylation in mammals: who, what, and why. *Mol. Cell* 33, 1–13.

Bhalla, T., Rosenthal, J.J.C., Holmgren, M., and Reenan, R. 2004. Control of human potassium channel inactivation by editing of a small mRNA hairpin. *Nat. Struct. Mol. Biol*. 11, 950–956

Bianchi, R., Chuang, S.-C., Zhao, W., Young, S.R., and Wong, R.K.S. 2009. Cellular plasticity for group I mGluR-mediated epileptogenesis. *J. Neurosci*. 29, 3497–3507.

Blichenberg, A., B. Schwanke, M. Rehbein, C.C. Garner, D. Richter, and S. Kindler. 1999. Identification of a cis-acting dendritic targeting element in MAP2 mRNAs. *J Neurosci*. 19:8818-8829.

Bliss, T.V., and T. Lomo. 1973. Long-lasting potentiation of synaptic transmission in the dentate area of the anaesthetized rabbit following stimulation of the perforant path. *J Physiol*. 232:331-356.

Bolognani, F., T. Contente-Cuomo, and N.I. Perrone-Bizzozero. 2010. Novel recognition motifs and biological functions of the RNA-binding protein HuD revealed by genome-wide identification of its targets. *Nucleic acids research*. 38:117-130.

Bolognani, F., M.A. Merhege, J. Twiss, and N.I. Perrone-Bizzozero. 2004. Dendritic localization of the RNA-binding protein HuD in hippocampal neurons: association with polysomes and upregulation during contextual learning. *Neuroscience letters*. 371:152-157.

Bolognani, F., and N.I. Perrone-Bizzozero. 2008. RNA-protein interactions and control of mRNA stability in neurons. *Journal of neuroscience research*. 86:481-489.

Bolognani, F., S. Qiu, D.C. Tanner, J. Paik, N.I. Perrone-Bizzozero, and E.J. Weeber. 2007. Associative and spatial learning and memory deficits in transgenic mice overexpressing the RNA-binding protein HuD. *Neurobiology of learning and memory*. 87:635-643.

Bolognani, F., D.C. Tanner, M. Merhege, J. Deschenes-Furry, B. Jasmin, and N.I. Perrone-Bizzozero. 2006. In vivo post-transcriptional regulation of GAP-43 mRNA by overexpression of the RNA-binding protein HuD. *Journal of neurochemistry*. 96:790-801.

Bramham, C.R., Worley, P.F., Moore, M.J., and Guzowski, J.F. 2008. The immediate early gene arc/arg3.1: regulation, mechanisms, and function. *J. Neurosci*. 28, 11760–11767.

Brennan, C.M., and Steitz, J.A. 2001. HuR and mRNA stability. *Cell. Mol. Life Sci*. CMLS 58, 266–277.

Brew, H.M., J.L. Hallows, and B.L. Tempel. 2003. Hyperexcitability and reduced low threshold potassium currents in auditory neurons of mice lacking the channel subunit Kv1.1. *J Physiol*. 548:1-20.

Brewster, A.L., Lugo, J.N., Patil, V.V., Lee, W.L., Qian, Y., Vanegas, F., and Anderson, A.E. 2013. Rapamycin reverses status epilepticus-induced memory deficits and dendritic damage. *PloS one* 8, e57808.

Bronicki, L.M., and Jasmin, B.J. 2013. Emerging complexity of the HuD/ELAVl4 gene; implications for neuronal development, function, and dysfunction. *RNA N. Y. N* 19, 1019–1037.

Carninci, P. 2010. RNA dust: where are the genes? *DNA Res. Int. J. Rapid Publ. Rep. Genes Genomes* 17, 51–59.

Carpentier, A.F., Rosenfeld, M.R., Delattre, J.Y., Whalen, R.G., Posner, J.B., and Dalmau, J. 1998. DNA vaccination with HuD inhibits growth of a neuroblastoma in mice. *Clin. Cancer Res. Off. J. Am. Assoc. Cancer Res*. 4, 2819–2824.

Chen, X., and Johnston, D. 2006. Voltage-gated ion channels in dendrites of hippocampal pyramidal neurons. *Pflugers Arch* 453, 397-401.

Chen, X., and D. Johnston. 2010. The Elusive D-current: Shaping Action Potentials in the Dendrites? Nova Science Publishers, Inc., Hauppauge, NY.

Costa-Mattioli, M., and Monteggia, L.M. 2013. mTOR complexes in neurodevelopmental and neuropsychiatric disorders. *Nat. Neurosci.* 16, 1537–1543.

Costa-Mattioli, M., W.S. Sossin, E. Klann, and N. Sonenberg. 2009. Translational control of long-lasting synaptic plasticity and memory. *Neuron*. 61:10-26.

D'Adamo, M.C., Catacuzzeno, L., Di Giovanni, G., Franciolini, F., and Pessia, M. 2013. K+ CHANNELEPSY: progress in the neurobiology of potassium channels and epilepsy. *Frontiers in Cellular Neuroscience* 7.

Dalmau, J., Furneaux, H.M., Gralla, R.J., Kris, M.G., and Posner, J.B. 1990. Detection of the anti-Hu antibody in the serum of patients with small cell lung cancer--a quantitative western blot analysis. *Ann. Neurol.* 27, 544–552.

Dalmau, J., Furneaux, H.M., Cordon-Cardo, C., and Posner, J.B. 1992. The expression of the Hu (paraneoplastic encephalomyelitis/sensory neuronopathy) antigen in human normal and tumor tissues. *Am. J. Pathol*. 141, 881–886.

Davis, G.W., and C.S. Goodman. 1998. Genetic analysis of synaptic development and plasticity: homeostatic regulation of synaptic efficacy. *Curr Opin Neurobiol*. 8:149-156.

Deschenes-Furry, J., K. Mousavi, F. Bolognani, R.L. Neve, R.J. Parks, N.I. Perrone-Bizzozero, and B.J. Jasmin. 2007. The RNA-binding protein HuD binds acetylcholinesterase mRNA in neurons and regulates its expression after axotomy. *The Journal of neuroscience : the official journal of the Society for Neuroscience*. 27:665-675.

Di Liegro, C.M., Schiera, G., and Di Liegro, I. 2014. Regulation of mRNA transport, localization and translation in the nervous system of mammals (Review). *Int. J. Mol. Med.*

Dyrskjøt, L., Ostenfeld, M.S., Bramsen, J.B., Silahtaroglu, A.N., Lamy, P., Ramanathan, R., Fristrup, N., Jensen, J.L., Andersen, C.L., Zieger, K. 2009. Genomic profiling of microRNAs in bladder cancer: miR-129 is associated with poor outcome and promotes cell death in vitro. *Cancer Res*. 69, 4851–4860.

Fabian, M.R., N. Sonenberg, and W. Filipowicz. 2010. Regulation of mRNA translation and stability by microRNAs. *Annual review of biochemistry*. 79:351-379.

Fan, Y., Fricker, D., Brager, D.H., Chen, X., Lu, H.C., Chitwood, R.A., and Johnston, D. 2005. Activity-dependent decrease of excitability in rat hippocampal neurons through increases in I(h). *Nature neuroscience* 8, 1542-1551.

Filipowicz, W., S. Bhattacharyya, and N. Sonenberg. 2008. Mechanisms of post-transcriptional regulation by microRNAs: are the answers in sight? *Nat Rev Genet*. 9:102-114.

Fujiwara, T., Mori, Y., Chu, D.L., Koyama, Y., Miyata, S., Tanaka, H., Yachi, K., Kubo, T., Yoshikawa, H., and Tohyama, M. 2006. CARM1 regulates proliferation of PC12 cells by methylating HuD. *Mol. Cell. Biol*. 26, 2273–2285.

Fukao, A., Y. Sasano, H. Imataka, K. Inoue, H. Sakamoto, N. Sonenberg, C. Thoma, and T. Fujiwara. 2009. The ELAV protein HuD stimulates cap-dependent translation in a Poly(A)- and eIF4A-dependent manner. *Mol Cell*. 36:1007-1017.

Gallagher, S.M., Daly, C.A., Bear, M.F., and Huber, K.M. 2004. Extracellular signal-regulated protein kinase activation is required for metabotropic glutamate receptor-dependent long-term depression in hippocampal area CA1. *J. Neurosci.* 24, 4859–4864.

Geiger, J.R., and P. Jonas. 2000. Dynamic control of presynaptic Ca(2+) inflow by fast-inactivating K(+) channels in hippocampal mossy fiber boutons. *Neuron*. 28:927-939.

George, A.D., and S.A. Tenenbaum. 2006. MicroRNA modulation of RNA-binding protein regulatory elements. *RNA biology*. 3:57-59.

Golding, N.L., H.Y. Jung, T. Mickus, and N. Spruston. 1999. Dendritic calcium spike initiation and repolarization are controlled by distinct potassium channel subtypes in CA1 pyramidal neurons. *J Neurosci*. 19:8789-8798.

Gong, R., Park, C. S., Abbassi, N. R., and Tang, S. J. 2006. *The Journal of biological chemistry* 281: 18802-18815

Govindarajan, A., Israely, I., Huang, S. Y., and Tonegawa, S. 2010. *Neuron* 69: 132-146

Graus, F., Keime-Guibert, F., Reñe, R., Benyahia, B., Ribalta, T., Ascaso, C., Escaramis, G., and Delattre, J.Y. 2001. Anti-Hu-associated paraneoplastic encephalomyelitis: analysis of 200 patients. *Brain J. Neurol*. 124, 1138–1148.

Grundhoff, A., C.S. Sullivan, and D. Ganem. 2006. A combined computational and microarray-based approach identifies novel microRNAs encoded by human gamma-herpesviruses. *RNA*. 12:733-750.

Henson, R.A., Urich, H. Encephalomyelitis with carcinoma. 1982 In: Henson RA. Urich, H. editors. *Cancer and nervous system.* Oxford: Blackwell Scientific 314-345.

Higgs, M.H., and Spain, W.J. 2011. Kv1 channels control spike threshold dynamics and spike timing in cortical pyramidal neurones. *The Journal of physiology* 589, 5125-5142.

Hinman, M.N., and Lou, H. 2008. Diverse molecular functions of Hu proteins. *Cell. Mol. Life Sci.* CMLS 65, 3168–3181.

Hoeffer, C.A., and Klann, E. 2009. NMDA Receptors and Translational Control. In Biology of the NMDA Receptor, A.M. Van Dongen, ed. (Boca Raton (FL): CRC Press),.

Hoeffer, C.A., and E. Klann. 2010. mTOR signaling: at the crossroads of plasticity, memory and disease. *Trends in neurosciences*. 33:67-75.

Hoffman, D. A., Magee, J. C., Colbert, C. M., and Johnston, D. 1997. K+ channel regulation of signal propagation in dendrites of hippocampal pyramidal neurons. *Nature* 387, 869-875.

Holth, J.K., Bomben, V.C., Reed, J.G., Inoue, T., Younkin, L., Younkin, S.G., Pautler, R.G., Botas, J., and Noebels, J.L. 2013. Tau loss attenuates neuronal network hyperexcitability in mouse and Drosophila genetic models of epilepsy. *J. Neurosci. Off. J. Soc. Neurosci. 33*, 1651–1659.

Hopkins, W.F., M.L. Allen, K.M. Houamed, and B.L. Tempel. 1994. Properties of voltage-gated K+ currents expressed in Xenopus oocytes by mKv1.1, mKv1.2 and their heteromultimers as revealed by mutagenesis of the dendrotoxin-binding site in mKv1.1. *Pflugers Archiv : European journal of physiology*. 428:382-390.

Hubers, L., Valderrama-Carvajal, H., Laframboise, J., Timbers, J., Sanchez, G., and Côté, J. 2011. HuD interacts with survival motor neuron protein and can rescue spinal muscular atrophy-like neuronal defects. *Hum. Mol. Genet*. 20, 553–579.

Jain, R.G., Andrews, L.G., McGowan, K.M., Pekala, P.H., and Keene, J.D. 1997. Ectopic expression of Hel-N1, an RNA-binding protein, increases glucose transporter (GLUT1) expression in 3T3-L1 adipocytes. *Mol. Cell. Biol*. 17, 954–962.

Jimenez-Mateos, E.M., and Henshall, D.C. 2013. Epilepsy and microRNA. *Neuroscience* 238, 218–229.

Kelleher, R.J., 3rd, Govindarajan, A., Jung, H.-Y., Kang, H., and Tonegawa, S. (2004). Translational control by MAPK signaling in long-term synaptic plasticity and memory. Cell *116*, 467–479.

Kim, J., and D.A. Hoffman. 2008. Potassium channels: newly found players in synaptic plasticity. *Neuroscientist*. 14:276-286.

Kim, J., A. Krichevsky, Y. Grad, G.D. Hayes, K.S. Kosik, G.M. Church, and G. Ruvkun. 2004. Identification of many microRNAs that copurify with polyribosomes in mammalian neurons. *Proceedings of the National Academy of Sciences of the United States of America*. 101:360-365.

Klann, E., and T.E. Dever. 2004. Biochemical mechanisms for translational regulation in synaptic plasticity. *Nat Rev Neurosci*. 5:931-942.

Konecna, A., J.E. Heraud, L. Schoderboeck, A.A. Raposo, and M.A. Kiebler. 2009. What are the roles of microRNAs at the mammalian synapse? *Neurosci Lett.* 466:63-68.

Kosik, K.S. 2006. The neuronal microRNA system. *Nature reviews. Neuroscience.* 7:911-920.

Krestel, H., Raffel, S., von Lehe, M., Jagella, C., Moskau-Hartmann, S., Becker, A., Elger, C.E., Seeburg, P.H., and Nirkko, A. 2013. Differences between RNA and DNA due to RNA editing in temporal lobe epilepsy. *Neurobiol. Dis.* 56, 66–73.

Kundu, P., M.R. Fabian, N. Sonenberg, S.N. Bhattacharyya, and W. Filipowicz. 2012. HuR protein attenuates miRNA-mediated repression by promoting miRISC dissociation from the target RNA. *Nucleic acids research*. 40:5088-5100.

Kuwano, Y., H.H. Kim, K. Abdelmohsen, R. Pullmann, Jr., J.L. Martindale, X. Yang, and M. Gorospe. 2008. MKP-1 mRNA stabilization and translational control by RNA-binding proteins HuR and NF90. *Mol Cell Biol*. 28:4562-4575.

Landgraf, P., M. Rusu, R. Sheridan, A. Sewer, N. Iovino, A. Aravin, S. Pfeffer, A. Rice, A.O. Kamphorst, M. Landthaler, C. Lin, N.D. Socci, L. Hermida, V. Fulci, S. Chiaretti, R. Foa, J. Schliwka, U. Fuchs, A. Novosel, R.U. Muller, B. Schermer, U. Bissels, J. Inman, Q. Phan, M. Chien, D.B. Weir, R. Choksi, G. De Vita, D. Frezzetti, H.I. Trompeter, V. Hornung, G. Teng, G. Hartmann, M. Palkovits, R. Di Lauro, P. Wernet, G. Macino, C.E. Rogler, J.W. Nagle, J. Ju, F.N. Papavasiliou, T. Benzing, P. Lichter, W. Tam, M.J. Brownstein, A. Bosio, A. Borkhardt, J.J. Russo, C. Sander, M. Zavolan, and T. Tuschl. 2007. A mammalian microRNA expression atlas based on small RNA library sequencing. *Cell*. 129:1401-1414.

Lee, H.Y., Ge, W.P., Huang, W., He, Y., Wang, G.X., Rowson-Baldwin, A., Smith, S.J., Jan, Y.N., and Jan, L.Y. 2011. Bidirectional regulation of dendritic voltage-gated potassium channels by the fragile X mental retardation protein. *Neuron* 72, 630-642.

Lee, K.F.H., Soares, C., and Béïque, J.-C. 2013. Tuning into diversity of homeostatic synaptic plasticity. *Neuropharmacology.*

Lim, C.S., and Alkon, D.L. 2012. Protein kinase C stimulates HuD-mediated mRNA stability and protein expression of neurotrophic factors and enhances dendritic maturation of hippocampal neurons in culture. *Hippocampus* 22, 2303–2319.

Liu DZ, Tian Y, Ander BP, Xu H, Stamova BS, Zhan X, Turner RJ, Jickling G, Sharp FR 2010. Brain and blood microRNA expression profiling of ischemic stroke, intracerebral hemorrhage, and kainate seizures. *J Cereb Blood Flow Metab* 30:92–101.

Losonczy, A., Makara, J. K., and Magee, J. C. 2008. Compartmentalized dendritic plasticity and input feature storage in neurons. *Nature* 452, 436-441.

Lukong, K.E., Chang, K., Khandjian, E.W., and Richard, S. 2008. RNA-binding proteins in human genetic disease. *Trends Genet.* TIG 24, 416–425.

Ma, T., Hoeffer, C.A., Capetillo-Zarate, E., Yu, F., Wong, H., Lin, M.T., Tampellini, D., Klann, E., Blitzer, R.D., and Gouras, G.K. 2010. Dysregulation of the mTOR pathway mediates impairment of synaptic plasticity in a mouse model of Alzheimer's disease. *PloS one* 5.

Ma, D., N. Zerangue, K. Raab-Graham, S.R. Fried, Y.N. Jan, and L.Y. Jan. 2002. Diverse trafficking patterns due to multiple traffic motifs in G protein-activated inwardly rectifying potassium channels from brain and heart. *Neuron*. 33:715-729.

Magee, J. C., and Johnston, D. 1997. A synaptically controlled, associative signal for Hebbian plasticity in hippocampal neurons. *Science* 275, 209-213.

Mameli, M., Balland, B., Luján, R., and Lüscher, C. (2007). Rapid synthesis and synaptic insertion of GluR2 for mGluR-LTD in the ventral tegmental area. Science 317, 530–533.

Martin, K.C., and R.S. Zukin. 2006. RNA trafficking and local protein synthesis in dendrites: an overview. *J Neurosci*. 26:7131-7134.

Mascott, C.R., Gotman, J., and Beaudet, A. 1994. Automated EEG monitoring in defining a chronic epilepsy model. *Epilepsia* 35, 895-902.

Mathews, P. J., Jercog, P. E., Rinzel, J., Scott, L. L., and Golding, N. L. 2010. Control of submillisecond synaptic timing in binaural coincidence detectors by K(v)1 channels. *Nat Neurosci* 13, 601-609.

Matsumoto, T., Ryuge, S., Kobayashi, M., Kageyama, T., Hattori, M., Goshima, N., Jiang, S.-X., Saegusa, M., Iyoda, A., Satoh, Y. 2012. Anti-HuC and -HuD autoantibodies are differential sero-diagnostic markers for small cell carcinoma from large cell neuroendocrine carcinoma of the lung. *Int. J. Oncol.* 40, 1957–1962.

Matthew, E.M., Hart, L.S., Astrinidis, A., Navaraj, A., Dolloff, N.G., Dicker, D.T., Henske, E.P., and El-Deiry, W.S. 2009. The p53 target Plk2 interacts with TSC proteins impacting mTOR signaling, tumor growth and chemosensitivity under hypoxic conditions. *Cell Cycle* 8, 4168-4175.

Mayford, M., Bach, M. E., Huang, Y. Y., Wang, L., Hawkins, R. D., and Kandel, E. R. 1996. *Science* 274: 1678-1683

McCarthy, N., Wetherill, L., Lovely, C.B., Swartz, M.E., Foroud, T.M., and Eberhart, J.K. 2013. Pdgfra protects against ethanol-induced craniofacial defects in a zebrafish model of FASD. *Development* 140, 3254–3265.

Meisner, N.C., and W. Filipowicz. 2011. Properties of the Regulatory RNA-Binding Protein HuR and its Role in Controlling miRNA Repression. *Advances in experimental medicine and biology*. 700:106-123.

Merlin, L.R., Bergold, P.J., and Wong, R.K. 1998. Requirement of protein synthesis for group I mGluR-mediated induction of epileptiform discharges. *J. Neurophysiol.* 80, 989–993.
Metz, A.E., N. Spruston, and M. Martina. 2007. Dendritic D-type potassium currents inhibit the spike afterdepolarization in rat hippocampal CA1 pyramidal neurons. *J Physiol*. 581:175-187.

Miller, S., Yasuda, M., Coats, J. K., Jones, Y., Martone, M. E., and Mayford, M. 2002. *Neuron* 36: 507-519

Miska, E.A., E. Alvarez-Saavedra, M. Townsend, A. Yoshii, N. Sestan, P. Rakic, M. Constantine-Paton, and H.R. Horvitz. 2004. Microarray analysis of microRNA expression in the developing mammalian brain. *Genome Biol*. 5:R68.

Monaghan, M.M., J.S. Trimmer, and K.J. Rhodes. 2001. Experimental localization of Kv1 family voltage-gated K+ channel alpha and beta subunits in rat hippocampal formation. *J Neurosci*. 21:5973-5983.

Nakamoto, M., Nalavadi, V., Epstein, M.P., Narayanan, U., Bassell, G.J., and Warren, S.T. 2007. Fragile X mental retardation protein deficiency leads to excessive mGluR5-dependent internalization of AMPA receptors. *Proc. Natl. Acad. Sci. U.S.A.* 104, 15537–15542.
Narayanan, R., and Johnston, D. 2010. The h current is a candidate mechanism for regulating the sliding modification threshold in a BCM-like synaptic learning rule. *Journal of neurophysiology* 104, 1020-1033.

Narayanan, U., Nalavadi, V., Nakamoto, M., Pallas, D.C., Ceman, S., Bassell, G.J., and Warren, S.T. 2007. FMRP phosphorylation reveals an immediate-early signaling pathway triggered by group I mGluR and mediated by PP2A. *The Journal of neuroscience : the official journal of the Society for Neuroscience* 27, 14349-14357.

Origanti, S., S.L. Nowotarski, T.D. Carr, S. Sass-Kuhn, L. Xiao, J.Y. Wang, and L.M. Shantz. 2012. Ornithine decarboxylase mRNA is stabilized in an mTORC1-dependent manner in Ras-transformed cells. *Biochem J*. 442:199-207.

Pascale, A., Amadio, M., Scapagnini, G., Lanni, C., Racchi, M., Provenzani, A., Govoni, S., Alkon, D.L., and Quattrone, A. 2005. Neuronal ELAV proteins enhance mRNA stability by a PKCalpha-dependent pathway. *Proc. Natl. Acad. Sci. U. S. A.* 102, 12065–12070.

Pascale, A., and Govoni, S. 2012. The complex world of post-transcriptional mechanisms: is their deregulation a common link for diseases? Focus on ELAV-like RNA-binding proteins. *Cell. Mol. Life Sci.* CMLS 69, 501–517.

Pascale, A., P.A. Gusev, M. Amadio, T. Dottorini, S. Govoni, D.L. Alkon, and A. Quattrone. 2004. Increase of the RNA-binding protein HuD and posttranscriptional up-regulation of the GAP-43 gene during spatial memory. *Proc Natl Acad Sci U S A*. 101:1217-1222.

Pei, J.J., and Hugon, J. 2008. mTOR-dependent signalling in Alzheimer's disease. *Journal of cellular and molecular medicine* 12, 2525-2532.

Pfaffl, M.W. 2001. A new mathematical model for relative quantification in real-time RT-PCR. *Nucleic Acids Res*. 29:e45.

Pende, M., Um, S.H., Mieulet, V., Sticker, M., Goss, V.L., Mestan, J., Mueller, M., Fumagalli, S., Kozma, S.C., and Thomas, G. 2004. S6K1−/−/S6K2−/− Mice Exhibit Perinatal Lethality and Rapamycin-Sensitive 5′-Terminal Oligopyrimidine mRNA Translation and Reveal a Mitogen-Activated Protein Kinase-Dependent S6 Kinase Pathway. *Mol. Cell. Biol.* 24, 3112–3124.

Poolos, N.P., and Johnston, D. 2012. Dendritic ion channelopathy in acquired epilepsy. *Epilepsia* 53 *Suppl 9*, 32-40.

Potter, W.B., Basu, T., O'Riordan, K.J., Kirchner, A., Rutecki, P., Burger, C., and Roopra, A. 2013. Reduced Juvenile Long-Term Depression in Tuberous Sclerosis Complex Is Mitigated in Adults by Compensatory Recruitment of mGluR5 and Erk Signaling. *PLoS Biol* 11.

Quinlan, E.M., B.D. Philpot, R.L. Huganir, and M.F. Bear. 1999. Rapid, experience-dependent expression of synaptic NMDA receptors in visual cortex in vivo. *Nat Neurosci*. 2:352-357.

Raab-Graham, K.F., P.C. Haddick, Y.N. Jan, and L.Y. Jan. 2006. Activity- and mTOR-dependent suppression of Kv1.1 channel mRNA translation in dendrites. *Science*. 314:144-148.

Rho, J.M., Szot, P., Tempel, B.L., and Schwartzkroin, P.A. 1999. Developmental seizure susceptibility of kv1.1 potassium channel knockout mice. *Developmental neuroscience* 21, 320-327.

Richter, J.D., and E. Klann. 2009. Making synaptic plasticity and memory last: mechanisms of translational regulation. *Genes Dev*. 23:1-11.

Robbins, C.A., and Tempel, B.L. (2012). Kv1.1 and Kv1.2: similar channels, different seizure models. *Epilepsia* 53 Suppl 1, 134-141.

Robertson, B., Owen, D., Stow, J., Butler, C., and Newland, C. 1996. Novel effects of dendrotoxin homologues on subtypes of mammalian Kv1 potassium channels expressed in Xenopus oocytes. *FEBS Lett* 383, 26-30.

Ronesi, J.A., and K.M. Huber. 2008. Homer interactions are necessary for metabotropic glutamate receptor-induced long-term depression and translational activation. *The Journal of neuroscience : the official journal of the Society for Neuroscience*. 28:543-547.

Sahin, M. 2012. Targeted treatment trials for tuberous sclerosis and autism: no longer a dream. *Current opinion in neurobiology*. 22:895-901.

Schechter, L.E. 1997. The potassium channel blockers 4-aminopyridine and tetraethylammonium increase the spontaneous basal release of [3H]5-hydroxytryptamine in rat hippocampal slices. *J Pharmacol Exp Ther*. 282:262-270.

Schratt, G. 2009. Fine-tuning neural gene expression with microRNAs. *Current opinion in neurobiology*. 19:213-219.

Scott, L. L., Mathews, P. J., and Golding, N. L. 2005. Posthearing developmental refinement of temporal processing in principal neurons of the medial superior olive. *J Neurosci* 25, 7887-7895.

Sharma, A., C.A. Hoeffer, Y. Takayasu, T. Miyawaki, S.M. McBride, E. Klann, and R.S. Zukin. 2010. Dysregulation of mTOR signaling in fragile X syndrome. *J Neurosci*. 30:694-702.

Sharma, A.K., Reams, R.Y., Jordan, W.H., Miller, M.A., Thacker, H.L., and Snyder, P.W. 2007. Mesial temporal lobe epilepsy: pathogenesis, induced rodent models and lesions. *Toxicol. Pathol.* 35, 984–999.

Shen, R., Pan, S., Qi, S., Lin, X., and Cheng, S. 2010. Epigenetic repression of microRNA-129-2 leads to overexpression of SOX4 in gastric cancer. *Biochem. Biophys. Res. Commun.* 394, 1047–1052.

Shin, M., Brager, D., Jaramillo, T.C., Johnston, D., and Chetkovich, D.M. 2008. Mislocalization of h channel subunits underlies h channelopathy in temporal lobe epilepsy. *Neurobiology of disease* 32, 26-36.

Siddeek, B., Inoubli, L., Lakhdari, N., Rachel, P.B., Fussell, K.C., Schneider, S., Mauduit, C., and Benahmed, M. 2014. MicroRNAs as potential biomarkers in diseases and toxicology. *Mutat. Res.*

Smart, S.L., V. Lopantsev, C.L. Zhang, C.A. Robbins, H. Wang, S.Y. Chiu, P.A. Schwartzkroin, A. Messing, and B.L. Tempel. 1998. Deletion of the K(V)1.1 potassium channel causes epilepsy in mice. *Neuron*. 20:809-819.

Sosanya, N.M., Huang, P.P.C., Cacheaux, L.P., Chen, C.J., Nguyen, K., Perrone-Bizzozero, N.I., and Raab-Graham, K.F. 2013. Degradation of high affinity HuD targets releases Kv1.1 mRNA from miR-129 repression by mTORC1. *J. Cell Biol.* 202, 53–69.

Southan, A.P., and D.G. Owen. 1997. The contrasting effects of dendrotoxins and other potassium channel blockers in the CA1 and dentate gyrus regions of rat hippocampal slices. *Br J Pharmacol*. 122:335-343.

Spilman, P., Podlutskaya, N., Hart, M.J., Debnath, J., Gorostiza, O., Bredesen, D., Richardson, A., Strong, R., and Galvan, V. 2010. Inhibition of mTOR by rapamycin abolishes cognitive deficits and reduces amyloid-beta levels in a mouse model of Alzheimer's disease. *PloS one* 5, e9979.

Spruston, N., Schiller, Y., Stuart, G., and Sakmann, B. 1995. Activity-dependent action potential invasion and calcium influx into hippocampal CA1 dendrites. *Science* 268, 297-300.

Srikantan, S., K. Tominaga, and M. Gorospe. 2012. Functional interplay between RNA-binding protein HuR and microRNAs. *Current protein & peptide science*. 13:372-379.

Stafstrom, C.E., Hagerman, P.J., and Pessah, I.N. 2012. Pathophysiology of Epilepsy in Autism Spectrum Disorders. In Jasper's Basic Mechanisms of the Epilepsies, J.L. Noebels, M. Avoli, M.A. Rogawski, R.W. Olsen, and A.V. Delgado-Escueta, eds. (Bethesda (MD): National Center for Biotechnology Information (US)),.

Storm, J.F. 1988. Temporal integration by a slowly inactivating K+ current in hippocampal neurons. *Nature*. 336:379-381.

Sun, H., Kosaras, B., Klein, P.M., and Jensen, F.E. 2013. Mammalian target of rapamycin complex 1 activation negatively regulates Polo-like kinase 2-mediated homeostatic compensation following neonatal seizures. *Proceedings of the National Academy of Sciences of the United States of America* 110, 5199-5204.

Tang, S.J., Reis, G., Kang, H., Gingras, A.-C., Sonenberg, N., and Schuman, E.M. 2002. A rapamycin-sensitive signaling pathway contributes to long-term synaptic plasticity in the hippocampus. *Proc. Natl. Acad. Sci. U.S.A.* 99, 467–472.

Tanouye, M.A., and A. Ferrus. 1985. Action potentials in normal and Shaker mutant Drosophila. *J Neurogenet*. 2:253-271.

Thiels, E., Kanterewicz, B.I., Norman, E.D., Trzaskos, J.M., and Klann, E. 2002. Long-term depression in the adult hippocampus in vivo involves activation of extracellular signal-regulated kinase and phosphorylation of Elk-1. *J. Neurosci.* 22, 2054–2062.

Tiffany, A.M., L.N. Manganas, E. Kim, Y.P. Hsueh, M. Sheng, and J.S. Trimmer. 2000. PSD-95 and SAP97 exhibit distinct mechanisms for regulating K(+) channel surface expression and clustering. *The Journal of cell biology*. 148:147-158.

Tiruchinapalli, D.M., M.D. Ehlers, and J.D. Keene. 2008. Activity-dependent expression of RNA binding protein HuD and its association with mRNAs in neurons. *RNA biology*. 5:157-168.

Tsutsui, H., Karasawa, S., Okamura, Y., and Miyawaki, A. 2008. Improving membrane voltage measurements using FRET with new fluorescent proteins. *Nat Methods* 5, 683-685.

Turchinovich, A., Weiz, L., Langheinz, A., and Burwinkel, B. 2011. Characterization of extra-cellular circulating microRNA. *Nucleic Acids Res.* 39:7223–7233.

Turrigiano, G.G., and S.B. Nelson. 2000. Hebb and homeostasis in neuronal plasticity. *Current opinion in neurobiology*. 10:358-364.

Udagawa, T., Swanger, S. A., Takeuchi, K., Kim, J. H., Nalavadi, V., Shin, J., Lorenz, L. J., Zukin, R. S., Bassell, G. J., and Richter, J. D. 2012. *Molecular cell*

Volk, L.J., B.E. Pfeiffer, J.R. Gibson, and K.M. Huber. 2007. Multiple Gq-coupled receptors converge on a common protein synthesis-dependent long-term depression that is affected in fragile X syndrome mental retardation. *The Journal of neuroscience : the official journal of the Society for Neuroscience*. 27:11624-11634.

Wang, D.O., Martin, K.C., and Zukin, R.S. 2010. Spatially restricting gene expression by local translation at synapses. *Trends Neurosci* 33, 173–182.

Wang, X., and T.M. Tanaka Hall. 2001. Structural basis for recognition of AU-rich element RNA by the HuD protein. *Nature structural biology*. 8:141-145.

Wells, D.G., X. Dong, E.M. Quinlan, Y.S. Huang, M.F. Bear, J.D. Richter, and J.R. Fallon. 2001. A role for the cytoplasmic polyadenylation element in NMDA receptor-regulated mRNA translation in neurons. *J Neurosci*. 21:9541-9548.

Williams, C., Shai, R.M., Wu, Y., Hsu, Y., Sitzer, T., Spann, B., McCleary, C., Mo, Y, and Miller, C. 2009. Transcriptome analysis of synaptoneurosomes identifies neuroplasticity genes overexpressed in incipient Alzheimer's disease. *PLoS ONE.* 3: e4936.

Winden, K.D., Karsten, S.L., Bragin, A., Kudo, L.C., Gehman, L., Ruidera, J., Geschwind, D.H., and Engel, J., Jr. 2011. A systems level, functional genomics analysis of chronic epilepsy. *PloS One* 6, e20763.

Wong, M., and Crino, P.B. 2012. mTOR and Epileptogenesis in Developmental Brain Malformations. In Jasper's Basic Mechanisms of the Epilepsies, J.L. Noebels, M. Avoli, M.A. Rogawski, R.W. Olsen, and A.V. Delgado-Escueta, eds. (Bethesda (MD): National Center for Biotechnology Information (US)),.

Wong, M. 2013. Mammalian target of rapamycin (mTOR) pathways in neurological diseases. *Biomed. J.* 36, 40–50.

Wu, J., J. Qian, C. Li, L. Kwok, F. Cheng, P. Liu, C. Perdomo, D. Kotton, C. Vaziri, C. Anderlind, A. Spira, W.V. Cardoso, and J. Lu. 2010. miR-129 regulates cell proliferation by downregulating Cdk6 expression. *Cell Cycle*. 9:1809-1818.

Wu, L., Wells, D., Tay, J., Mendis, D., Abbott, M. A., Barnitt, A., Quinlan, E., Heynen, A., Fallon, J. R., and Richter, J. D. 1998. *Neuron* 21: 1129-1139

Wykes, R.C., Heeroma, J.H., Mantoan, L., Zheng, K., MacDonald, D.C., Deisseroth, K., Hashemi, K.S., Walker, M.C., Schorge, S., and Kullmann, D.M. 2012. Optogenetic and potassium channel gene therapy in a rodent model of focal neocortical epilepsy. *Sci. Transl. Med.* 4, 161ra152.

Xue, Y., K. Ouyang, J. Huang, Y. Zhou, H. Ouyang, H. Li, G. Wang, Q. Wu, C. Wei, Y. Bi, L. Jiang, Z. Cai, H. Sun, K. Zhang, Y. Zhang, J. Chen, and X.D. Fu. 2013. Direct Conversion of Fibroblasts to Neurons by Reprogramming PTB-Regulated MicroRNA Circuits. *Cell*. 152:82-96.

Yu, T., Li, J., Yan, M., Liu, L., Lin, H., Zhao, F., Sun, L., Zhang, Y., Cui, Y., Zhang, F., Li, J., He, X., and Yao, M. 2014. MicroRNA-193a-3p and -5p suppress the metastasis of human non-small-cell lung cancer by downregulating the ERBB4/PIK3R3/mTOR/S6K2 signaling pathway. *Oncogene.*

Zeng, L.H., Rensing, N.R., Zhang, B., Gutmann, D.H., Gambello, M.J., and Wong, M. (2011). Tsc2 gene inactivation causes a more severe epilepsy phenotype than Tsc1 inactivation in a mouse model of tuberous sclerosis complex. *Human molecular genetics* 20, 445-454.

Zeng, L.H., Rensing, N.R., and Wong., M. 2009. The mammalian target of rapamycin signaling pathway mediates epileptogenesis in a model of temporal lobe epilepsy. *The Journal of neuroscience : the official journal of the Society for Neuroscience*. 29:6964-6972.

Zerr, P., J.P. Adelman, and J. Maylie. 1998. Episodic ataxia mutations in Kv1.1 alter potassium channel function by dominant negative effects or haploinsufficiency. *J Neurosci*. 18:2842-2848.

Zhang, W., and D.J. Linden. 2003. The other side of the engram: experience-driven changes in neuronal intrinsic excitability. *Nat Rev Neurosci*. 4:885-900.

VITA

Natasha Marie Sosanya graduated from Taft High School in San Antonio, TX in May 2003. She earned her Bachelor of Science from the University of Texas at San Antonio in May 2007. She entered the Institute for Cell and Molecular Biology at The University of Texas at Austin in June 2007.

Permanent address:

16619 Tenaca Trail

San Antonio, TX 78266

This manuscript was typed by Natasha Marie Sosanya.